14

# Clad welding of steel with nickel-base alloys


E.M. Jorritsma


November 1996

Supervision : Prof. Dr. G. den Ouden
Ir. T. Luijendijk, TU Delft
Ir. R.P.M. van Houdt, IHC Parts & Services


Delft University of Technology
Department of Materials Science and Technology
Welding Technology and Non-Destructive Testing

# Preface

This is the final report of my M.Sc. thesis project at the Delft University of Technology, section Welding technology and Non-destructive Testing. The research is done at IHC Parts & Services in Kinderdijk.

This graduation project followed after earlier research I did at IHC, studying the same matter. It proved rather difficult to solve the "indication problem" to which one was often referring. Many came to me with *the* solution to the problem and, considering all, I tried to maintain a objective look at the matter and conduct a logical research….This was not always that simple because I had to work with very difficult materials which cracked when used in the industrial situation but did not want to come apart when (water)cut, machined or sawn for research purposes. Many helpful souls saw their machines been tortured whenever this student came up with supposedly an ordinary piece of steel. Eventually the test pieces (30 - 80 kg) were reduced to handier proportions and I gradually gained more insight in the actual causes of the fissuring problem of the cladding. It was interesting to see that a problem occurring in a 7 tonne part can actually be seen under a electron microscope at a magnification of 4000 times. When the cause of cracking was found, the next step would be to eliminate this cause changing as little as possible in the production process. This proved to be rather difficult but eventually three plausible solutions came out of the research. One of them, using Hot-wire GTAW for the cladding, is already successfully applied and proves to have much more possibilities than just the solution to the "indication problem".

During my quest to eliminate the fissures and obtain my degree I enjoyed the help of many people for which I thank them all, but I would like to express my special thanks to the following:
My two mentors, Ralph van Houdt and Theo Luijendijk of whom the first kept me thinking in all directions and provided me with the proper work environment for *practical* research. The second gave me hard-core theoretical material science background and put pressure on me to deliver an academic research. Furthermore I would like to thank Archie Frame from SBM/IHC who often put my feet back on the floor when I considered myself as an expert on this matter based on hardly two years of experience opposed to his vast experience on much more than the welding of Inconel 625. Finally I say thanks to my fellow students, friends and staff of the Laboratory of Material Science who helped me to overcome all sorts of problems from grinding a test piece to copying this report. It was a pleasant and instructive way of finishing my education and my life as a student.

# Samenvatting

De oppervlakte-eigenschappen van constructiestaal kunnen verbeterd worden door op te lassen met een hoogwaardiger legering. In dit geval wordt, vanuit een industrie, voor een specifieke toepassing in de off-shore, een foutloos oppervlak geëist dat daarnaast corrosie- en slijtvast is. Voor deze toepassing worden naast koolstofstalen onderdelen ook (super)duplex constructies opgelast met de nikkellegering Inconel 625. Er worden drie tot vier lagen aangebracht door middel van onder poeder lassen met enkele (massieve) draad. Vervolgens wordt de opgelaste laag mechanisch bewerkt tot een zeer glad en vlak oppervlak omdat in de praktijk onder zeer corrosieve omstandigheden Teflon (PTFE) afdichtingen over het bewerkte oppervlak glijden. Bij de produktie van deze gelaste lagen worden bij penetrant onderzoek na het bewerken onacceptabele indicaties gevonden, welke door scheurtjes blijken te worden veroorzaakt.
De oorzaak van deze scheurtjes moet gezocht worden in de combinatie van het lassen van zeer hoogwaardige materialen en het bewerken tot lage ruwheid. Met behulp van "Bead-on-Plate" lasproeven is gekeken naar het eerste aspect, waarbij de lasbadvorm, het stollingsmechanisme van Inconel 625 en de invloed hierop van de lasparameters, een belangrijke rol speelden. Het bleek dat een plat lasbad en een snelle stolling van het lasmetaal het beste resultaat opleverden. Het tweede aspect is vervolgens belicht door de gelaste laag in stappen te bewerken waaruit volgde dat defecten vooral optreden in het overgangsgebied tussen de bovenste en de tweede laslaag. Microscopisch onderzoek wees verder uit dat de scheuren ontstonden als gevolg van interdendritische verbindingen zoals de Laves fase, $(Ni,Cr)_2(Nb,Mo)$, welke ontstaan als gevolg van microsegregatie tijdens het stollen. Het element niobium speelt hierbij een prominente rol.
Er zijn naar aanleiding van dit onderzoek, drie oplossingen voorgesteld om indicaties te voorkomen of op zijn minst het aantal te minimaliseren: Ten eerste kan men, mits de huidige lasmethode gehandhaafd wordt, uitsluitend de toplaag van Inconel 625 bewerken, daar in dit gebied zelden indicaties gevonden zijn. Ten tweede kan men kiezen voor een ander lasproces, TIG-lassen met voorverwarmde draad, omdat, waarschijnlijk door snelle stolling, geen scheurtjes in het bewerkte lasmetaal gevonden zijn. Tenslotte kan worden overwogen om, in plaats van Inconel 625, met de vergelijkbare Hastelloy C-4 legering op te lassen, welke geen niobium bevat waardoor de kans op interdendritische verbindingen sterk verlaagd wordt.

# Summary

The surface properties of construction steel can be improved by clad welding with a high grade material. In the present case a zero defect surface is required, which is also very resistant to wear and corrosion, for a specific off-shore application.

For this application, carbon steel and (super)duplex parts are clad welded with Inconel 625, a nickel-base alloy. Three to four layers are applied, by means of the submerged arc welding process using a single (massive) electrode wire. Then the cladding is machined up to very low roughness, because in service and in a highly corrosive environment, Teflon (PTFE) seals glide on the surfaces. During the fabrication of these overlays, unacceptable indications are found after dye penetrant testing, caused by fissuring of the material.

The cause of the fissures should be found in the combination of welding very high grade material and machining to low roughness. Applying "Bead-on-Plate" tests, the first aspect has been examined. The bead geometry, the solidification process of Inconel 625 and the influence of the welding parameters on this, played an important role. Best results were obtained creating a flat weld bead and ensuring a high solidification rate.

The second aspect was investigated by step-wise machining of the cladding. It was concluded that the defects occurred in the boundary zone between the top layer and the second layer. Further microscopic research revealed that fissuring took place as a result of the presence of interdendritic constituents like laves phase $(Ni,Cr)_2(Nb,Mo)$, which are formed due to microsegregation during solidification. The element niobium plays a prominent role in this respect.

After this research, three solutions are suggested to prevent or at least minimize the defects:

Firstly, when the current welding method is maintained, one should only machine the toplayer, as in this part of the cladding very few indications were found. Secondly, one could choose to apply another welding process, Hot-wire TIG. Probably due to a high solidification rate, no indications were found in the machined surface when this process was used. Finally it is suggested to weld with the comparable Hastelloy C-4, which, contrary to Inconel 625, does not contain any niobium, thereby reducing the chance that interdendritic compounds occur.

# CONTENT

# List of abbreviations

| | |
|---|---|
| ASME | = American Society of Mechanical Engineers |
| BOP | = Bead-on-Plate |
| DAZ | = Differently Affected Zone |
| EMPA | = Electron Microprobe Analyses |
| FPSO | = Floating Production and Storage Off-loading |
| FSO | = Floating and Storage Off-loading |
| GTAW | = Gas Tungsten Arc Welding |
| HAZ | = Heat Affected Zone |
| HI | = Heat-input |
| HWGTAW | = Hot-wire Gas Tungsten Arc Welding |
| IHC | = Industriële Handels Combinatie |
| MC | = Metal Carbide |
| MIG | = Metal Inert Gas |
| NDT | = Non Destructive Testing |
| PREn | = Pitting Resistance Equivalent number |
| PSR | = Product Status Report |
| PT | = Penetrant Testing |
| PWHT | = Post Weld Heat Treatment |
| SAW | = Submerged Arc Welding |
| SBM | = Single Buoy Moorings |
| SEM | = Scanning Electron Microscopy |
| TEM | = Transmission Electron Microscopy |
| TIG | = Tungsten Inert Gas |
| WPS | = Welding Procedure Specification |

# 1. Introduction

In this report the results of a study are described dealing with clad welding of steel products with nickel-base alloys. Clad welding is often applied with the aim to improve the surface properties of construction steel parts. The present study shows that during clad welding of steel, in particular of swivel joints for off-shore applications, certain defects occur. These defects can be explained in terms of the metallurgy of welding this alloy.

The research has been conducted in co-operation with IHC Parts & Services and SBM Off-shore Systems as a M.Sc. thesis project at Delft University of Technology, section Welding Technology and Non-Destructive Testing.

In chapter 2 the industrial application of the clad welding and the appearing problems will be unfolded, resulting in the aim of this research programme. The results of some preliminary experiments will be presented in this chapter as well.

Chapter 3 describes the experiments performed to evaluate the problem and to optimize the welding of Inconel 625. This is generally done by means of Bead-on-Plate tests followed by microscopic investigation. In addition there also have been done some tests on clad welding of test rings under practical conditions.

The results of the experiments are evaluated and discussed in chapter 4 giving three possible solutions to eliminate the problem. To ensure the desired quality suggestions are given to control and follow the production process.

The conclusions and recommendations for further research are given in chapter 5.

Table 2.1 Compositions (wt%) and properties of used alloys

| | **Nickel-base alloys** | | | | **Duplex steel** | | **C-steel** |
|---|---|---|---|---|---|---|---|
| **Chemical composition** | Inconel 625 | S59 | Low Nb Inconel 625 | Hastelloy C-4 | Duplex Zeron 25 | Super Duplex Zeron 100 | ASTM A508 Cl.A |
| Ni | >58 | 59 | Bal | 65 | 4.5 - 6.5 | 6.0 - 8.0 | 0.5 - 1.0 |
| Cr | 20 - 23 | 23 | 20.3 | 16 | 21 - 23 | 24 - 26 | 0.25 - 0.45 |
| Fe | <5.0 | 1.0 | 3.9 | 2 | Bal. | Bal. | Bal. |
| Cu | - | 0.02 | - | - | - | <0.7 | - |
| Mo | 8.0-10.0 | 16 | 8.3 | 16 | 2.5 - 3.5 | 3.5 | 0.55 - 0.70 |
| Nb | 3.15-4.15 | - | **0.6** | - | - | - | - |
| Al | <0.40 | - | 0.1 | - | - | - | - |
| Ti | <0.40 | 0.02 | 0.12 | 0.25 | - | - | - |
| S | <0.015 | 0.002 | 0.004 | <0.002 | <0.02 | - | <0.025 |
| W | - | 0.1 | - | <0.10 | - | 0.7 | - |
| Co | <0.1 | 0.02 | - | 0.10 | - | - | - |
| C | <0.10 | 0.02 | - | 0.10 | <0.03 | <0.03 | <0.27 |
| Mn | <0.50 | 0.1 | 0.36 | 0.20 | <2.0 | <1.0 | 0.5 - 1.0 |
| Si | <0.50 | 0.13 | 0.3 | 0.03 | <1.0 | - | 0.15 - 0.40 |
| P | <0.015 | 0.005 | 0.16 | <0.005 | <0.030 | 0.03 | <0.025 |
| V | - | 0.1 | - | 0.02 | - | - | <0.05 |
| N | - | - | - | - | 0.08-0.20 | 0.25 | - |
| **Mechanical properties** | | | | | | | |
| Yield ≥ (0.2% offset) | 480 Mpa | 520 Mpa | | 305 MPa | 450 MPa | 400 MPa | 450 MPa |
| Tensile ≥ | 65 MPa | 770 MPa | | 700 MPa | 650 - 900 MPa | 650 - 900 MPa | 620 - 795 MPa |
| Elongation ≥ | 54% | 45% | | 40% | 30% | 25% | 16% |
| Hardness | 95 HRB | | | | 270 - 300 HB | 200 - 270 HB | |
| Charpy-V ≥ | 85 J at -196°C | 62 J at -196°C | | | 112 J at -196°C | 75 J at -40°C | 34 - 27 J at -20°C |
| PREn | 51 | 76 | | | 35 | 42 | |

# 2. Aim of research

## § 2.1 Industrial situation

The aim of the research described in this report is to solve an industrial problem. During the fabrication of certain components for off-shore applications, parts have to be cladded with Inconel 625. The problem is that when the claddings of this material are machined and dye penetrant tested often unacceptable defects (indications) appear. The final aim of this research project is to explain the occurrence of these defects and eventually propose possible solutions to eliminate them.
In this section the problem is described from the industrial point of view.

This research has been carried out in co-operation with and in assessment of IHC (Industriële Handels Combinatie) Holland, business unit Parts & Services. IHC Holland is a member of the exchange quotated IHC Caland Group, and originates from several shipyards. Its core business is capital goods for the international dredging industry. For some years, IHC Holland is diverging to other marine areas like off-shore oil exploitation. The aim is to generate 25% of the turn-over from non-dredging products. A growing market in this field of business are production installations for small oil fields, for instance in the North Sea, which are currently not exploited by permanent production platforms. IHC P & S fabricates certain parts for these installations, the so-called swivel stack consisting of multiple swivel - joints. These parts are designed by SBM (Single Buoy Moorings) in Monaco and constructed at IHC P & S at Kinderdijk. SBM is a sister enterprise of IHC Holland and has participated in the research as well.

### § 2.1.1 Parts

The parts to be considered are swivel joints used in exploiting relatively small oil fields. For these fields it is too expensive to build a permanent production platform, so instead a smaller, semi-permanent anchored tanker is used. Basically there are two types of tankers:
Firstly, the Floating Storage Off-loading (FSO), a tanker that functions as a buffer, which is positioned at an oil well and stores the crude oil before it is off-loaded by another tanker to take it ashore. Usually an older tanker is used which is reconstructed and has a V-shaped boom on the bow with the actual connection between riser and vessel.

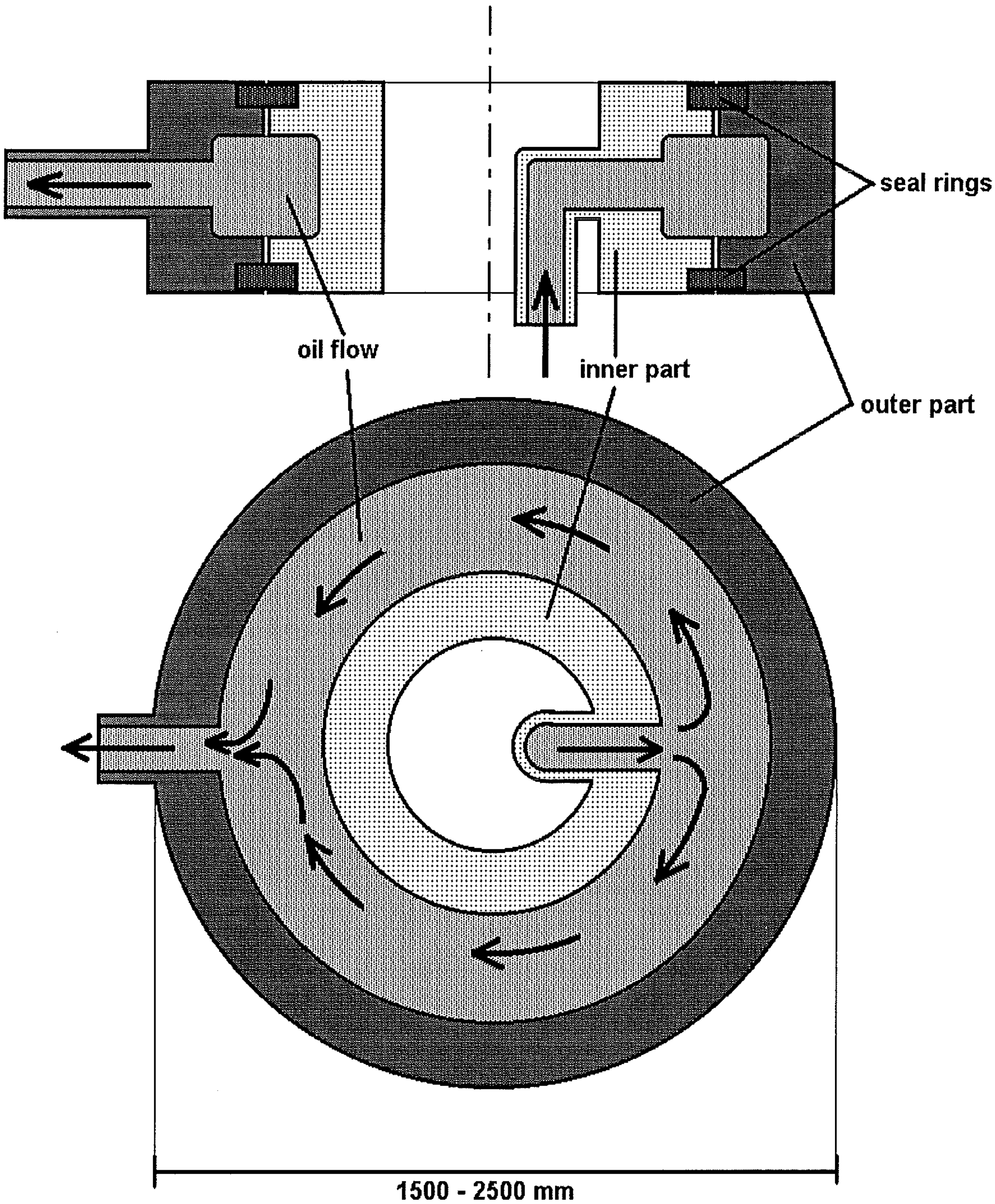


Figure 2.1 Schematic view of swiveljoint

Secondly, the Floating Production and Storage Off-loading (FPSO), a tanker that besides storing also separates the crude oil from sea water and gaseous phases. For this purpose also old tankers are in use, but recently vessels with fully integrated production facilities are constructed as well. These vessels have the connection **in** the bow and produce the oil before it is stored in the hold.

The actual coupling between riser and vessel is called the swivel. It consists of a fixed inner part which is connected to the riser, and the rotating outer part, which is connected to the vessel. Both parts are ring-like constructions. The oil enters through the inner part and leaves the swivel through the outer part (fig. 2.1). Between these two parts there is a complicated system of bearings and seals to prevent leakage. This system has to meet rather high requirements on corrosion resistance and rigidity. After all it is operating in a marine environment and the oil is hot and rich in sulphur. Besides that, the pressures can rise up to several hundred bar.

The seal system consists of seal rings and plastic seals. The seal rings are bolted to both the inner and the outer part and are interconnected. Between the rings and swivel parts the plastic seals have to glide on the metal surface to sustain minimum leakage.

The swivels have a functional life of 10 years minimum without major maintenance. Therefore, the seal wear has to be kept at a minimum, and corrosion of the gliding surfaces has to be avoided at all times. To satisfy these requirements the rubbing surfaces which are in direct contact with the seals are made of Inconel 625 a nickel-base superalloy. This means that a layer of this material has to be put on the seal rings and swivel part which are in contact with the seals. This is done by means of welding a layer of certain thickness on these parts which are then machined to their final dimensions. After this the surface is tested before fitting by means of NDT according to the specifications of ASME and of the client.

### § 2.1.2 Materials

The swivel parts are made of different base materials depending on the fluid that is transported through the swivel. If the oil is rich in sulphur a material of high corrosion resistance is used. If water is injected through the swivel into the well to maintain pressure, a lower quality of steel can be used. In the current designs three kinds of steel are used. Most seal rings are forgings and the inner and outer parts are in general castings. For the chemical composition of the steels see right part of table 2.1:

**Carbon steel** is used for low corrosive oil and water injection. When the pressures remain low these steels also fulfil the requirements.

**Duplex steel** is used if the environment is rather corrosive. This is a high alloy steel with about

22 wt% Cr and 5.5 wt% Ni (see table 2.1). It consists of a ferrite matrix with austenite "islands". This structure has a high strength and corrosion resistance and is obtained after heat treatment of the casting. The austenite/ferrite ratio is about 40/60 and the Pitting Resistance Equivalent number (PREn) is ± 35. This dimensionless quantity indicates the resistance to pitting corrosion and is solely determined by the chemical composition of the alloy.

**Super duplex steel** has roughly the same chemical composition as duplex steel but has a higher Cr an Ni content and contains more N. The $\gamma/\alpha$ ratio is 50/50 and it has generally a better corrosion resistance (PREn >40). Due to the high alloy content of Ni and Cr it is relatively expensive.

Clad welding the last two alloys requires extra care because the (super)duplex materials have a relatively low heat conductivity so they can reach high temperatures during welding which can cause intolerable thermal deformation and disturbance of the $\gamma/\alpha$-ratio which yields a decrease in corrosion resistance.

Different cladding materials can be used (see left hand side of table 2.1). **Inconel 625** is a nickel-base alloy with very good corrosion resistance and mechanical properties. It is often used in offshore applications especially as clad material for piping and chemical installations. The particular use in this application as clad material is not common but prescribed by the client. Important elements besides nickel and chromium are niobium, molybdenum, silicon and carbon. These elements may be involved in the fissuring problem of the weld metal.

When the (super)duplex steel parts of the swivel are cladded a buffer layer is needed. In this case **S59** is used as cladding material which is also a nickel-base alloy with the distinction that it does not contain any niobium. The buffer layer is used for (super)duplex steels because these alloys contain for steels high concentrations of nitrogen (0.08 - 0.25 wt%). N is used to stabilize the austenite phase. This element has been found to form Nb-nitrides which can cause cracking during side-bend tests which are required by the client for the specification of the cladding procedure. When carbon steel is used for the swivels no buffer layer is needed as this material does not contain any nitrogen. Finally, **C4** and **Inconel 625 with low Nb content** are mentioned in Table 2.1 which are used as a substitute for Inconel 625 to investigate the influence of the Nb content on the number of indications in § 3.5.

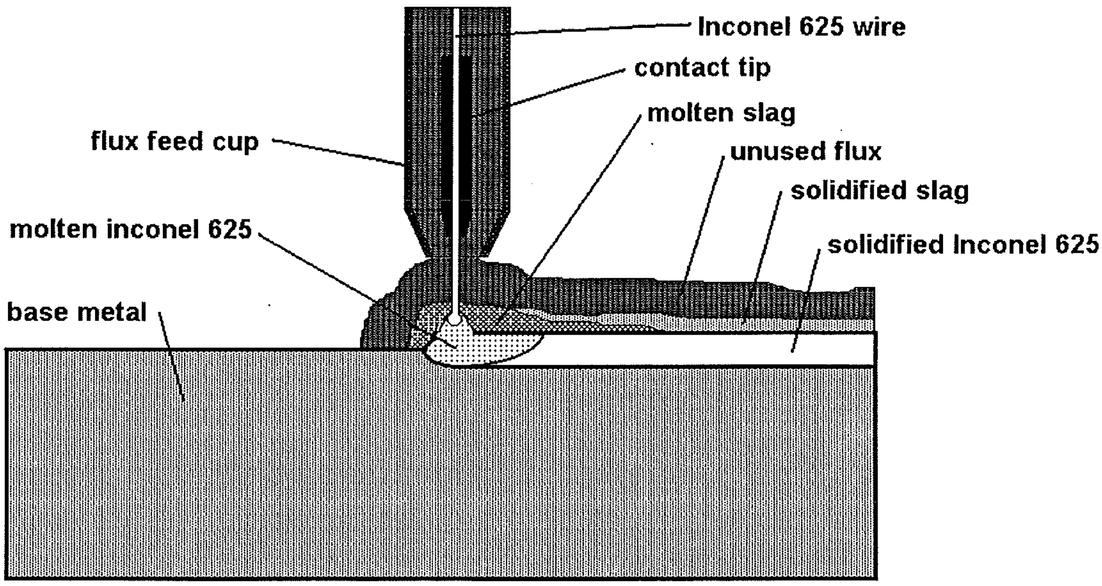


Figure 2.2 The principle of submerged arc welding

## § 2.1.3 Welding

Layers of Inconel 625 or S59 are clad welded on certain swivel parts. Currently this is done by means of submerged arc welding (SAW) (fig. 2.2). This is an arc welding process with a melting electrode-wire. Most welding is done by use of a massive electrode wire but S59 is currently welded with metal cored wire as this is an unusual alloy. The wire consists of a more commonly used alloy cover (pure nickel for example) with the alloying elements in the metal powder core. During welding the correct alloy composition is thus created in the bead. No cast batch of S59 is therefore needed to fabricate the specified electrode wire.

A powder flux which is added externally is also melted by the arc and forms a protective layer of slag. In general, a specific combination of wire and flux is used, provided by the manufacturer of the filler metal. The clad welding has proved to be a critical factor in the production process and has to be monitored carefully.

Producing a "perfect" cladding involves a number of aspects regarding the welding process. This includes among other things base metal and weld metal, flux, equipment, welding parameters and metallurgy. Furthermore, the machining of the cladding plays an important role.

In this research most attention has been paid to the actual welding process and the influence of the welding parameters on the results. In addition, microscopic investigation has to reveal further insight in the solidification of the weld and the problem of fissuring after the machining of the cladding. Several welding tests have been performed under industrial conditions to approach the real situation as close as possible.

To ensure that the corrosion resistance of the overlay is comparable with that of the material Inconel 625, the client prescribes that 2 mm below the machined surface of the cladding the chemical composition has to be equal to the specified composition of Inconel 625 (table 2.1). To achieve this, the cladding thickness after machining has been set at a minimum thickness of 5 mm and should consist of three deposited layers including the buffer layer.

## § 2.1.4 Machining

The inner and outer parts of the swivel and the seal rings are rough castings or forgings and are delivered in unfinished shape with a tolerance of several millimetres. All parts are machined by turning. The parts that need cladding are pre-machined before welding. After welding the welded surfaces are

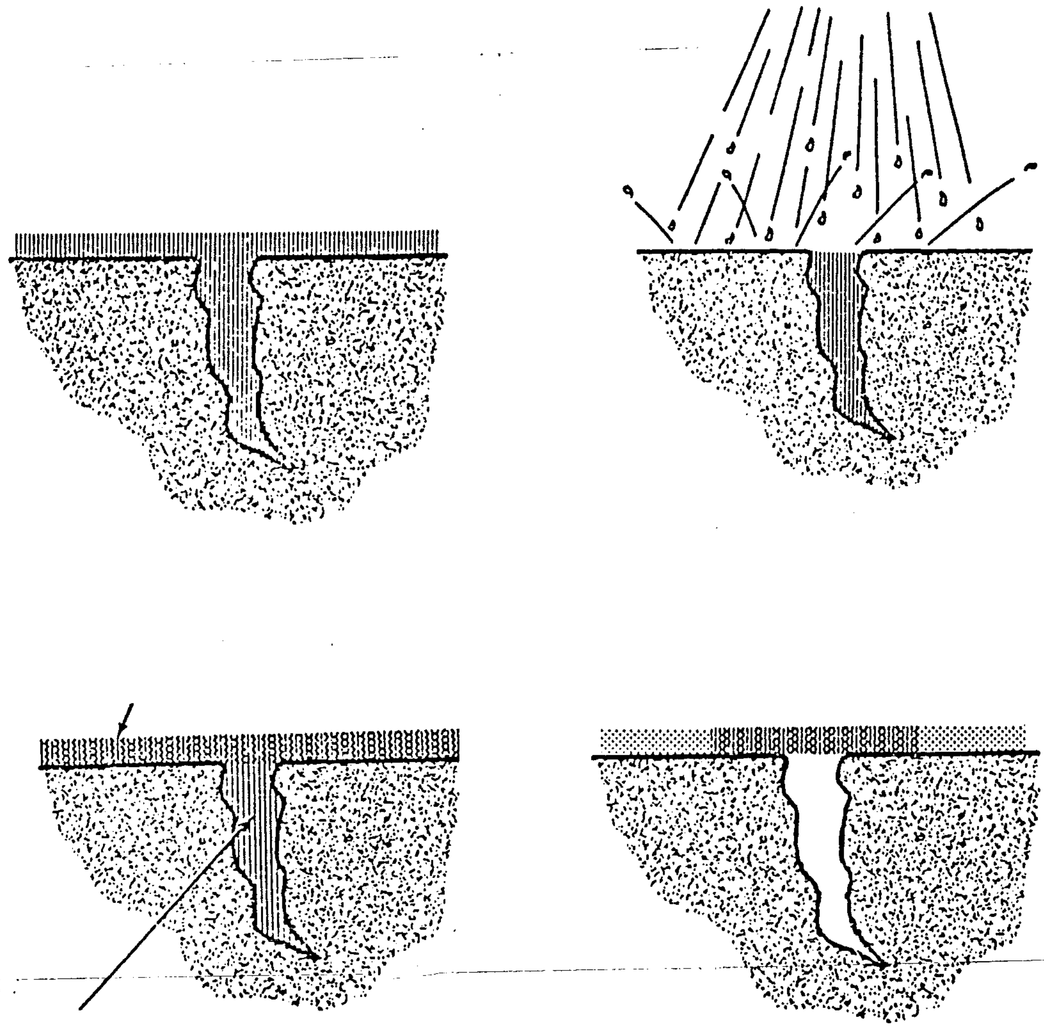

Figure 2.3 The principle of dye penetrant testing [6]

pre-machined and final-machined. Because the cladded surfaces are in contact with plastic seals these surfaces must have very small tolerances and a low surface roughness is vital. The specified tolerance is 0.1 mm on a diameter of approximately 1500 - 2000 mm. The gliding surfaces of the seals must have a roughness of Ra < 0.4 μm. To achieve this, a third machining stage, the superfinish, has to be performed. In the past this was done by grinding the surface with a grinding disc. With this method virtually no material was taken off, and the specified roughness requirement could be met. On the other hand it was unknown what actually happened during the grinding in terms of material take-off, glazing and grinding disc wear. At the moment the superfinish is carried out by fine machining. With a very sharp tool less than 0.1 mm material is removed. This method is quite reproducible and the final roughness requirement is met.

However, some problems are arising during machining of the cladding. Nickel alloys like Inconel 625 are widely used for wear resistant layers, sometimes at high temperatures as well. During normal machining of a material (regular steel) the metal is taken off by means of shearing. During this process the temperature of the material to-be-taken-off rises dramatically at the tool tip. This causes a large decrease in strength and the material can be cut easily. The heat is extracted by the chip and the tool does not wear too much and remains relatively cool. This mechanism can only be applied for ferrous alloys and not for nickel alloys. Nickel alloys hold their strength at high temperatures, in fact that is what they are used for, and are not as easily machined as carbon steels. What happens is that a small stressed zone is created just ahead of the cutting tool where the material is plastically deformed. Inconel 625 has the property to *workharden* while deforming. It has been found that due to this phenomenon a hardened layer is formed at the surface with a thickness of approximately 0,15 mm [1]. This causes a substantial increase in tool wear. To prevent this excessive wear one should machine with a cutting depth of more than 0,15 mm and use sharp tools at all times. Later in this report the relation between the indication problem and the machining will be described.

## § 2.1.5 NDT and repair welding of cladding

The machined cladding is non-destructive tested using **dye penetrant testing**. This method involves spraying the surface to be tested with red coloured dye which penetrates in possible cracks or cavities. After a specified period (20 min.) the abundant dye is removed and a developer is sprayed on the surface. This is a white calcareous substance that absorbs the penetrated fluid from the cavities (see fig. 2.3). These cavities subsequently show as red indications. ASME VIII (Appendix 8) specifies the

dimensions and shape of the indications of so-called "relevant" indications as follows [2]:

Relevant indication: major dimensions > 1.6 mm

Linear = length : width > 3 : 1

Rounded/elliptical = length : width ≤ 3 : 1

Acceptance criteria:

All surfaces to be examined shall be free of:

a. relevant linear indications;

b. relevant rounded indications greater than 4.8 mm in diameter;

c. four or more relevant indications in a line, separated 1.6 mm or less from each other.

NB. An indication of an imperfection may be larger than the imperfection that causes it; however, the size of the indication is the basis for the acceptance evaluation.

For the application in swivels, the sections of the surface that are in actual contact with the seals are not allowed to show any indications and other parts are evaluated according to the ASME specification.
Relevant indications are ground away or, if they are to large, milled with a small handmill and then repair-welded with GTAW. Specified by a special Welding Procedure Specification (WPS) the small milled holes (less than 1 mm in depth) are then filled with one droplet of Inconel 625 or S59 filler metal. When multiple indications are welded the repaired surfaces, i.e. the reinforcements of the droplets, are machined up to ± 0.05 mm above the final dimensions. The redundant metal is then ground off till the final dimensions are obtained.

## § 2.2 Preliminary research

Before the present research was started, preliminary investigations were carried out on this subject. In a first approach the company itself (IHC), in collaboration with the client (SBM) made an investigations to acquire adequate knowledge on the cladding of Inconel 625 for industrial application [3]. This resulted in the choice for the single wire submerged arc welding process and the use of a buffer layer when clad welding on duplex steels.
As a next step a study was carried out to reduce the number of indications in the cladding and to determine the cause of the PT indications. The most important conclusion of this project was that the

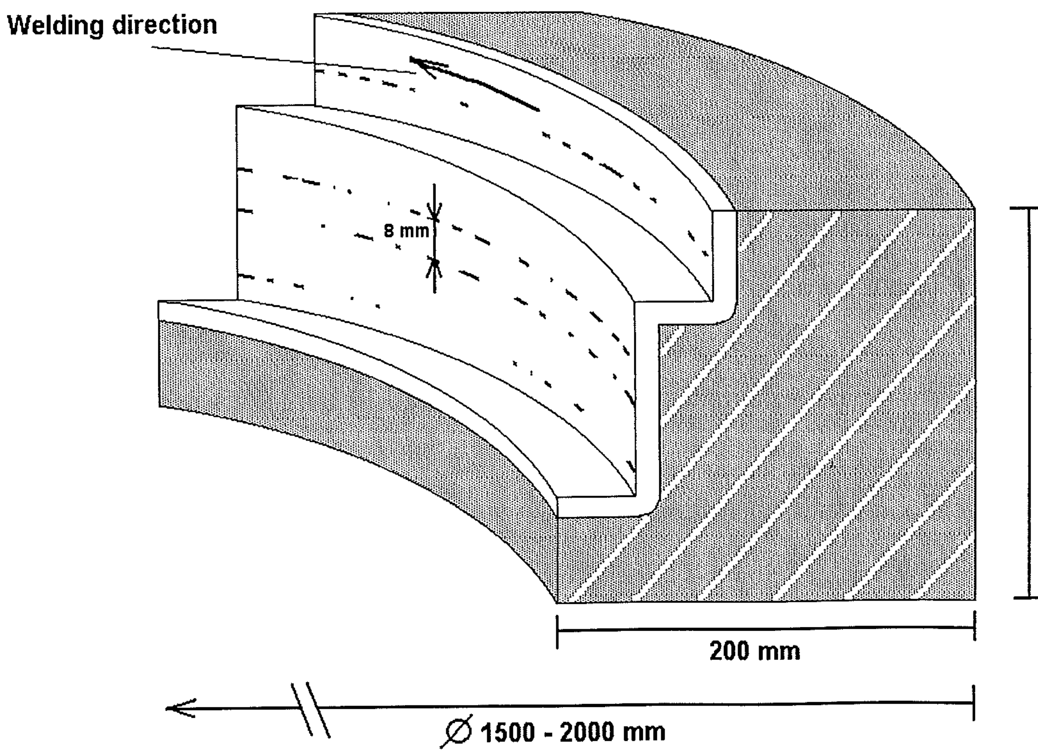


Figure 2.4 Linear pattern of PT-indications in a seal surface

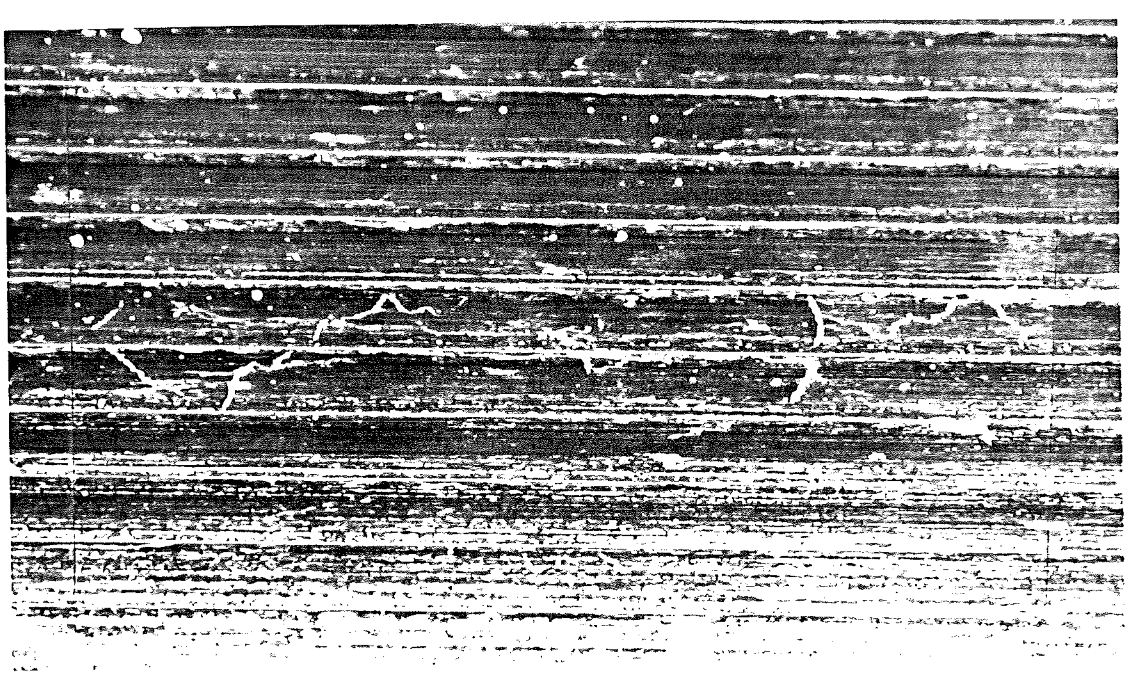

Figure 2.5 Photograph of actual fissure in machined production ring (60x)

indications were caused by micro-fissures and not, as previously assumed, by slag inclusions [4]. Furthermore, it was shown that the problem was probably caused by a combination of welding and machining. The base material itself was ruled out as a major cause because indications showed after welding on different materials. On this basis it was concluded that there was no simple solution to the problem, and to gain more theoretical background a literature survey was conducted on the welding of nickel alloys in general and the cladding of Inconel 625 in particular from a metallurgical point of view. This revealed that the following aspects are of great importance: the type of microstructure, segregation pattern of alloying elements and the formation of interdendritic compounds during solidification. In this respect the elements niobium, carbon and silicon appear to be of major importance in the solidification process of Inconel 625 [5].

## § 2.3 Description of the problem

The problem which led to this investigation presented in this report can be described as follows.
During dye penetrant testing of the welded and machined Inconel 625 cladding of swivel parts defect indications are found. Some of the areas which show indications are in direct contact with the plastic seals ("seal surfaces") and will not be accepted by the client. It is possible to remove the defects but at a very high costs, especially when these defects occur in as high numbers as 150 per surface in some cases).

Most indications have a linear shape and are situated in lines, parallel to the welding and machining direction (see fig. 2.4). These lines are separated in a regular manner at a distance of roughly 7 to 10 mm, which suggests that they are caused by welding. Previously, it was assumed that the indications were caused by slag inclusions, a common feature of submerged arc welding. Further research showed however that the indications were caused by fissuring of the weld metal. These fissures are small, irregular, closed cracks < 1.5 mm in length (see fig. 2.5). The fissures are **not** visible with the untrained eye. There are several questions to be answered in relation with this fissuring problem:

* What causes the material to fissure?
* When does the material fissure?
* Which parameters influence the final result?

- **How can the PT-indications in the machined Inconel 625 surface be eliminated or at least minimised.**

In the following chapters these questions will be addressed.

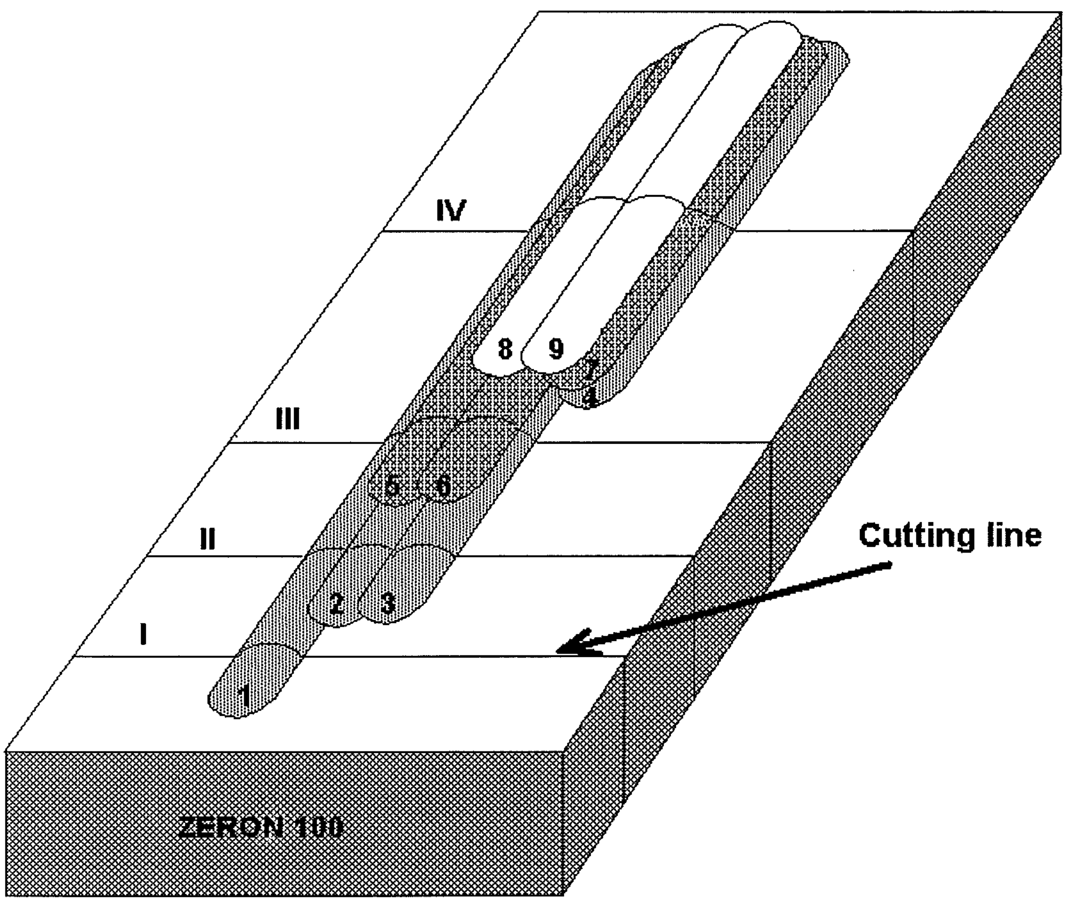


Figure 3.1a Welding sequence of BOP I

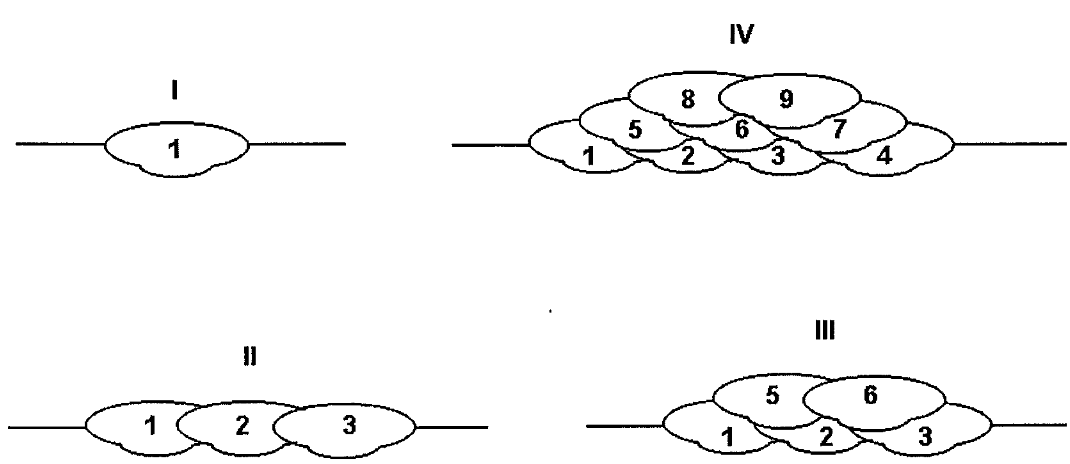


Figure 3.1b Cross-section of BOP I

# 3. Experiments and Results

In this chapter the experiments are described which were performed in order to answer the questions mentioned in chapter 2. The experiments were carried out in the form of Bead-on-Plate tests because it is a relatively simple method to investigate a welding process and its critical aspects. Using optical research, the solidification behaviour of Inconel 625 and the influence of the welding parameters on the structure were determined. Finally the machining of the cladding was given a close look in an attempt to understand what happens during the finish of an Inconel 625 overlay.

## § 3.1 The Bead-on-Plate test

The Bead-on-Plate (BOP) test is a simple test which can be used to obtain information about the bead geometry of a weld. One or more weld beads are deposited on a test piece of base metal. A cross-section is made for optical investigation to determine the influence of the welding parameters on the properties including the macrostructure and microstructure.

All BOP tests were performed using the production facilities at the welding shop at IHC with help of qualified welders.

## § 3.2 Bead-on-Plate test I - *General welding test* -

The first BOP test series had the following objectives:

- to obtain general information about the geometry of the cladded layer;
- to evaluate the influence of multi-layer welding on the shape and structure of the cladding;
- to determine the influence of the welding parameters (in particular the travel speed and the arc voltage) on the geometry of the weld beads;
- to compare the current claddings with the experimental ones, made for the original qualification of the welding procedure.

The last objective is added because when the first Inconel 625 claddings were welded in earlier projects the number of indications was much lower than in the current situation. Some macro-specimens of the

Table 3.1 Welding parameters and bead dimensions of BOP I

| | A I | B I | C I |
|---|---|---|---|
| I (A) | 260 | 260 | 260 |
| V (V) | 26 | 26 | 28 |
| v (mm/min) | 400 | 500 | 500 |
| HI (kJ/mm) | 1.02 | 0.81 | 0.88 |
| W (mm) | 16 | 12 | 12 |
| D (mm) | 6.4 | 5.0 | 4.4 |
| D/W | 0.39 | 0.42 | 0.37 |
| R (mm) | 3.4 | 2.2 | 2.1 |
| P (mm) | 3.0 | 2.8 | 2.3 |

W = Bead width

D = Bead depth

R = Reinforcement

P = Penetration

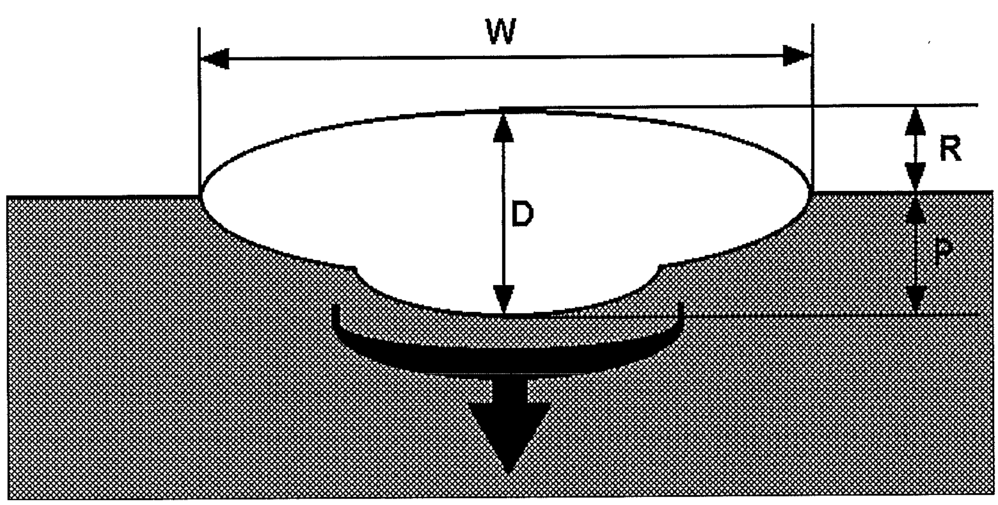


Figure 3.2 Schematic view of typical SAW weld bead

qualification tests were still available and could be compared with the BOP I specimens. Three Zeron 100 testplates were produced with each a cladding with specific parameters (A, B, and C) (see fig. 3.1 and table 3.1). This was done in such a way that cross-sections for microscopic investigation could be made with one, two or three layers. The welding parameters and the bead dimensions obtained are given in table 3.1.

Of each welded test piece cross-sectional macro-specimens were obtained, which were used to determine the macrostructure of the bead cross-section (fig. 3.2). Of every section photographs were taken which are included in appendix I. These photos reveal the following characteristic features.

**General bead geometry**

The weld beads have rather large penetration and not a smooth fusion line. This is partly due to the process in which the electrode wire is melting and the drops create locally a finger print shaped penetration. The beads are not really flat and tend to thicken when the number of layers increases, i.e. the depth-width ratio increases.

**Multiple layer cladding**

When a multiple layer cladding is applied, the fingers sometimes penetrate the underlying layer and touch the base metal or the buffer layer. This probably leads to too much dilution in the top layers. Another aspect of multiple layer welding is the epitaxial growth of the grains. This is clearly visible in the macrographs in which columnar coarse grains run through the different beads (see appendix I). The grains grow perpendicular to the fusion line and meet at the top of the bead. The region where the final stages of the solidification take place can prove to be a "risk zone" where possible hot cracks may occur. In fact, one hot crack was found in one of the specimens with three cladded layers. It is an apparent solidification crack that runs between the dendrites and extends through two layers starting in the second layer and progressing upwards. These type of cracks are probably not the cause of the indications as the fissures found during the production process are smaller and not visible with the untrained eye while most hot cracks are clearly visible directly after welding.

**Welding parameters**

In table 3.1 the welding parameters and the bead dimensions of the single bead test are given. It appears that an increase in the travel speed (A $\rightarrow$ B) makes the bead less wide, and the penetration depth

Table 3.2 Welding parameters and interpass temperatures of BOP II

| Weld no. | T (before) °C | T (after) °C | I (A) | V (V) |
|---|---|---|---|---|
| Layer A (S59) | Travelspeed : 470 mm/min | | | |
| 1 | 23 | 43 | 174 | 28 |
| 2 | 42 | 53 | 177 | 28 |
| 3 | 34 | 58 | 168 | 28 |
| 4 | 40 | 60 | 171 | 28 |
| 5 | 43 | 65 | 165 | 28 |
| 6 | 37 | 67 | 166 | 28 |
| 7 | 46 | 63 | 170 | 28 |
| 8 | 41 | 56 | 170 | 28 |
| **Average** | **38** | **58** | **172** | **28** |
| Layer B (Inconel 625) | Travelspeed : 500 mm/min | | | |
| 9 | 32 | 68 | 275 | 28 |
| 10 | 43 | 70 | 274 | 28 |
| 11 | 46 | 64 | 269 | 28 |
| 12 | 46 | 79 | 266 | 28 |
| 13 | 51 | 69 | 267 | 28 |
| **Average** | **43** | **70** | **270** | **28** |
| Layer C (Inconel 625) | Travelspeed : 500 mm/min | | | |
| 14 | 31 | 74 | 286 | 28 |
| 15 | 45 | 90 | 293 | 28 |
| 16 | 42 | 71 | 288 | 28 |
| 17 | 40 | 70 | 284 | 28 |
| **Average** | **39** | **76** | **287** | **28** |
| Layer D (Inconel 625) | Travelspeed : 500 mm/min | | | |
| 18 | 38 | 83 | 276 | 28 |
| 19 | 37 | 80 | 280 | 28 |
| 20 | 37 | 93 | 281 | 28 |
| **Average** | **37** | **85** | **279** | **28** |

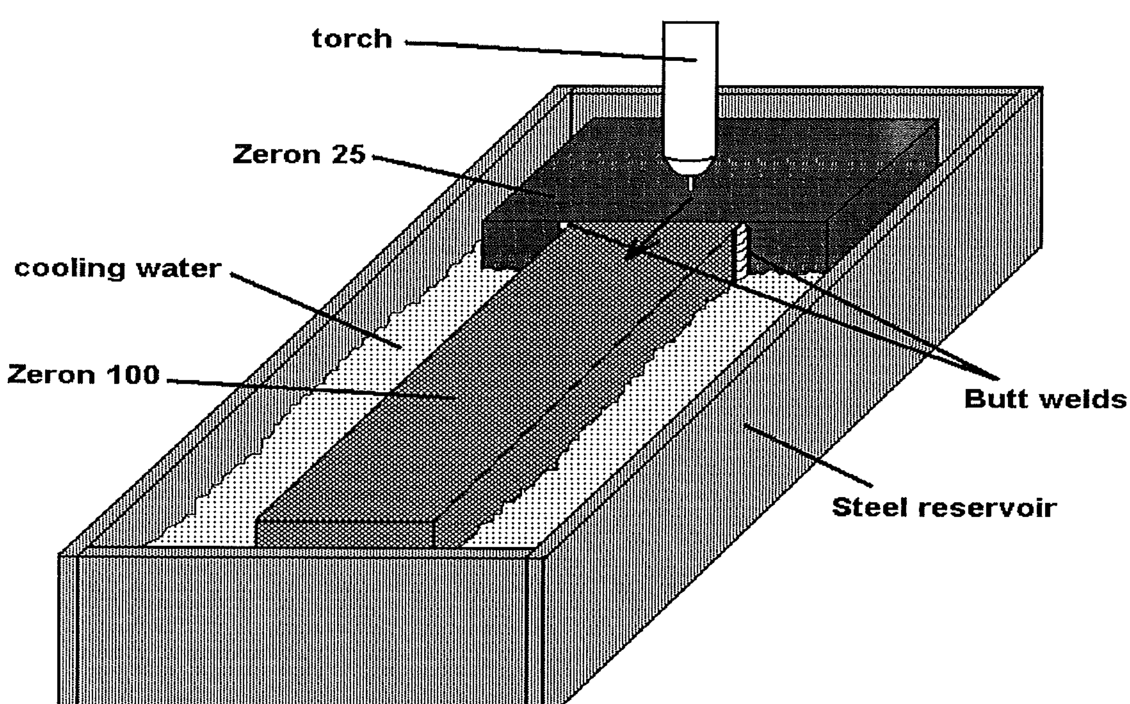


Figure 3.3 Experimental setup of BOP II

decreases which in this case is the aim. An increase in voltage (B $\rightarrow$ C) reduces the penetration and has apparently no significant influence on the bead width. The most idealized bead geometry (flat and wide) can be obtained by high travel speed and relatively high arc voltage.

**Comparison with earlier tests**

When the current (test)cladding is compared to the results of the original qualification tests, two important differences can be observed (see App. 1). Firstly, a clear difference appeared in the bead geometry. The fusion lines of the qualification tests are smoother and the top layers do not penetrate the lower layers. The different layers are clearly separated and the buffer layer hardly penetrates in the base metal.

Secondly, the macrostructure of the qualification tests tends to be less coarse than the BOP I specimens. Epitaxial grain growth is also observed but the grains are smaller. Moreover, the claddings fabricated shortly after the qualification test showed a small number of indications. The number of indications seemed to be influenced by the structure of the weld, in particular by the fineness of the grains. This might indicate different welding parameters. Another aspect could be a difference in plate thickness on which the claddings were welded. Unfortunately the original plate thickness could not be traced back.

## § 3.3 Bead-on-Plate Test II - *Cooled welding* -

Bead-on-Plate test II was carried out to determine the influence of the cooling rate on the structure of the weld metal. Smaller grains, found in the qualification specimens, can be obtained by higher cooling rates. It is rather difficult to control the cooling rate during submerged arc welding as the relatively thick slag layer thermally isolates the bead. In this test cooling of the weld was realized by welding on a test plate in a water basin to promote the interpass temperature to remain below 50°C (fig. 3.3). The water was additionally cooled by liquid nitrogen. Table 3.2 shows the various temperatures measured on the welds. The last column shows the time between the welds to indicate how long it took to cool the testpiece.

The cooled test plate consisted of two sections butt-welded together. One section of duplex steel (Zeron 25) and the other made of superduplex steel (Zeron 100). These two base metals are currently used in the swivel joints. Four layers were deposited: one buffer layer of S59 and three layers of Inconel 625. For the material compositions see table 2.1.

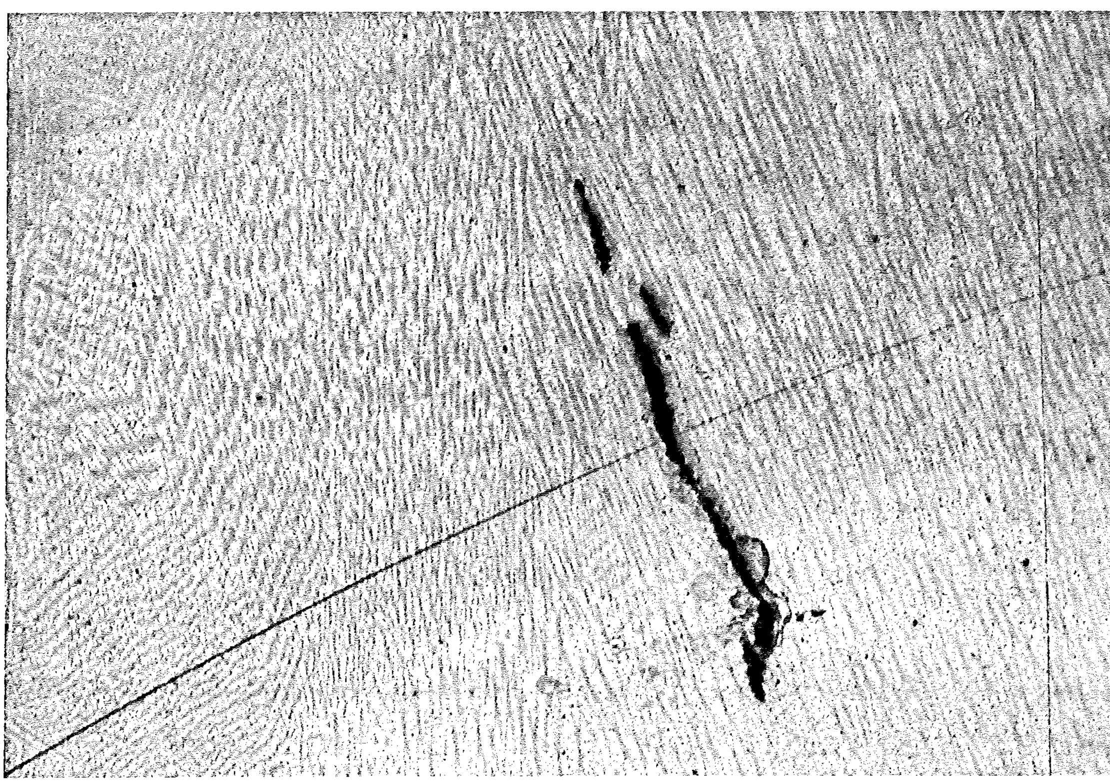

Figure 3.4 Photograph of hot-crack found in BOP II specimen perpendicular to the weld direction (60x).

**Macroscopic investigation**

Four cross-sectional macrospecimens were made of the cladding (2x on Zeron 100; 2x on Zeron 25). The specimens were photographed and compared to the results obtained in Bead-on-Plate I (See appendix I and II). The macrostructure of the specimens is finer than in BOP I. Columnar grain growth is also observed but the grains are smaller. Furthermore, the penetration and the bead geometry is comparable to BOP I. Yet another effect was observed. All cross-sections showed hot cracking in the second and/or third layer (layer B, C). All cracks were parallel to the weld direction and perpendicular to the base metal.

**Microscopic investigation**

Of every macro specimen a section was taken to be used for microscopic research. Those parts were taken which contained (hot)cracks. The cracks are interdendritic (see fig. 3.4) and run through the different layers. The crack surfaces are dendritic planes which seem to be torn apart. This indicates solidification cracking due to weld stresses.

## § 3.4 Bead-on-Plate test III - *Varying the parameters* -

The object of BOP III was to optimize the welding parameters and create an acceptable bead geometry. The previous test showed that by increasing the cooling rate the macrostructure was refined but hot cracks were introduced. Furthermore, no change in bead geometry was found indicating that only variation in the welding parameters could create an acceptable bead geometry.

This test consisted of eight single-bead welds, in which the parameters were varied considerably. At first no attention was paid to the level of the heat-input (HI) which is an important aspect of cladwelding (stainless) steels. A too large heat-input, which cannot be conducted by the base metal, can create unacceptable stresses and deformations in particular in stainless steels. The value of the heat-input is determined by the welding parameters and can be calculated as follows:

$$HI = \frac{\eta_p * I * U * 60}{v} \text{ [kJ/mm]} \qquad (3.1)$$

with v in mm/min.

In this formula $\eta_p$ represents the process efficiency which is >90% for SAW. Therefore $\eta_p$ can be set at a value of 1 in this case.

Table 3.3a Proposed welding parameters for BOP III

| | A | B | C | D | E | F | G | H |
|---|---|---|---|---|---|---|---|---|
| I (A) | 270 | 270 | 270 | 270 | 250 | 280 | 280 | 280 |
| V (V) | 25 | 29 | 33 | 33 | 29 | 37 | 37 | 37 |
| v (mm/min) | 500 | 500 | 500 | 575 | 500 | 440 | 500 | 560 |
| HI (kJ/mm) | 0.81 | 0.93 | 1.07 | 0.93 | 0.87 | 1.41 | 1.24 | 1.11 |

Table 3.3b Measured parameters for BOP III

| Result | A | B | C | D | E | F | G | H |
|---|---|---|---|---|---|---|---|---|
| I (A) | 279 | 283 | 286 | 291 | 266 | 298 | 296 | 290 |
| V (V) | 25 | 28 | 32 | 33 | 25 | 37 | 37 | 37 |
| v (mm/min) | 500 | 500 | 500 | 560 | 500 | 440 | 500 | 560 |
| HI (kJ/mm) | 0.84 | 0.96 | 1.13 | 1.03 | 0.80 | 1.50 | 1.31 | 1.14 |
| W (mm) | 12 | 14 | 15 | 14 | 11 | 17 | 16 | 14 |
| D (mm) | 6.1 | 5.2 | 4.9 | 5.3 | 5.9 | 5.8 | 5.9 | 5.1 |
| D/W | 0.51 | 0.37 | 0.34 | 0.37 | 0.51 | 0.34 | 0.37 | 0.36 |
| R (mm) | 2.8 | 2.5 | 2.1 | 2.3 | 2.6 | 2.4 | 2.3 | 2.1 |
| P (mm) | 3.3 | 2.7 | 2.8 | 3.0 | 3.3 | 3.4 | 3.6 | 3.0 |

HI = Heat Input

W = Bead Width

D = Bead Depth

R = Reinforcement

P = Penetration

After welding of the eight test beads, the best bead geometry and combination of parameters was to be selected. The "best" bead geometry for overlaying purposes is a flat and wide bead with not too much penetration. This is achieved, taking notice of the results of BOP I, with low current and relatively high arc voltage and travel speed. At this point, the heat-input was considered and a value <0.90 kJ/mm was taken to be ideal. Therefore the ideal combination of parameters was to be submitted to the above mentioned conditions: heat-input and bead geometry. With the selected set of parameters an additional bead was deposited, to find out whether the shape could be reproduced and had the intentioned shape. The combination of parameters as well as the bead dimensions are given in Table 3.3.

**Investigation of BOP III**

Of every weld bead a cross-sectional macrospecimen was made and all weld beads were then photographed (see appendix III). Comparison of the photographs led to the following observations:

- All beads have the finger print shaped penetration as described in § 3.2. When altering the parameters this zone varies in dimension.
- When the voltage is increased, keeping the other parameters at a constant value, the bead becomes wider and flatter (*A*,*B*,*C*).
- A high current, voltage and also increasing the travel speed compared to (*C*) gives an acceptable bead geometry (*D*) which has a slightly smaller bead width than *C*. The finger print is flat and not very pronounced.
- A low current and voltage and a medium travel speed result in a narrow bulb-shaped bead (*E*).
- Beads *F*, *G* and *H* are welded with rather high voltage and current varying the travel speed. Wide beads and high dilution are the result.

In fig. 3.6 the relation between the voltage and the dimensions is plotted (*A*,*B*,*C*) and fig. 3.7 shows the bead width as a function of the travel speed (*F*,*G*,*H*).

From the data acquired of BOP III and after a careful examination of the Qualification Report [3], a provisional set of parameters was obtained to be used in further tests. A low current to keep the heat-input at an acceptable value (< 0.90 kJ/mm). A rather high voltage to smoothen the fusion line and widen the bead. The voltage could not be too high as this would increase the heat-input to much. Finally a relatively high travel speed to reduce the penetration depth. Too large travel speed would create such a narrow bead that the deposition rate would be too low and more than three layers would be needed to

Table 3.4a Bead dimensions versus the arc voltage of beads A to B

| | A | B | C |
|---|---|---|---|
| Voltage (V) | 25.2 | 28.4 | 32.8 |
| Bead width (mm) | 12.0 | 14.1 | 14.6 |
| Bead depth (mm) | 6.1 | 5.2 | 4.9 |
| depth/width | 0.51 | 0.37 | 0.34 |
| Reinforcement (mm) | 2.8 | 2.5 | 2.1 |

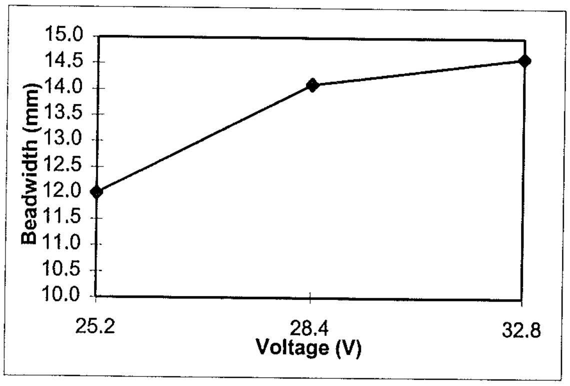


Figure 3.6a Bead width versus voltage of beads A to C of BOP III

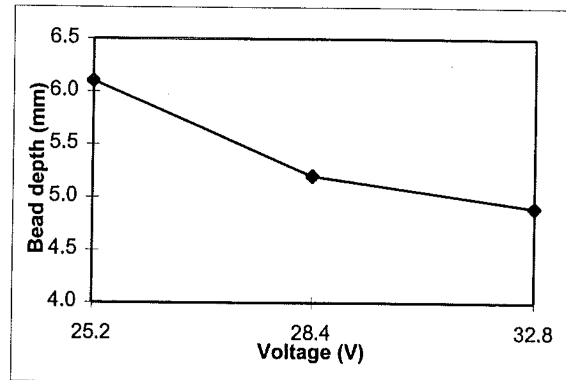


Figure 3.6b Bead depth versus voltage of beads A to C of BOP III

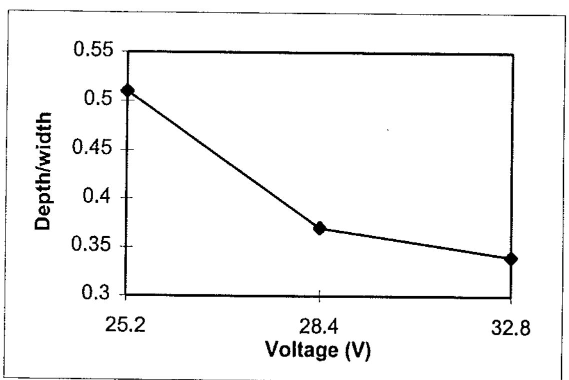


Figure 3.6c Depth-width ratio versus voltage of beads A to C of BOP III

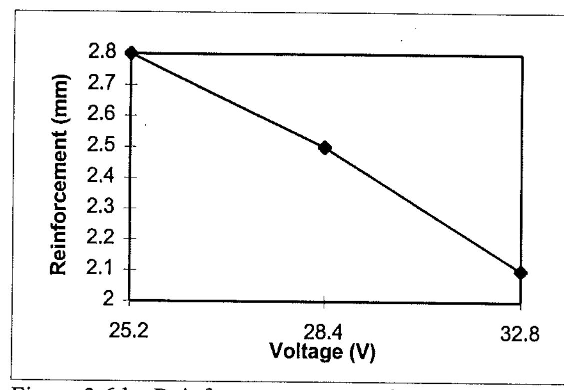


Figure 3.6d Reinforcement versus the voltage of beads A to C of BOP III

Table 3.4b Beadwidth versus the travelspeed of beads F to G

| | F | G | H |
|---|---|---|---|
| Travelspeed (mm/min) | 440 | 500 | 560 |
| Bead width (mm) | 16.9 | 15.8 | 14.1 |

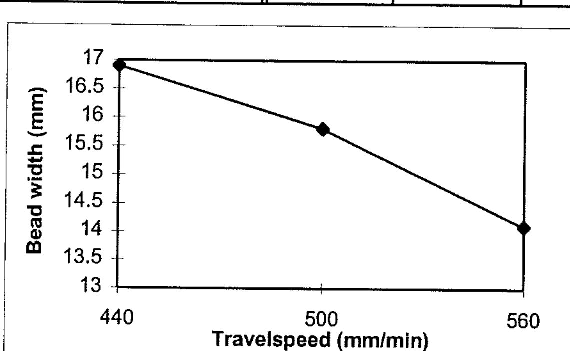


Figure 3.7 Bead width versus travelspeed of beads F to H of BOP III

ensure a sufficient layer thickness. Taking notice of all these aspects the following set of parameters was used for the additional test:

**I = 250 - 260 A; U = 28 V;** v = **500 mm/min** resulting in a **heat-input of 0.84 kJ/mm.**

Two remarks have to be made regarding this set of parameters:

1. A current **range** is given because the power source is set at CV (Constant Voltage). This means that the welding is done with a flat (horizontal) current-voltage plot. The system is therefore self-regulating. A small change in the voltage, for instance because of a change in the arc length, will create a rather large shift in the current to reinstall the original arc length. Many power sources have a U/I plot coefficient of about 1V/100A. Because of this, the current is never constant but alters within the specific range.
2. As mentioned before, the heat-input is an important parameter to characterise a process. The value of 0,90 kJ/mm is arbitrary and derived from the best set of parameters. It is known that a high heat-input, besides creating unacceptable stresses and deformations, has a negative influence on the cracking susceptibility of the weld metal.

This set of parameters was not used in any of the Bead-on-Plate tests so far. Photographs of macrospecimens are included in appendix III. The macros show the following characteristics :

- The general geometry is satisfactory and matches the intended shape, as described in the first part of this section, rather well. The fusion line is smooth and the finger is limited.
- The different beads show quite a variation in shape although the cross-sectional specimens were taken 10 to 15 mm apart. Especially the fusion line and the finger display a diversity in shape. This is probably due to current variations mentioned, which can hardly be avoided.

## § 3.5 Bead-on-Plate test IV - *Industrial simulation* -

The set of parameters determined in BOP III was then implemented in the production process and the results were promising at first. A dramatic decline in the number of indications was found. Unfortunately it was not a structural change in the behaviour as, after a certain period of time, some of the overlays even showed more indications than before the change in parameters. An explanation for this could not immediately be given. Hence an analysis of the whole production process had to be done including the machining of the cladding.

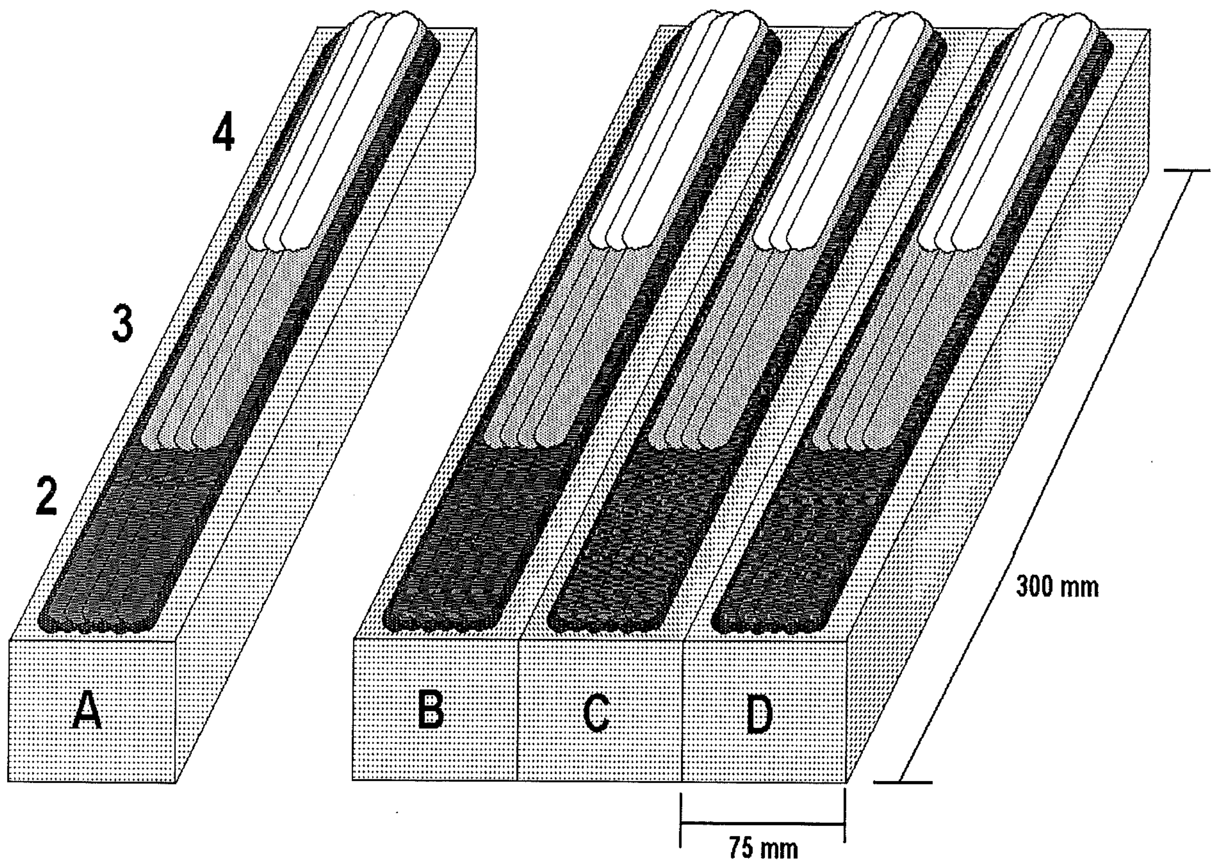


Figure 3.8 Welding sequence of BOP IV

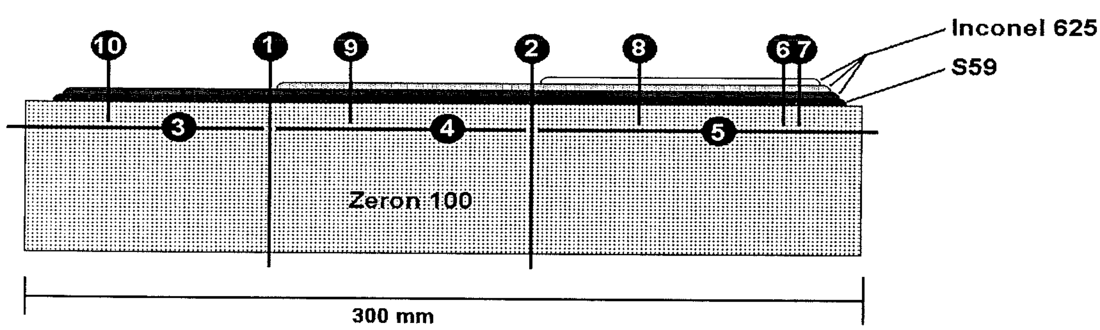


Figure 3.9 Cutting lines in test piece of BOP IV

In the literature survey conducted on this subject it was concluded that the solidification process of Inconel 625 and the constituents present in the solidified material are of major importance for producing a "perfect" cladding. In reference of this conclusion and the previous Bead-on-Plate tests the final welding test was performed in which the following questions had to be answered:

1. What is the influence of the welding parameters on the susceptibility to fissuring of the weld.
2. What is the influence of the niobium content in the filler metal on the number of indications?
3. What is the role of the solidification constituents like Laves-phase $(Ni,Cr)_2(Nb,Mo)$ on the occurrence of the indications?
4. Does the machining depth have any influence on the number of indications?

**Welding**

A Zeron 100 testpiece (300x350x85mm) with four different claddings was manufactured and examined (fig. 3.8). The claddings were welded stepwise having two, three and four layers. This experiment was carried out to do a bulk analysis of the machined surface and determine whether the composition the pure material Inconel 625, specified by the client, could be met for the different numbers of layers. This was eventually cancelled because the indication problem had the priority.

Cladding A was welded using the former parameters (280 A; 28 V; 400 mm/min) (see app. IV). A buffer layer of S59 (metal cored wire; ∅2.0 mm) and three layers of Inconel 625 (massive wire; ∅1.6 mm) were deposited. Total width of the cladding was set to be approximately 60 - 70 mm.

Cladding B was welded using the current (BOP III) parameters (250 A; 28 V; 500 mm/min) (see app. IV). Further features are equal to cladding A.

Cladding C consisted of four layers of Inconel 625 with reduced niobium content (0.6 wt% in stead of ±3.5 wt%). The as-welded chemical composition of this flux cored wire is given in table 3.1. The cladding was welded using the current parameters and no buffer layer was applied.

Cladding D consisted of four layers of HASTELLOY C4 (table 3.1), a nickel-base alloy comparable to S59 but more often used. This alloy does not contain any Nb and is known to produce no dangerous solidification constituents [8].

**Specimens**

Specimens were made for macro- and microscopic examination, machining tests and chemical analysis. Firstly the claddings were separated (fig. 3.8) by using high-pressure waterjet cutting. Further cutting

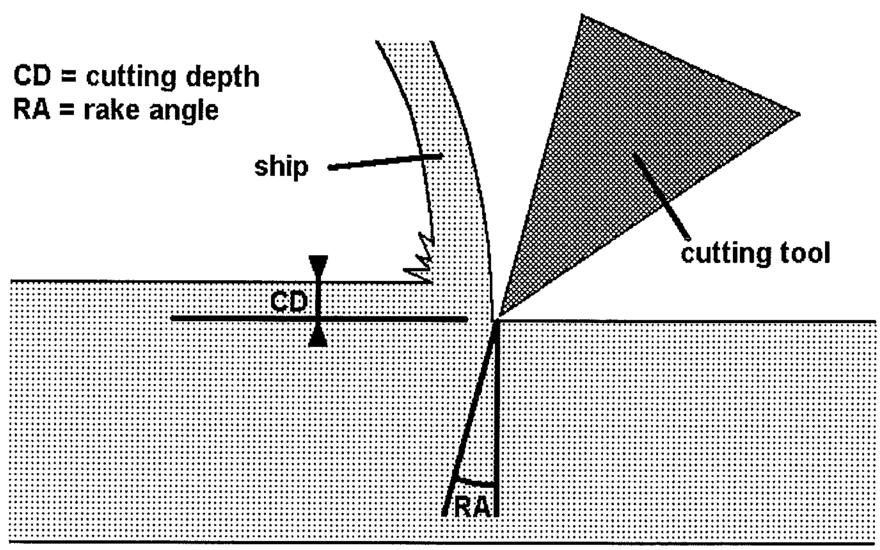


Figure 3.10 Relevant machining parameters

lines are illustrated in figure 3.9. The resulting bread-shaped pieces were cut **(1,2)** in three sections containing two, three or four layers of cladding, labelled A2, A3, A4, B2 etc. The larger part of the base metal was removed **(3,4,5)** by sawing to a specimen thickness of approx. 3 cm including cladding. Then the nine specimens were cut **(8,9,10)** in such manner that square parts were obtained which were easy to fixate in the four clamp lathe to be machined. Of the remaining parts, cross-sections were made **(6,7)** of all claddings with four layers (A4..D4) for etching and microscopic investigation.

## § 3.5.1 Machining of cladding

When metal is machined, several parameters are important to obtain a well machined surface. For the machining of this nickel-alloy cladding, a hard and sharp cutting tool is needed (see § 2.1.4) with a positive rake angle (fig. 3.10). In this case only a tool with an angle of 0° was available. How much material is taken off each rotation during turning depends on the feed rate and cutting depth. These two parameters have to be rather small to reduce tool wear. Furthermore the cutting speed has to be rather high especially when the cutting depth is small to prevent tearing of the material and smearing of metal ships.

Since the specimens are machined by turning and the lathe axis is in the middle of the square piece two other aspects have to be considered. First, the cutting speed is not constant because the tool starts cutting outward at the largest radius and travels inward at a constant rate to the axis of the lathe. Thus the speed decreases at a constant rate. Another aspect is the fact that a square surface is turned. This means that when machining starts, only the most distant parts, the corners, of the square surface are machined. In other words, not a full circle is cut but just sections of it. This deteriorates the quality, i.e. the sharpness, of the tool tip dramatically. According to the literature a minimum cutting speed is required of 50 m/min [1]. For these tests the cutting parameters were set in this way that the speed of cutting was 50 m/min when a full circle is described by the tool.

All claddings (A2..D4) were first machined until the surface was flat, ergo, the separate beads were no longer visible. This required about 0.5 to 1 mm of machining in depth.

When dye penetrant tested, **no** indications were found except for two indications in specimen A3. This specific specimen was the first cladding which was machined and as a trial more than 3 mm was taken off.

The fact that there were found no indications in the other specimens was a positive result, but as the indications found in A3 proved to be fissures and in line with the welding direction it was concluded

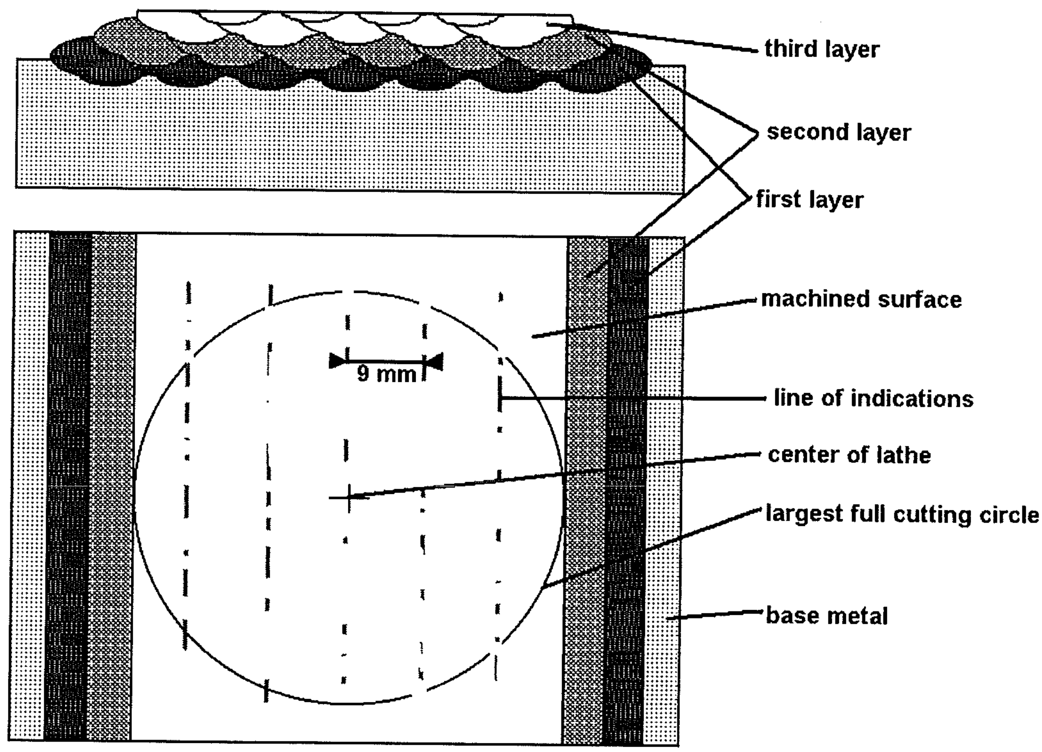


Figure 3.11 Indication pattern in the machined BOP IV specimens

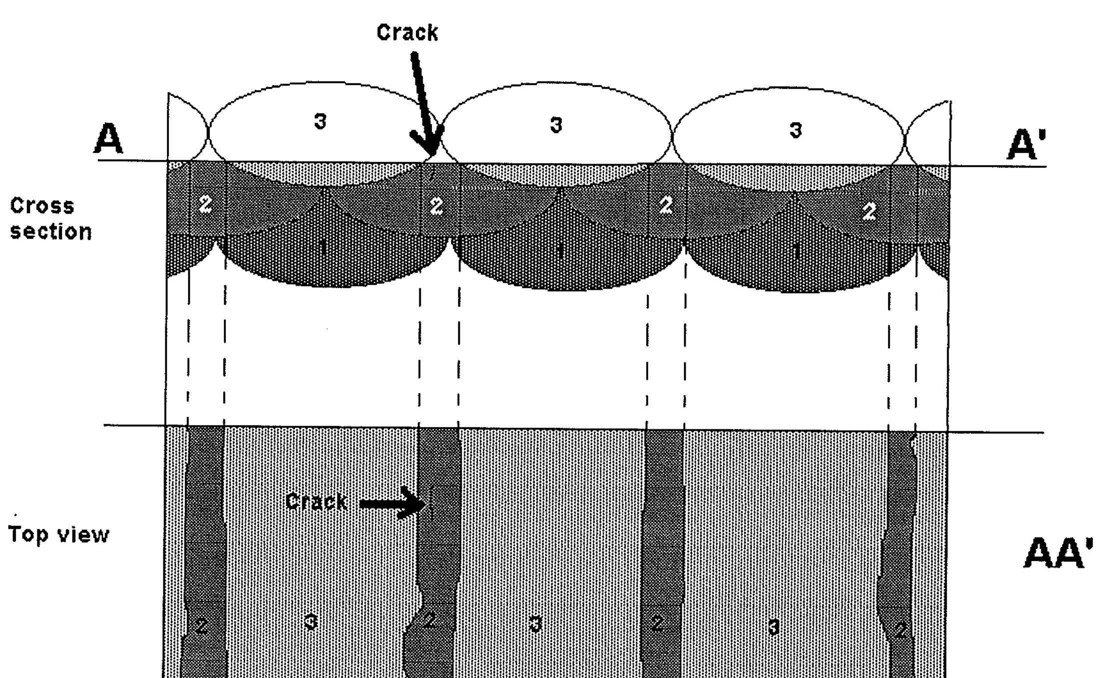


Figure 3.12 Position of cracks in the weld beads

that the indications had something to do with the machining depth. In order to confirm this, specimens A4 and B4 were further machined in steps of 0.5 mm and PT tested after each machining sequence. For the first few steps no indications were found, but when about 4.0 to 4.5 mm (in total) was taken off from the original cladding thickness multiple indications started to appear. These were found in a linear pattern and the "indication lines" had a typical spacing of 9 mm (A4) and 7 mm (B4) (see fig. 3.11). Specimens C4 and D4 were also machined deeper. C4 showed two indications when machined only 1 mm in depth and D4 showed no indications even when machined several millimetres in depth.

## § 3.5.2 Microscopic investigation

In the etched cross-sections several features could be seen (app. IV). The mean difference in total cladding thickness of A4 and B4 was roughly 1 mm (total thickness 10 -11 mm). The separate beads of the *A* specimens were larger but also showed more penetration depth and a less smooth fusion line. The individual layers of *B* were more separated than in *A*. In all, the beads and layers of *B* had a more constant shape than *A*.

Interesting features of the *C* specimen were remarkable flat beads and a smooth fusion line. This resulted in a cladding thickness of only 7 to 8 mm containing four layers. The fact that the cladding is relatively thin compared to the *A* and *B* specimens is probably due to the welding with metal cored wire. On average these wires produce thinner beads and low dilution.

The cross-section of *D* showed a cladding thickness of 10 to 11 mm, relatively flat beads and well-separated layers. The fusion lines were smooth but the beads sometimes had a little irregular shape compared to the beads in specimen *B*.

The indication pattern in the machined surface was compared with the etched cross-sections. It appeared that a spacing of 9 mm (A4) and 7 mm (B4) was exactly equal to the overlap of the beads in the top layer. The cladding was machined to such an extent that the tops of the second layer beads were "touched" (see fig. 3.12). The fissures thus typically arose in the second layer. There seems to be no relation between the occurrence of indications and the distance to the centre of the specimen, implicating that the machining speed has no influence on the fissuring in the weld metal (see fig. 3.11). However, when the speed is too low or the tool becomes less sharp, the tearing and smearing of pieces of metal increases. Furthermore, this phenomenon did specifically appear at the edges of the square surface when no full cutting circle was described. Sometimes this also resulted in indications.

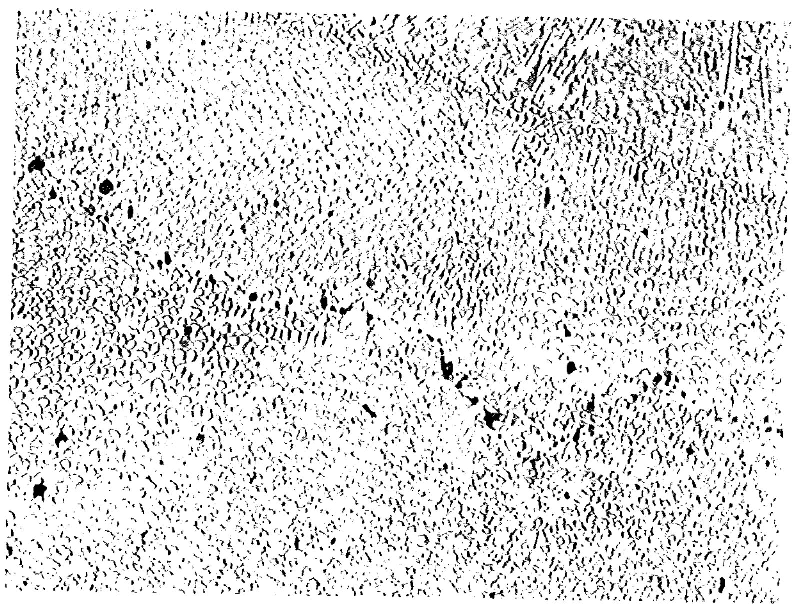

Figure 3.13 Fissure in etched surface (85x)

The marked indications were cut out to prepare for polishing and etching. These specimens were ground up to P 600 and then polished with diamond paste of 3 or 1 μm. After grinding and polishing the fissures are not visible any more under the microscope.

The specimens were then etched in a solution of 20 ml $H_2O$, 20 ml $HNO_3$, 20 ml HCl and 10 ml $H_2O_2$ (all components highly concentrated). After approximately 30 second of etching the microstructure and also the fissures (again) become visible. The following observations need mentioning (see fig. 3.12; 3.13):

The fissures

- occur between the bead penetrations of the top layer in the second layer;
- are positioned near the fusion line parallel to the welding direction;
- are interdendritic;
- seem to follow a pattern of interdendritic constituents.

The first remark can directly be deduced from the cross-sections and the known machining depth mentioned before. The second remark implies the influence of the top layer on the fissuring of the second one.

The last two remarks are closely related and point to a solidification problem. Alloys like Inconel 625 with multiple alloying elements, have a solidification temperature range depending on the composition. From the literature survey [5] it was concluded that in the final stages of the solidification process interdendritic compounds can be formed as a result of microsegregation. An example of such a solidification constituent is Laves-phase $(Ni,Cr)_2(Nb,Mo)$. Due to these components such alloys are prone to hot cracking. For one crack, distinctively longer than the others (>1.5 mm), a cross section was made (see App.IV). The indication found in the machined surface proved to be the top of a hot crack running 0.25 mm under the surface. The crack was 0.7 mm in width, visible with untrained eye and extending exactly perpendicular to the surface. Such cracks are probably not the main cause for the indication problem since most fissures are not visible with the untrained eye even when the surface is machined at a greater depth.

The two indications found in specimen **C4** (low Nb) also proved to be caused by fissuring (See appendix IV). However, these cracks had different features compared to the ones in the A and B specimens:

Both cracks were not closed but slightly open indicating it could be hot cracks. One of the cracks runs clearly between two grains which were not connected to well probably during the final stages of the

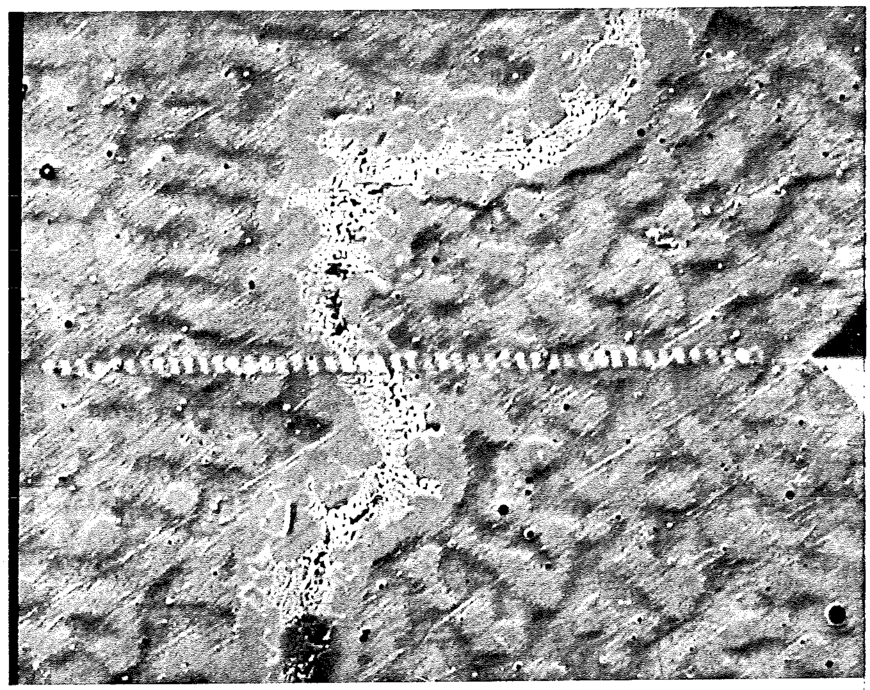

Figure 3.14 Line of scanning points across fissure (1000x)

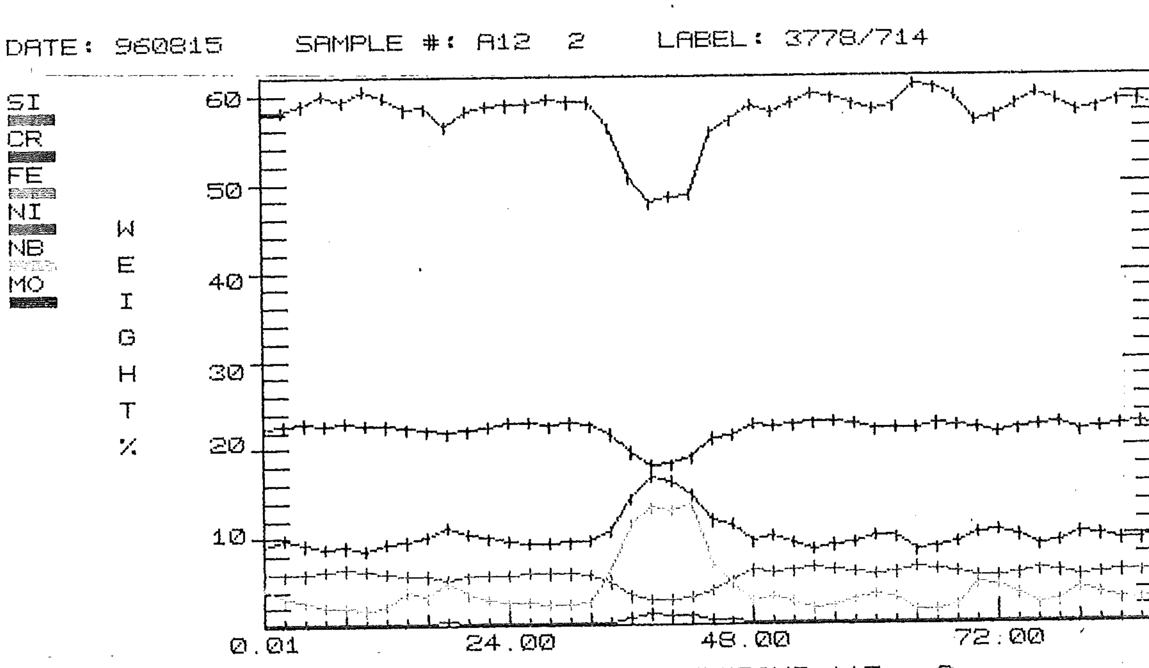


Figure 3.15 Composition scan of the fissure in fig. 3.14

solidification. The other crack runs perpendicular to the fusion line not between two grains. Further research on these (hot)cracks has not been done.

No indications have been found so far in the **D4** specimen so no microscopic investigation was done on this specimen.

### § 3.5.3 Chemical analysis of defects

At large magnifications (>600 X) the interdendritic phases show a dendritic or lamellar structure. Furthermore a region with a certain width besides the fissures is visible which seems to be differently affected by the etching agent. A chemical analysis of this region and the interdendritic compound should reveal more insight in the compositional effects around the defects.

The defects have been analyzed using EPMA (Electron Probe Micro Analysis). With this method the local composition of an area (spot) of 2 μm in diameter can be analyzed using a voltage of about 12 KeV. The elements scanned for are: Ni, Cr, Fe, Nb, Mo and Si. In the specified composition of Inconel 625 these elements add up to about 97 to 99 wt%. When scanning for these elements the local changes in the composition can therefore be determined.

In this case a line-scan has been done, built up of 35 - 64 spots of 2 μm in a row. The line scan was perpendicular to the defect and across the interdendritic phase (see fig. 3.14). Four scans have been drawn on two separate fissures both of the A4 specimen. The scanned areas are photographed using SEM (Scanning Electron Microscopy) and BEI-H (Backscattering Electron Ionoscopy with $H^+$-ions) with magnifications of 720 to 4000. As an example scan 2 is displayed in figure 3.15. The data of the other scans are attached to Appendix IV.

In figure 3.14 it can be seen that when the scanning-line crosses the defect and the interdendritic compound quite a dramatic change in composition occurs. Most significant are a depletion of Ni and an increase in the Nb content. Less pronounced are a raise in the Mo and Si contents and a fall in Cr and Fe. The exact composition of every single spot is given in Appendix IV.

The composition graphs show various peaks. The compositions of the minima or maxima of these peaks are averaged and given in table 3.5. This table also gives the composition of the earlier mentioned Laves phase $(Ni,Cr)_2(Nb,Mo)$ for comparison. These data are found by Cieslak et al. in TIG-welding tests with Inconel 625 [9]. In that research the influence of the carbon, silicon and niobium content on the solidification behaviour are investigated. The averaged compositions of literature- and experimentally found constituents in Table 3.5 are graphically displayed in figures 3.16 and 3.17. In these comparison

Table 3.5 Compositions of detected interdendritic phases in scan 1+2

| | Ni | Cr | Nb | Mo | Fe | Si |
|---|---|---|---|---|---|---|
| Literature | 48.2 | 15.5 | 17.2 | 16.7 | 1.3 | 1.0 |
| Scan 1 | 43.2 | 17.4 | 18.4 | 16.6 | 3.1 | 1.4 |
| Scan 2 | 48.3 | 18.4 | 13.3 | 15.8 | 3.0 | 1.1 |

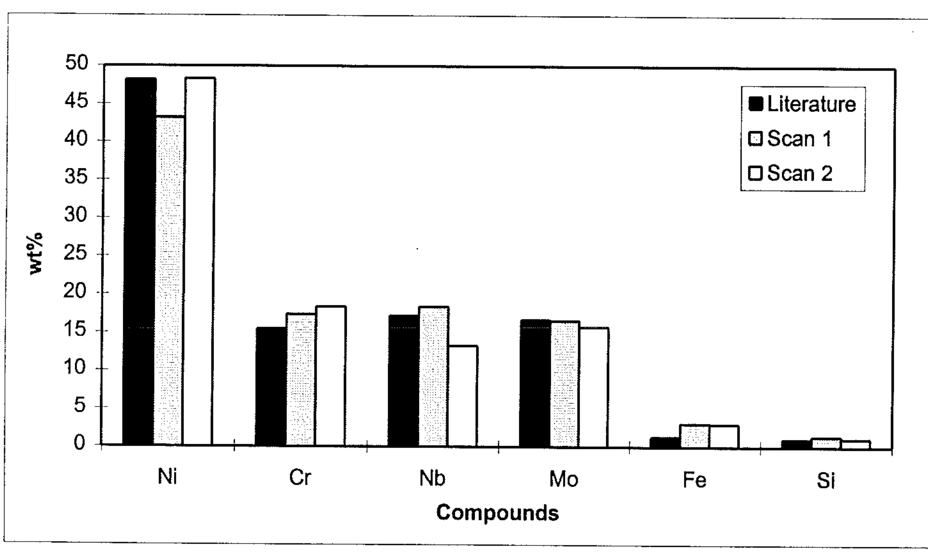


Figure 3.16 Comparison graph Laves-phase and detected phases in scan 1+2

graphs the experimentally found constituents can be identified.

The chemical formula for the Laves-phase is not stoichiometric as it is structurally not of the $A_2B$ type and no $Ni_2Nb$ has been found so far. When analysing the solidification constituents it can be stated that the Laves phase is found if the (Ni + Cr) content is twice the (Nb + Mo) content. Other, less recurrent phases are dendritic and blocky NbC and lamellar $M_6C$ which is rich in Nb, Mo and Si [9]. Only Laves and $M_6C$ have been found in the specimens. About scan 1 till 4 the following interesting features have to be mentioned:

Scan 1
- The composition graph displays three peaks. The fact that not one but three peaks are visible in the graph is probably due to porosity (see SEM 4000x of scan 1 in App. IV).
- If the peaks were considered as one large peak, the composition of this peak corresponds well with the literature value (fig. 3.16) indicating Laves-phase is present [9].
- Most elements show oscillations in the content over the entire scanned range. Comparing the scan to the SEM photograph shows that various dendrites and interdendritic regions are crossed by the scanning beam. The Ni and Cr lines show the same peaks and both are depleted in the interdendritic regions and enriched in the dendrite cores. Mo and Nb show the same behaviour but reversed. As Ni and Cr are enriched in the dendrite cores Mo and Nb are enriched in the interdendritic regions. The variation in the chromium content will be explained later by means of ternary Cr-Ni-Mo phase diagrams.

Scan 2
- Only one peak is visible in the graph. The photograph shows that in this case the constituent is much more homogeneous and there are apparently no porosities.
- "Finger print" comparison with Laves-phase composition in [9] displays a good match except for the Nb content which is a little low in this specimen (fig. 3.16)
- Again the oscillating behaviour in the different element concentrations is visible. Particularly, the oscillations are visible in the Ni, Mo and Nb concentrations, the Cr content again remains fairly constant.

Scan 3
- In this scan no pronounced peaks are visible. Only the oscillating behaviour is apparent.
- On the SEM photograph a distinctively affected zone (DAZ) is visible indicating a deviant composition. In the composition graph this is not clearly visible.

| | Ni | Cr | Nb | Mo | Fe | Si |
|---|---|---|---|---|---|---|
| Laves (lit.) | 48.2 | 15.5 | 17.2 | 16.7 | 1.3 | 1.0 |
| Scan 4 | 34.5 | 14.5 | 34.1 | 12.8 | 3.3 | 1.0 |

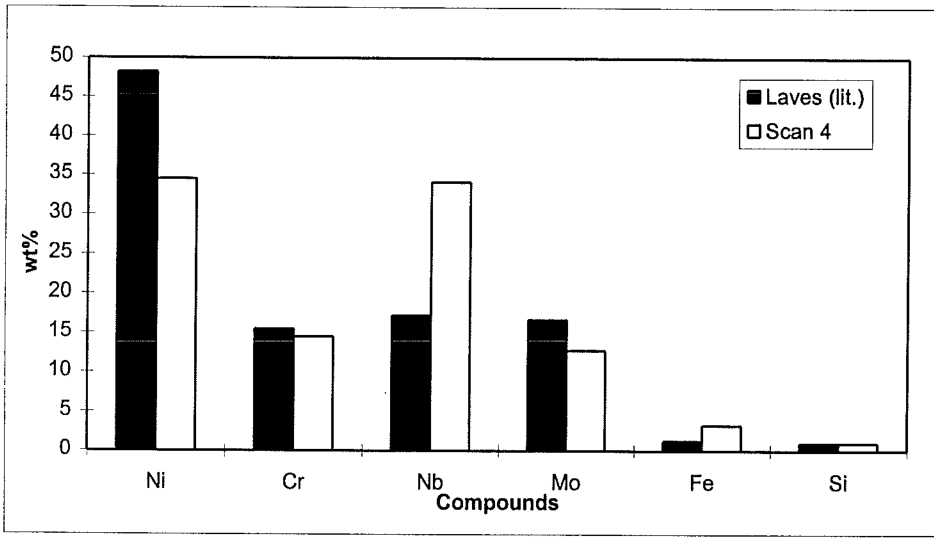


Figure 3.17a Comparison graph Laves-phase [8] and detected phase in scan 4

| | Ni | Cr | Nb | Mo | Fe | Si |
|---|---|---|---|---|---|---|
| $M_6C$ | 31.6 | 14.6 | 31.0 | 18.7 | 0.5 | 0.9 |
| Scan 4 | 34.5 | 14.5 | 34.1 | 12.8 | 3.3 | 1.0 |

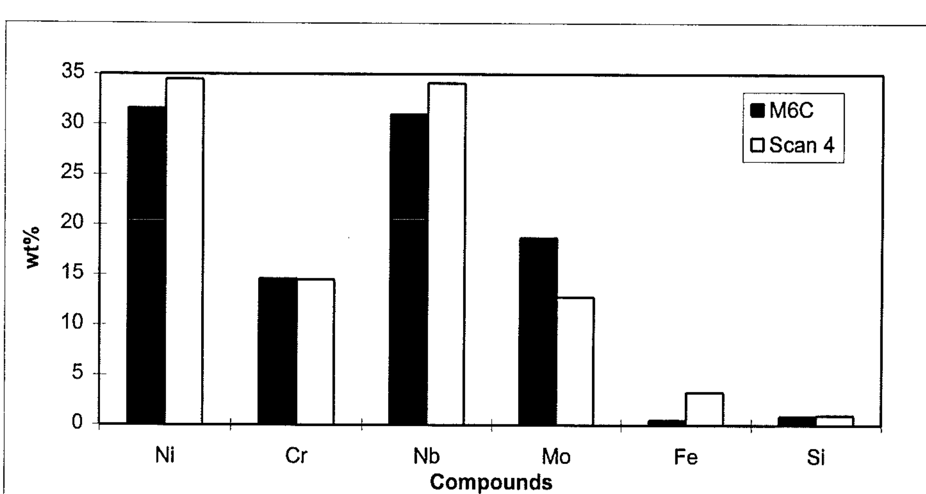


Figure 3.17b Comparison graph $M_6C$ [8] and detected phase in scan 4

Scan 4 - As in the previous scan the DAZ is analyzed but now a single peak is visible. On the SEM photographs a small constituent (∅ 2-3 μm) can be seen which is exactly crossed by the analysing line resulting in the peak.

- The composition of this compound does not match the Laves-phase (fig. 3.17a) but the $M_6C$ compound, also found by Cieslak in Si-rich Inconel 625. The match is not as close as the previous Laves-phase matches but except for the molybdenum content (Δwt% 6), quite good (fig. 3.17b).
- This scan also displays the oscillating behaviour and the DAZ is more distinct than in scan 3. The zone is clearly visible in the SEM photograph and has a width of approximately 40 μm. In the corresponding section of the composition graph the Nb content increases 2 to 3 wt% and the Ni content drops 5 wt%.

Finally it has to be mentioned that in the finger print graphs the iron content tends to be rather high compared to literature values. This is caused by a relatively high iron content in the electrode wire and possible dilution from the duplex stainless steel base metal. However, this supposedly will not have any effect on the number of indications as was stated in the research by Cieslak [9].

## § 3.6 Test rings

It could be stated that the indication problem is caused by fissuring of the cladding during machining. Heterogeneous solidification constituents play an important role in this. In order to implement the so far obtained results in the production process two test rings were fabricated comparable with the current products.

Test ring 1 was welded with the submerged arc process at IHC, using the currently used parameters (see § 3.4), and carefully monitored during welding. It was then stepwise machined to determine the "critical" depth.

Test ring 2 was welded using another process, Hot-wire GTAW, at Forth Tool & Valve Ltd. in Scotland. This company, specialized in cladding and machining offshore products, claimed not to have any PT-indications in their machined Inconel 625 claddings. On this ring a three layer overlay of Inconel 625 was deposited and with this new process and next machined at IHC in the same way as ring 1, to determine whether there was a critical depth in this overlay as well.

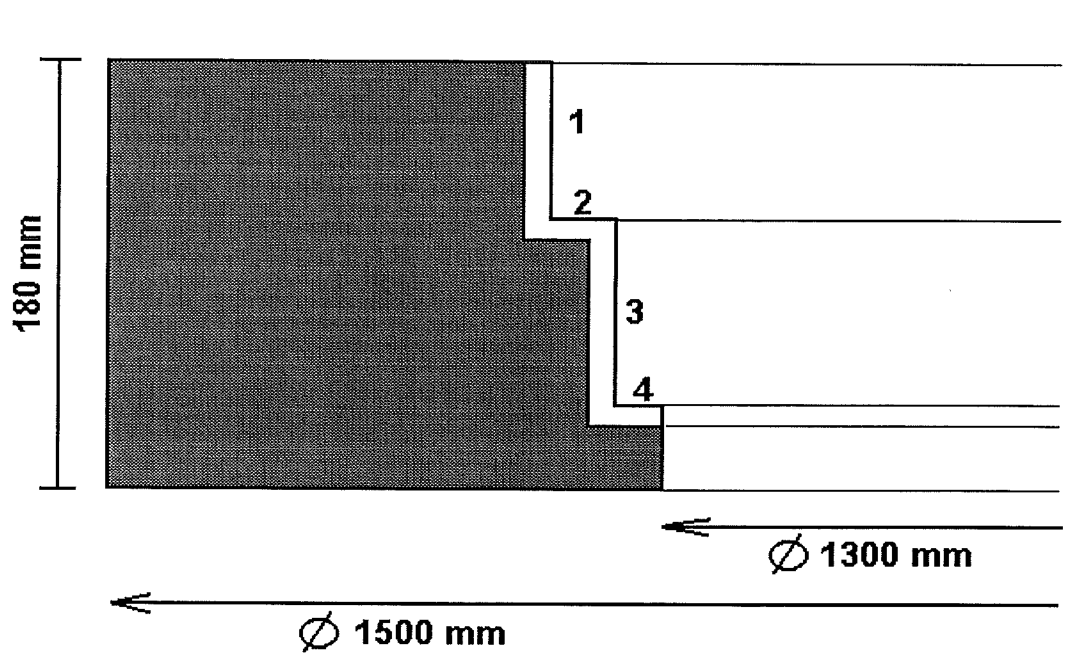


Figure 3.18 Cross-section of test ring

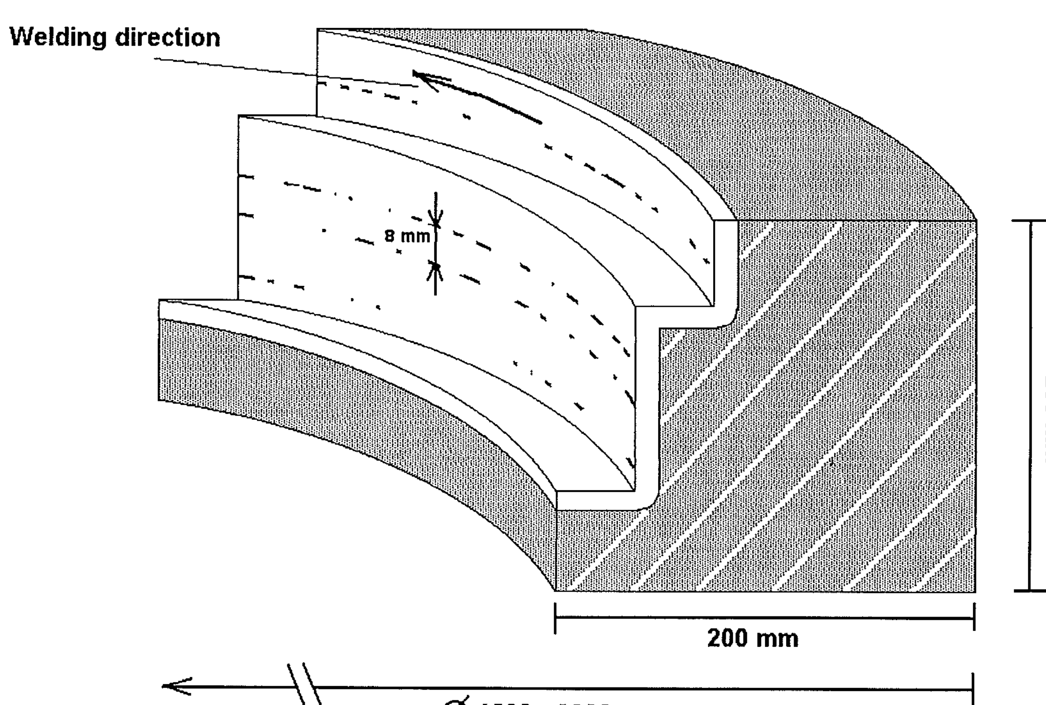


Figure 3.19 Linear pattern of PT-indications in a seal surface

**Test ring 1 :** ***Changed production process***

For this test a carbon-steel ring (St 52) was used with roughly the same dimensions and design as a swivel seal ring (see fig. 3.18). A Carbon staal ring was used as no Zeron 100 or 50 rings were available. Furthermore, when the basemetal was thick anough the influence of the basemetal was ruled out. It was internally cladded on two vertical (1, 3) and two horizontal (2, 4) surfaces. Three layers (85 beads) of Inconel 625 were deposited not using a buffer layer of S59. The complete process was controlled with a parameter-monitoring-system recording the welding parameters: current, voltage and wire speed.

After welding, the cladding thickness of the vertical surfaces was 7 ± 0.5 mm. Surface **2** had 11 ± 1 mm and surface **4** had 8 ± 1 mm of Inconel 625 cladding. The error in the horizontal cladding thickness is larger because surfaces **2** and **4** are only 16.5 mm in width being quite difficult to weld. On these surfaces and in the corner between the horizontal and vertical surfaces one cannot speak of three layers but just of a certain thickness.

After welding, the ring was machined according to a certain machining schedule divided in three sections (App. V).

<u>Section 1</u>: Machine the cladding just up to a clean surface. About 0.5 to 1 mm was machined off.

<u>Section 2</u>: Machining all surfaces with increasing cutting depths to see whether this had any influence on the PT result. Firstly, surfaces 1 to 4 were machined with a cutting depth of 0.05 to 0.35 mm (surface 1 with a cutting depth of 0.05 mm; 2 with 0.15 mm etc.). Then, all four surfaces were machined with cutting depths of 0.1 to 0.4 mm (surface 1 with a cutting depth of 0.4 mm; 2 with 0.3 mm etc.). In this way, all surfaces were machined 0.45 mm in depth. After this section, approximately 1 to 1.5 mm was machined of the original cladding thickness.

<u>Section 3</u>: To reach the presumed critical depth under the original welded surface, 2.0 mm was machined off further. Successive machining steps of 0.5 mm in cutting depth should reveal the critical depth in the cladding. This depth was found after one step of 0.5 mm. This meant that in total 3.5 to 4.0 mm was machined off. Section 3 was only performed on the vertical surfaces because of the larger dimensions a more accurate estimate of the critical depth could be made.

The results of this machining test are given in Appendix V including the number of indications. A dramatic increase in the number of indications of less than 10 to more than 70 gives a conclusive estimate of the critical depth of 4 mm. The indications had the same features as in the actual production

rings: line shaped in the welding direction at certain distance from each other (fig. 3.19). They had a linear character indicating it were fissures as well.

**Test ring 2 :** ***Cladding with Hot-wire GTAW***

A test ring with roughly the same design and dimensions as ring 1 was overlaid using the hot-wire GTAW process. The general characteristics of this process are:

- A 100% Ar shielded semi-automated welding process using a tungsten electrode and externally fed 1.6 mm massive Inconel 625 wire;
- The filler metal wire is heated to ± 700°C with an secondary current of 60 - 80 A before melting in the arc;
- It is a pulsed welding process using a programmed pulse time, peak- and base current; $I_b = 145A \pm 10A$; $I_p = 280A \pm 10A$; $t_{pulse} = 0.5$ sec.; $U = 13 - 15$ V; $v = 255$ mm/min.
- Arc length is voltage-controlled and deviations are adjusted through an X-Y slide on which the welding head is mounted;
- 1G and 3G positioned welding is possible.
- Measured dilution < 10%.

Forth Tool & Valve Ltd. has a vast experience in welding and machining Inconel 625 for off-shore purposes. On this ring three layers of Inconel 625 were deposited resulting in a cladding thickness varying from 6.0 to 9.2 mm depending on the surface (see Appendix V). The variation in thickness is caused by the fact that all surfaces, vertical and horizontal, were welded with the torch in the same (1G) position. Depositing the beads in an ascending, or vertical, mode the cladding thickness is larger than when welding horizontally. The unfinished surface looked good having a very regular solidification pattern. Since it is a pulsating process the weld beads depict solidification lines in a periodic mode in which the line spacing is determined by the pulse frequency and travel speed.

To see whether there is a critical machining depth resulting in PT-indications this ring was machined with a similar sequence as test ring 1. After machining sections 1 and 2 no indications were found. Machining section 3 was performed in eight steps of 0.5 mm cutting depth and only in one step a single indication was found. When this particular surface was machined again the indication disappeared.

The results of this test were very promising and proved that a perfect cladding of Inconel 625 in fact can be produced.

# 4. Discussion

In this chapter the results of the experiments will be discussed and evaluated resulting in some suggestions to improve the final quality of the welded overlay. Firstly the bead-on-plate tests will be discussed and secondly the test rings. In the discussion the conclusions of the literature survey on the solidification properties of Inconel 625 are regarded as well [5].

## § 4.1 Bead-on-Plate tests

The four bead-on-plate tests were done each with use of the previously gained knowledge. In this section the results are discussed of the BOP tests aiming to find the actual cause of the fissuring in the cladding. First the welding is evaluated, then the machining and finally the chemical analysis of the compounds found in the weld metal.

### § 4.1.1 Welding

BOP I and III showed that the applied parameters of the submerged arc welding of Inconel 625 have great influence on the bead geometry and should therefore be well monitored. Best results were obtained at medium current, relatively high arc voltage and high travel speed. For high current values penetration is too large. Low travel speed gives a pronounced "finger". For that reason the travelspeed should be relatively high. However, the voltage should not be too low, to ensure a relatively wide and flat bead. A bead geometry with an aspect ratio (width/depth) of 2,5 to 2,7 is considered optimal.
With these parameters the heat-input is limited, which is also beneficial for the weld bead structure. The solidification rate increases and consequently the columnar grain growth is reduced and the microstructure refined. This last aspect may also be achieved by extra cooling of the weld which was done in BOP II. This proved to be rather inpractable for production cladding and furthermore resulting in multiple hot cracks. However, the structure was refined and the columnar grain growth reduced.
BOP IV confirmed that the "new" well controlled parameters resulted in more reproducible bead geometry and layer thickness. Moreover, overlaying with alloys which are low or free of niobium proved to be an alternative. The literature survey on this subject revealed that this element has a large influence on the solidification behaviour of Inconel 625 and therefore the hot crack susceptibility of the

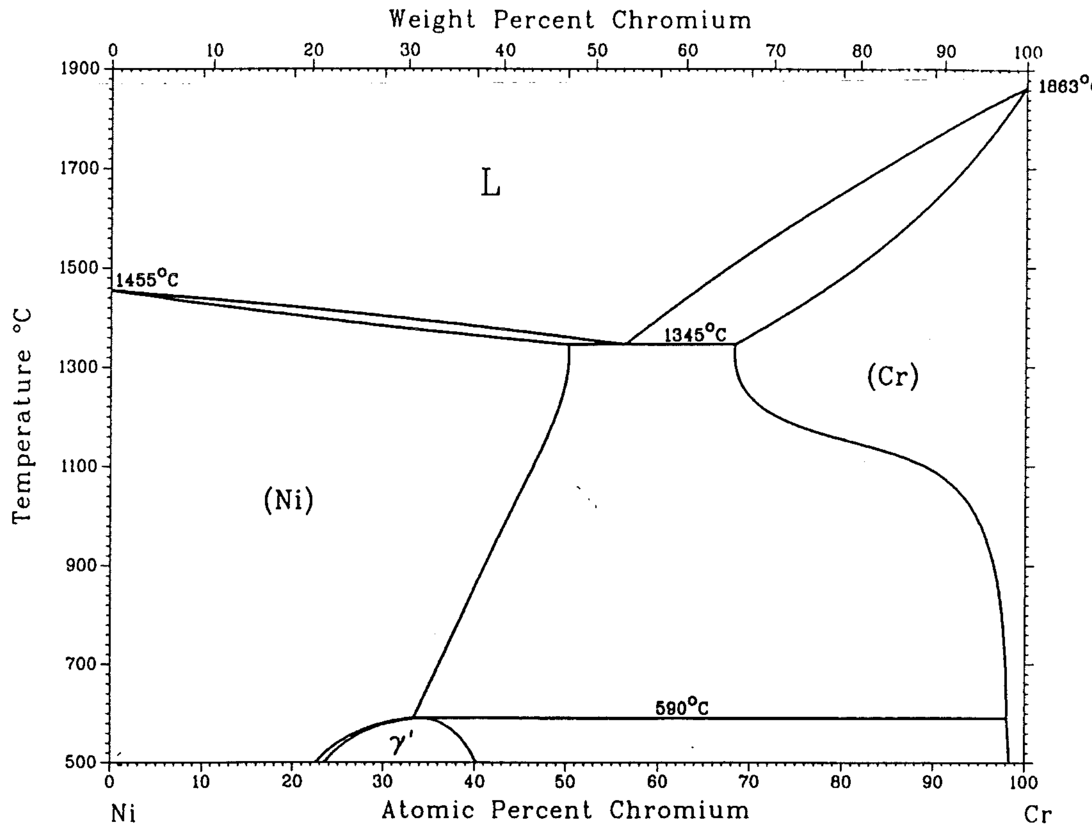


Figure 4.1a Binary phase diagram of nickel and chromium [11].

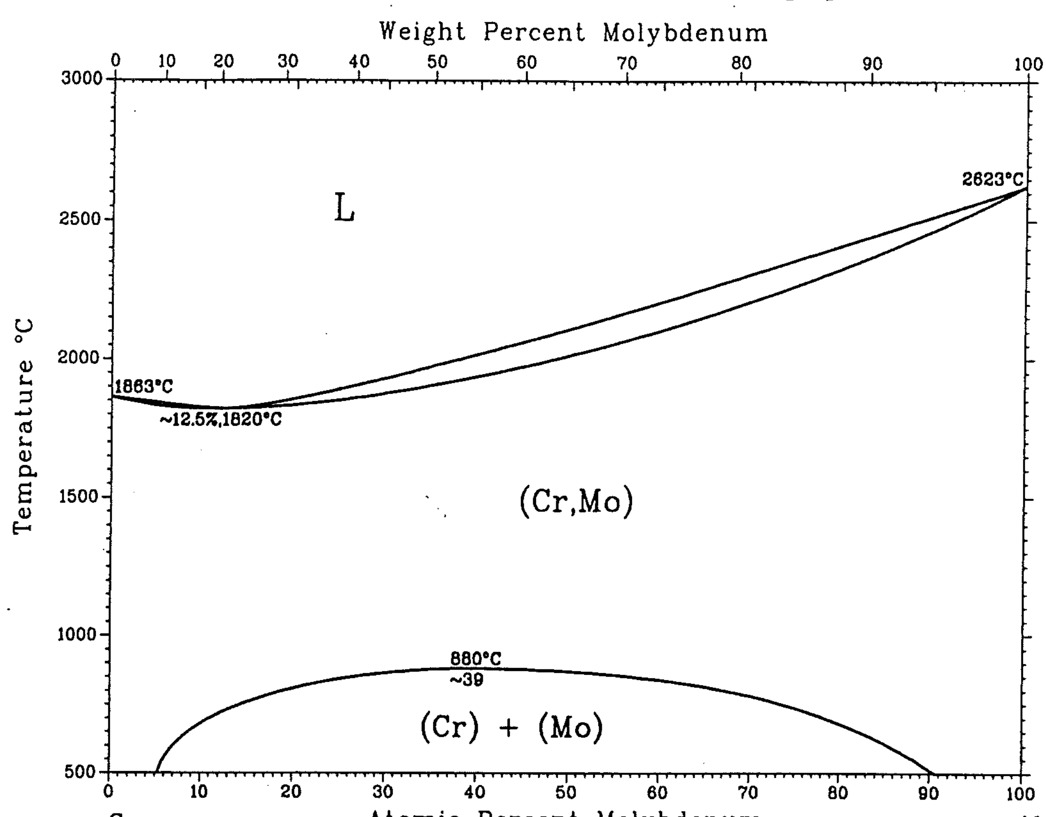


Figure 4.1b Binary phase diagram of chromium and molybdenum [11].

weld metal. Cladding with a low-Nb Inconel 625 flux-cored wire resulted nevertheless in small cracks whereas Nb-free Hastelloy C-4 have an indications free surface. The fact that the niobium content has a distinct influence on the number of indications was hereby confirmed.

### § 4.1.2 Machining

It can be stated that the indications are caused by a combination of the welding and the machining of the overlay. The indications emerge during machining in a well defined pattern obviously related to the welding process. Whether the defects are already present before machining remains uncertain and cannot be determined by NDT.

Cutting speed and depth seem to have no influence on the occurrence of indications. When the cladding is only machined in the top layer, no indications are found. The indications appear when the top layer is almost completely machined off and the beads in the second layer are "touched" (see fig. 3.12). This point is reached when, on average 3.5 to 4.0 mm is machined off.

The areas in which the PT indications appear are cut out from the machined specimen and are prepared for microscopic investigation. The indications are very small fissures (<1mm) which seem to follow a pattern of interdendritic phases. The phase is surrounded by a differently etched zone, probably as a result of segregation effects. All fissures found in the *A* and *B* specimens have these features. No interdendritic phases were found which were not cracked. This means that the material only fissures when this phase is present, or the inclusions are too small to detect when not causing a macroscopic PT indication. On the other hand, if such small inclusions were actually present they would not cause any problems.

The events taking place when the machining tool cuts the segregation zone and the interactions with the interdendritic phases are not exactly known. Due to the workhardening (§ 2.1.4) of the nickel-alloy the metal deforms drastically in front of the cutting tool. If a heterogenous phase is present, probably more brittle than the matrix, (micro)cracking occurs. However, the fissures are not pulled open. Looking at the photographs of the machined surface (appendix IV) the fissures seem to be covered by overlapping metal. The metal appears to be pulled over the fissure. Besides this, the photographs show loose metal parts which are pulled out and spread across the surface, which confirms the forces taking place during the machining.

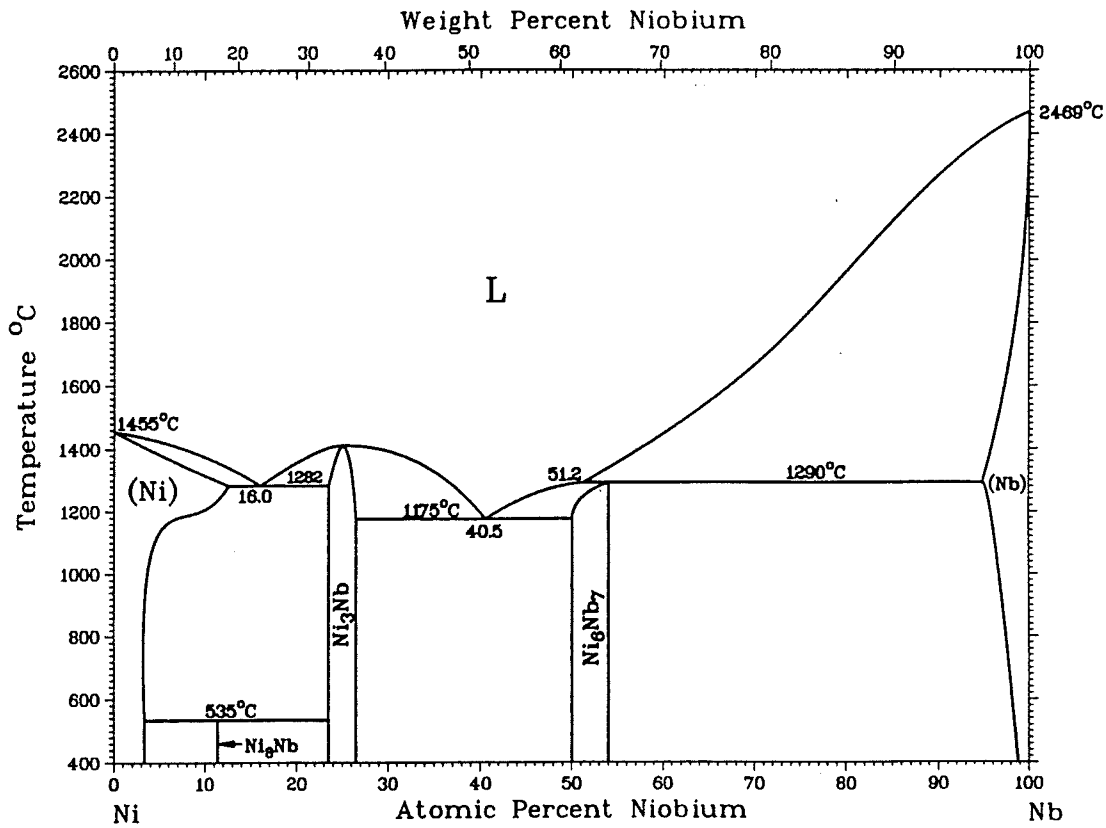


Figure 4.1c Binary phase diagram of nickel and niobium [11].

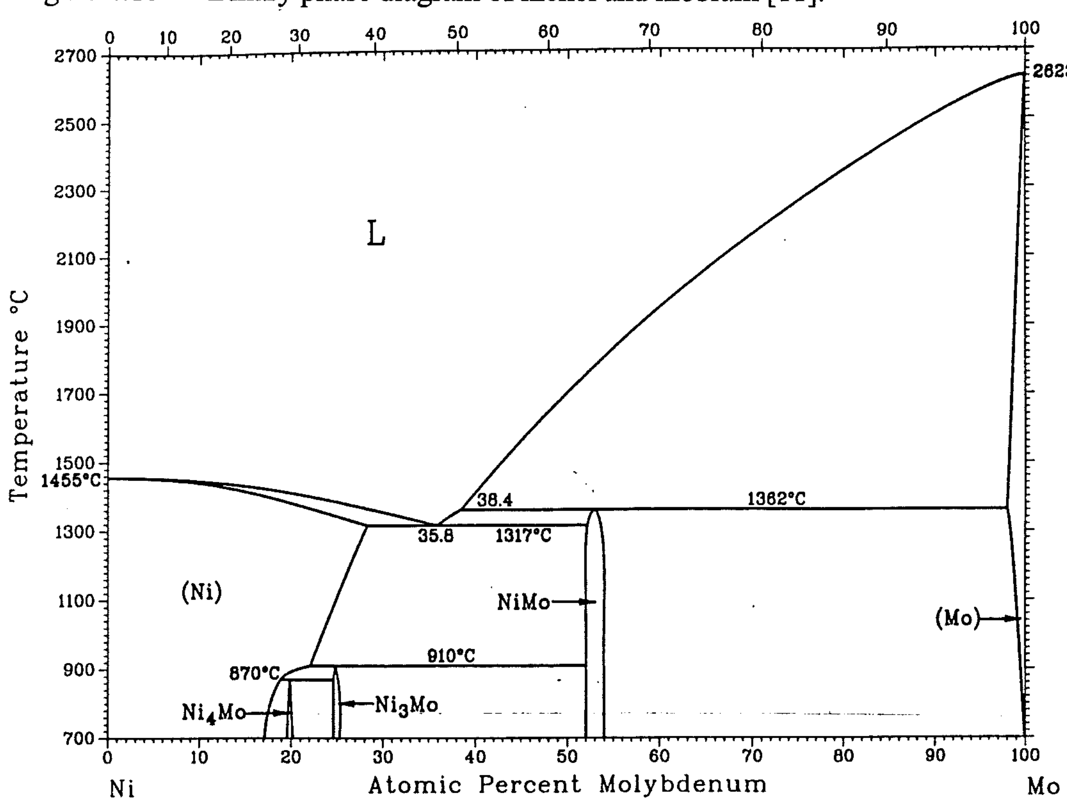


Figure 4.1d Binary phase diagram of nickel and molybdenum [11].

## § 4.1.3 Chemical analysis

The analyzed defects show a zone on the photographs which is differently affected by the etching agent. In the SEM photographs, this zone and the interdendritic regions display a difference in height. Which of these two is affected more cannot be deduced because of the shadowing effect of SEM. In defect I (scan 1 + 2) an interdendritic phase is visible roughly in the middle of the differently affected zone (DAZ). The zone in defect I is less wide (15 - 25 μm) than in defect II (30 - 40 μm; scan 3 + 4). This difference is probably due to segregation effects as alloying elements migrate to the inhomogeneous phase.

From the composition graphs several things can be concluded. The composition of the DAZ is more or less equal to the interdendritic regions. As the defect is scanned these regions show a decrease in the Ni and Fe content and an increase in the Nb, Mo and Si content. The Cr content remains relatively constant. The scanning lines of these elements have an oscillating character as dendrite cores and interdendritic regions are crossed. This variation in composition causes the difference in etching.

As Inconel 625 is a multi-element alloy it is very hard to predict the segregation effects during solidification. When the binary phase diagrams of Cr-Ni, Cr-Mo, Ni-Nb and Ni-Mo are observed, only the increase of the Mo and Nb content in the interdendritic regions can be explained in the Ni-Mo and Ni-Nb phase diagrams (see fig. 4.1a,b,c,d). As the Ni-Mo liquidus line is followed during solidification, molybdenum segregates towards the interdendritic region. The same happens when the Ni-Nb diagram is observed, the Nb content increases during solidification. However, no Laves-phase or Laves-phase like constituents are given in this phase diagram. The other combinations show the opposite behaviour compared to the experimental values [11]. Furthermore can the occurence of the Laves phase ($A_2B$) not be explained with these diagrams.

A (poor) explanation for the difference in composition between the dendrite core and the interdendritic region in terms of the three main alloying elements Ni, Cr and Mo can be given. This was done by comparing Inconel 625 to three other nickel base alloys: C4, C22 and C276. Cieslak conducted research on the welding metallurgy of these alloys in which the object was to explain the occurrence of various solidification constituents during GTA welding [8]. The main differences in composition between Inconel 625 and these alloys are the absence of Nb, a higher Mo content and alloying with W in C22 and C276. Segregation effects are reviewed by means of similar line scans of Ni, Cr Mo and Fe as were done in this research project. Then, the solidification and particularly the formation of various constituents are described by referring to isothermal ternary phase diagrams at 1250°C and 850°C of Ni,

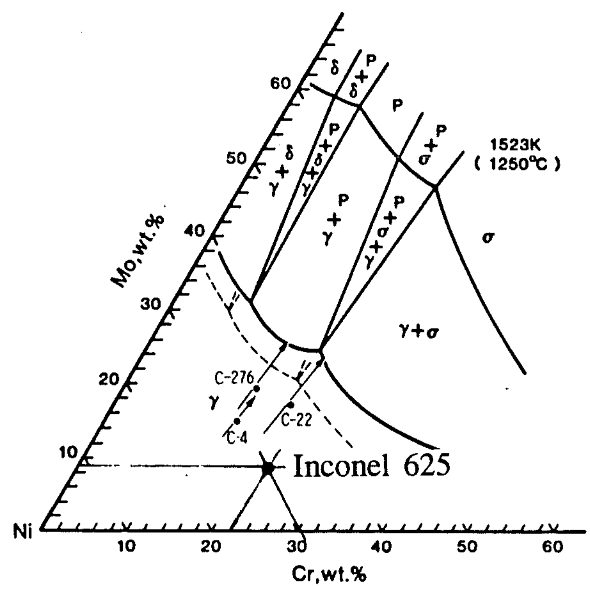


Figure 4.2 Ternary phase diagram of nickel, chromium and molybdenum at 1250°C [8].

Cr, and Mo. In figure 4.2 the segregation of the three elements is displayed by arrows for the investigated alloys. The tail of the arrow represents the composition of the initial solid to crystallize from the melt, the dendrite core region. The head of the arrow represents the final solidification composition, that of the interdendritic region. If a similar arrow for Inconel 625 is added, pointing in the same direction, the change in the solidifying Inconel 625 can be explained accordingly. This behaviour confirms the compositional oscillations found in the scans: When the scanning line enters the interdendritic region, the Ni content drops and the Mo content increases. The Cr content displays no distinct changes during solidification. The following remark, however, has to be made, reducing the applicability of this theory: In the phase diagrams, the compositions are depicted using the element **equivalents** $Ni_{eq}$, $Mo_{eq}$ and $Cr_{eq}$ in which major alloying elements like Ti, Fe and W are included. The Inconel 625 composition is added in figure 4.2, not considering the other important elements Nb, Fe and Si. Nevertheless, an indication for the displayed behaviour has been given.

Major deviations in the composition are found when the interdendritic phases are analyzed. The phase in defect I is identified as Laves-phase $(Ni,Cr)_2(Nb,Mo)$ (see fig. 3.16). The occurrence of this constituent is mainly caused by segregation of Nb and Mo to the interdendritic regions. In this context, niobium is the most important element.

The Si content also plays an important role according to Cieslak [9]. This element is present in low quantities (<0.4 wt%) but increases in the Laves-phase up to 1.9 wt% in scan 2.

In scan 2, the "Laves" peak seemingly consists of three smaller peaks. This can be explained as follows: When the electron beam strikes a porosity the near-average composition of the alloy is recorded. On the BEI-H photograph the porosities are visible as black spots and even have the shape of small hot cracks.

In scan 4 the scanning line (accidentally) crosses another constituent. It is not identified as Laves-phase but as $M_6C$, rich in Mo and Nb (fig. 3.17b). Carbon is not scanned for in this case, but the measured composition of the constituent matches the literature value quite good [9]. This inclusion is very small (< 3 μm), but also known to occur in welded Inconel 625.

**Metallurgical aspects**

From the foregoing it can be concluded that the fissuring of the metal is caused by the occurrence of interdendritic phases. In turn, these are solidificational effects. If it is a pure solidification problem, the question remains why no fissures are found in the top layer. The top layers must influence the underlying beads creating the susceptibility to fissuring. This points to the phenomenon of **reheat cracking**

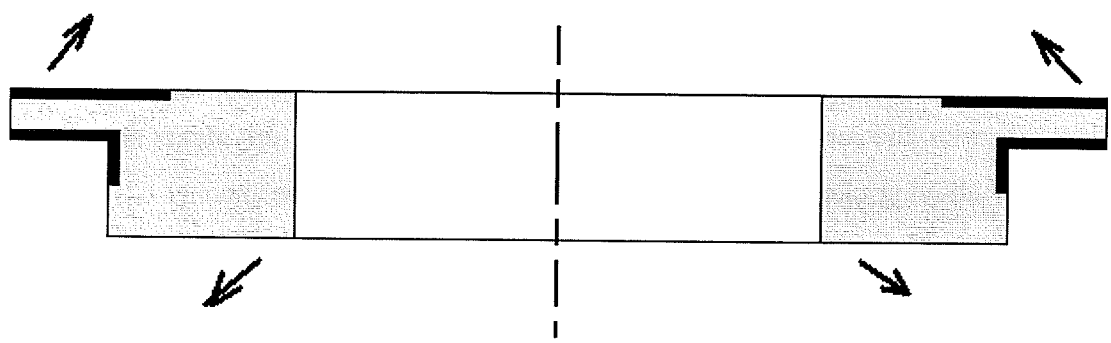

Figure 4.3 Deformation of seal ring due to "hoop stresses"

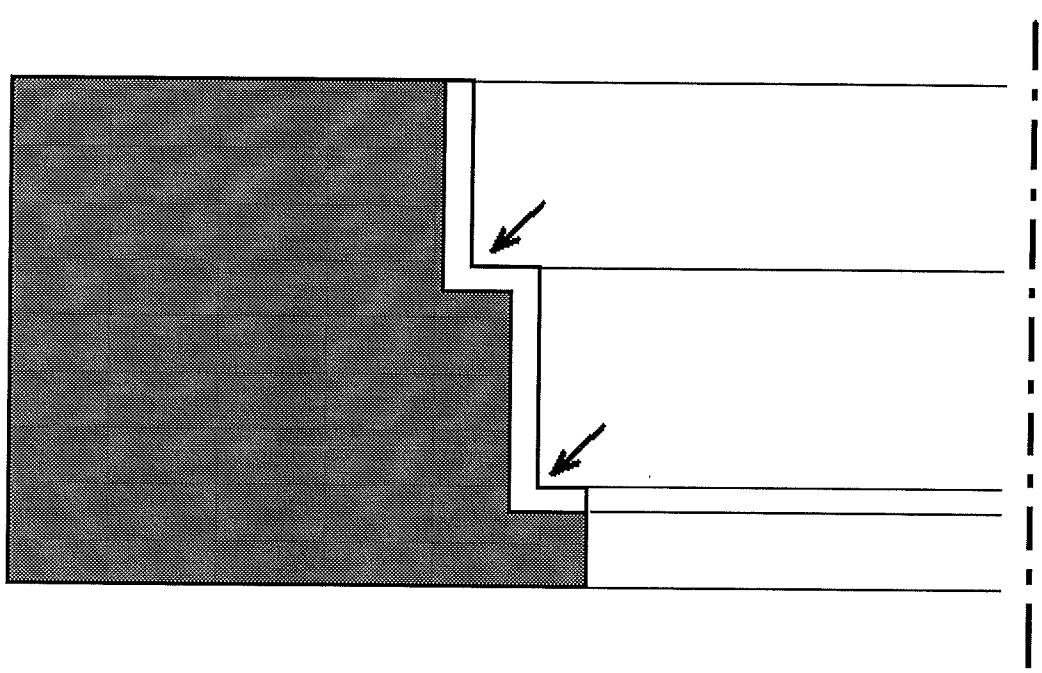

Figure 4.4 Possible location of stress concentration in cladded surface

which is defined as: "intergranular cracking in the heat affected zone (HAZ) or in the weld metal occurring during the exposure of welded assemblies to the elevated temperatures of post weld heat treatments (PWHT) or high temperature service". Reheat cracks are also known to occur in multi-layer welds. It is a very complex phenomenon caused by a combination of unfavourable macrostructure, precipitation hardening and segregation of alloying elements. In turn, these are related to the heat-input, cooling rate, alloy composition and heating temperature. The reheat cracks can have almost every orientation depending on the orientation of the grain boundary and therefore not only in the welding direction. The crack dimensions given for strip clad welding of steel are 2.5 to 3.5 mm which is significantly larger than these specimens and in the actual production welds. However, the fissure found in specimen C4, welded with low-niobium Inconel 625, could be a reheat crack.
Another fissuring phenomenon is **liquidation cracking** which is also related to the extensive reheat of the heat affected zone in multi-layer welding. What happens is that a particular phase remelts, for instance on the (former) grain boundary. The liquid phase may disperse like a film on the grain boundary and can weaken the structure. As a result of residual stresses, which obviously are present as the cladded parts deform during welding, these liquidation cracks occur. In low alloy steel, elements like phosphorus and sulphur form these low melting phases in combination with iron. Possibly, niobium may form this kind of phases in combination with nickel in Inconel 625.

In each of the above mentioned cracking phenomena stresses play an important role. In fact, stresses occurring during the welding are mentioned before as relatively less robust parts macroscopically deform as a result of the welding. Seal rings with a relatively small cross-section seem to turn "inside out" when the cladding is applied (fig. 4.3) due to so-called "hoop stresses". These stresses are caused by the fact that only one side of the rings is cladded inducing much stress. Furthermore, a weakened area and/or an extensive stress concentration is necessary to induce fissuring. The interdendritic phases possibly can be both on a microscopic scale. This combination may cause the material to crack. On a macroscopic scale, corners in machined claddings can cause stress concentrations as well (fig. 4.4). Until now no cracks have been found in these areas of the cladded parts. Whether residual stresses are the most important aspect of the fissuring mechanism requires more research.

## § 4.2 Test rings

The results from the test rings basically confirm the knowledge gained from BOP IV.

In test ring 1 very few indications were found in the top layer. When the cladding was machined 3.5 to 4 mm in depth, many indications started to appear proving the second layer was "touched". Moreover, machining with various cutting depths did not result in more indications. This machining sequence (section 2, § 3.6) was done in the top layer, therefore it can be said that the cutting depth has no influence on the number of indications. On the other hand, it is not clear wether variation in cutting depth causes a change in the occurrence of indications in the critical zone, compared to a cutting depth of 0.5 mm. The assumption is that there will not be much difference in using the former (A) parameters or the current (B) parameters. Even though the rather large difference in heat-input: 1.18 kJ/mm in *A* and 0.86 kJ/mm in *B*, the indications will appear anyhow in the Inconel 625, using this welding process.

Test ring 2 showed that another welding method (Hot-wire GTAW) resulted in no indications. The cladding material, number of layers (three) and machining sequence remained the same. Therefore this (good) result has to do with the solidification sequence of the weld metal.
The factors that influence the solidification rate are:

- the interpass temperature which is the same as in the SAW process (±100°C);
- the heat-input which is 0.8 to 1.0 kJ/mm for SAW and pulsating in the Hot-wire GTAW (HWGTA) process between 0.4 and 0.7 kJ/mm when $\eta_p$ is ±80% percent. These two values are relatively low because the contribution to the heat-input of the hot wire is not included which is heated by a current of 60 to 80 A;
- the shielding gas (100% Ar) which cools the bead during HWGTA welding whereas the flux is isolating the bead in the SAW process.

The alternating solidification process of the weld metal is visible in the pool. Due to the pulsating current the material solidifies during the base current and a re-melt of the this material takes place during the peak current. The fraction that is re-melted depends on the pulse frequency and the travel speed. This re-melt might play an important role, as possible segregation is partly abolished and a re-distribution of alloying elements is accomplished. This may have more influence than the heat-input.
The pulsed HWGTAW has an oscillating fusion line but in contrast with the generated smoothness of the SAW fusion line, this does not seem to enhance the occurrence of indications.

## § 4.3 Suggested solutions

After this research program there are three possible solutions which can be suggested to solve the indication problem. The first can be implemented in the current production process but has some practical problems. The second involves the acquisition of new equipment which requires an extensive investment both financially and from the personnel who will operate the new welding equipment. The third needs more metallurgical investigation and approval from the client and the final users of the swivel itself.

### § 4.3.1 Welding and machining

**1. Controlling the machining depth**

In BOP IV was found that when machining only in the top layer of the cladding the number of indications is minimized up to a zero defect surface. A minimum machined overlay thickness of 5 mm Inconel 625 is prescribed by the client. This thickness, including variation in bead depth and deformation of the cladded part, can be obtained by depositing three welded layers adding up to an unfinished thickness of 7 to 8 mm. In this case the "B" submerged arc welding parameters are used for a better reproducible cladding. The average top layer thickness is about 4 mm. So when the surface is machined to final dimensions to an overlay thickness of 5 mm, only metal will be removed in the top layer and no indications should occur.

The above can be applied to flat surfaces but problems may arise in the corners of step-wise shaped surfaces, which are often used in the swivel design. It can hardly be predicted if the machined corner will be positioned just in the critical zone. Another, closely related problem are unforseen deformations of the cladded part as a result of residual weld stresses. In that case the rough cladding thickness could prove to be too small or the cladding is machined into the second layer and indications appear. When these problems arise, a solution could be to machine for instance 1 mm under these final dimensions and deposit another layer on the machined surface and machine again. Albeit that the corner indications could reoccur.

In all, this suggested solution is definitely the cheapest and easiest one to apply but not 100% full proof as the problem is avoided and not resolved.

## 2. Using Hot-wire GTAW

The cladding of test ring 2, using the HWGTAW process, gave an indication free machined surface. Apart from this major advantage, the process and hardware have some further interesting features:

- The parameters are programmed in an integrated computer and are displayed at all times. The process can therefore be controlled easily and welding programmes for various applications can be retrieved and changed.
- Horizontal and vertical surfaces are welded without changing the position of the torch.
- No flux is applied so when welding in a clean room no dust or slag pollute the environment.

When choosing this process for future projects, several things have to be considered. The complete welding unit is quite costly (*f*300.000,- to *f*500.000,-) which is rather an investment for just one welding system. It is not only a financial investment but the welders operating the system have also to be trained and accustomed to this completely new machine. Finally, all current welding procedures have to be requalified and approved by the client. Although this will be the least of the possible problems of integrating a new welding process into the production process.

## 3. Using different cladding materials

In BOP IV cladding D was welded with the niobium free Hastelloy C4 and resulted in no indications. This confirms the important role of this element in the solidification process and the formation of interdendritic compounds. No bufferlayer of S59 is needed resulting in a reduction of the production time. C-4 contains, however, some miscellaneous alloying elements like Ti. Furthermore, the Cr content is relatively low and more Mo is added compared to Inconel 625. The interactions of the alloying elements with, for instance, nitrogen in duplex steel need more investigation, but most of these aspects are reviewed in the welding qualification tests, required for production welding.

Changing the filler metal, however, involves more. The alloy is less common than Inconel 625 and is more expensive (C4: *f*100,-/kg, Inconel 625: *f*60,-/kg). Just like changing the process, another filler metal requires new welding procedures and approval of the client. Although this alloy is comparable to Inconel 625, extensive (rubbing) tests with the seal material and corrosion tests have to be done. These tests determine whether the alloy is suitable for the application, or not.

In all, this option could be a relatively simple alternative if one decides to maintain the original submerged arc welding process.

## § 4.3.2 Quality assurance

**The Product Status Report (PSR)**

To guarantee the quality of the cladding it proved to be vital to carefully monitor the production process. In welding in general and in high quality submerged arc welding in particular, the final result depends on a wide array of parameters and external factors. In the first stages of this research the Product Status Report (PSR) was introduced in the production of the overlays. An example is attached in appendix VI. The object of the PSR was to follow the cladded parts and see if the changes in the welding parameter setting resulting from the research had any influence on the quality: the number of indications. Most attention was paid to the NDT and the repair welding of possible indications. To every cladded part a PSR was attached and updated by the project manager or myself.

One of the conclusions was that in the robust parts like the inner- and outer parts of the swivels less indications were found than in the smaller rings. The first results after the changes in consequence of BOP II and III were quite good but proved later to be short termed. After all, the PSR demonstrated to be a valuable but time-consuming way of recording research results in a fabrication process.

**The Jobsheet**

In the near future a large number of swivels has to be fabricated involving many Inconel 625 overlays. Since the PSR system proved to be too complicated and as the focus is more the welding itself and not the repair, the jobsheet was introduced to assure the quality of the claddings. An example is attached in appendix VI. To every part to-be-cladded a jobsheet is attached with registration number and WPS reference.

The object of the jobsheet is to monitor the welding and have a feedback system for the welding shop. In the past the whereabouts and status of some components were unclear and various registration systems were used. Irregularities can now be noticed earlier and not until the part is being machined or fitted. Also the batch number of the filler wire is written down to ensure the right material is welded and changes in the compositions can be recorded.

The jobsheet is no substitute for the PSR but is just focused on the welding. It is updated by the welders and will probably prove its value in the coming projects.

# 5. Conclusions

In this chapter the conclusions are given of the above described research on the fissuring problem in Inconel 625 overlays. These final remarks should give the answer to the questions posed in § 2.3. Next, some suggestions are given for future research for better understanding of the fissuring and metallurgy of Inconel 625.

## § 5.1 Conclusions

- The unacceptable indications found during the dye penetrant testing of machined Inconel 625 overlays are caused by fissures in the cladded surface.

- The fissures are interdendritic. The solidification process of Inconel 625 during welding has therefore to be considered as a critical step. The solidification rate has to be as high as possible to create a fine microstructure. However, extra cooling during welding has no significant effect on this and seems to increase the susceptibility to hot cracking.

- By changing the welding parameters the bead geometry can be altered and the heat-input minimized. This results in an optimized flat bead with limited penetration and epitaxial grain growth. It did not result in a substantial reduction in the number of indications.

- During the solidification of Inconel 625 microsegregation occurs and as a result of that, interdendritic phases like Laves $(Ni,Cr)_2(Nb,Mo)$ and Nb and Mo rich $M_6C$ are formed. These phases are found to cause the fissuring of the weld metal.

- The fissures appear at specific depth in the cladding. This depth is approximately 4 mm below the initial top surface of the cladding in the top of the second layer. No or very few indications are found in the top layer. This means that the top layer has some sort of reheat effect on the underlying layer.

- When Hot-wire GTAW is applied for the welding of Inconel 625 no indications are found after machining. This pulsating process provides a lower heat input and therefore a higher solidification rate and a finer structure.

- When another, niobium free, nickel-base alloy like the Hastelloy C4 is used, no indications are found. This alloy is known to form no interdendritic phases like the Laves-phase during solidification.

- To produce a high quality overlay it is vital to monitor and control the welding process. Therefore involvement and feedback to the welders is an important factor.

## § 5.2 Further research

Doing research in an industrial environment proved to be rather complex. At first, the problem to be studied seemed to be well-defined, but as the project evolved, more factors emerged and the matter became more complicated. For example, cooling the weld might be a possible solution, theoretically, but proved to be impractable. Nevertheless, three solutions have been given in section 4.3.1. For these solutions more research is needed and besides that, the following points should also be examined.

* The results of Bead-on-Plate IV point to a solidification problem but on the other hand no indications are found in the top layer. The earlier discussed aspect of reheating the welded material can be investigated further as microstructure refinement and secondary precipitation play an important role in reheat crack susceptibility.

* As solidification rate increases the microstructure becomes finer but the segregation increases as well. The exact relations between these two aspects and their influence on the cracking susceptibility may be important for this application.

* The mechanical properties of phases like Laves are probably of major influence in the machining of the cladding. The exact interactions of constituent and cutting tool are an interesting field of research.

* In this project the electrode wire and flux were not varied. It could be worthwhile investigating other combinations. In the industry, many different fluxes are available, some especially for high quality cladding.

* Finally, the macrostresses and microstresses occurring in the weld and base metal are not investigated in this research and need more attention. For example by means of finite element methods.

# REFERENCES

[1] Nickel Development Institute,
Machining Nickel Alloys, A Nickel Development Institute Reference Book, Series Nr. 11.008.**i - iii** and **1 - 22**.

[2] American Society of Mechanical Engineers,
ASME VIII, Pressure Vessels, Appendix 8, Rev 1989.

[3] H. Verschuren,
Research and Qualification Report, IHC/SBM, Kinderdijk, October 1993.

[4] E.M. Jorritsma,
Indicatie onderzoek aan opgelast Inconel 625, Delft University of Technology/IHC P & S, Kinderdijk, July 1995.

[5] E.M. Jorritsma,
Oplassen van roestvast staal met legeringen op nikkelbasis, Delft University of Technology/IHC P & S, Literature survey, March 1996.

[6] Drs. W.P.J. Vink,
Niet-destructief onderzoek, Delftse Universitaire Pers, Delft, 1995

[7] T. Sawai, Y. Ueshima, S. Mizoguchi,
Microsegregation and Precipitation Behaviour during Solidification in a Nickel-base Superalloy, ISIJ International, Vol. 30 (1990), No. 7, **520 -528**.

[8] M.J. Cieslak, T.J. Headley, A.D. Romig Jr.,
The Weldin Metallurgy of HASTELLOY Alloys C-4, C-22 and C-276, Metallurgical Transactions A, 17A (11), 1986, **2035 - 2047**.

[9] M.J. Cieslak, T.J. Headley, T. Kollie, A.D. Romig Jr.,
A Melting and Solidification Study of Alloy 625, Metallurgical Transactions A, 19A (9), 1988. **2319 - 2331**.

[10] A. Dhooge, A. Vickier,
Reheat Cracking - A Review of Recent Studies (1984-1990), Welding in the World, Vol. 30 (1992), No. 3/4, **44 - 71**.

[11] D.A. Porter, K.E. Easterling,
Phase Transformations in Metals and Alloys, T.J.Press (Padstow) Ltd, Padstow, Cornwall, 1981.

[12] T.B. Massalski (Ed.)
Binary Alloy Phase Diagrams, American Society of Metals, 2nd edition, 1990

# APPENDICES

I : Data and photographs of Bead-on-Plate I + WPS 91/91-2
II : Data and photographs of Bead-on-Plate II
III : Data and photographs of Bead-on-Plate III
IV : Data and photographs of Bead-on-Plate IV
V : Data of Test rings 1 and 2
VI : Product Status Report and Jobsheet

# APPENDIX I

**Data and photographs of Bead-on-Plate test I and WPS 91 & 91-2**

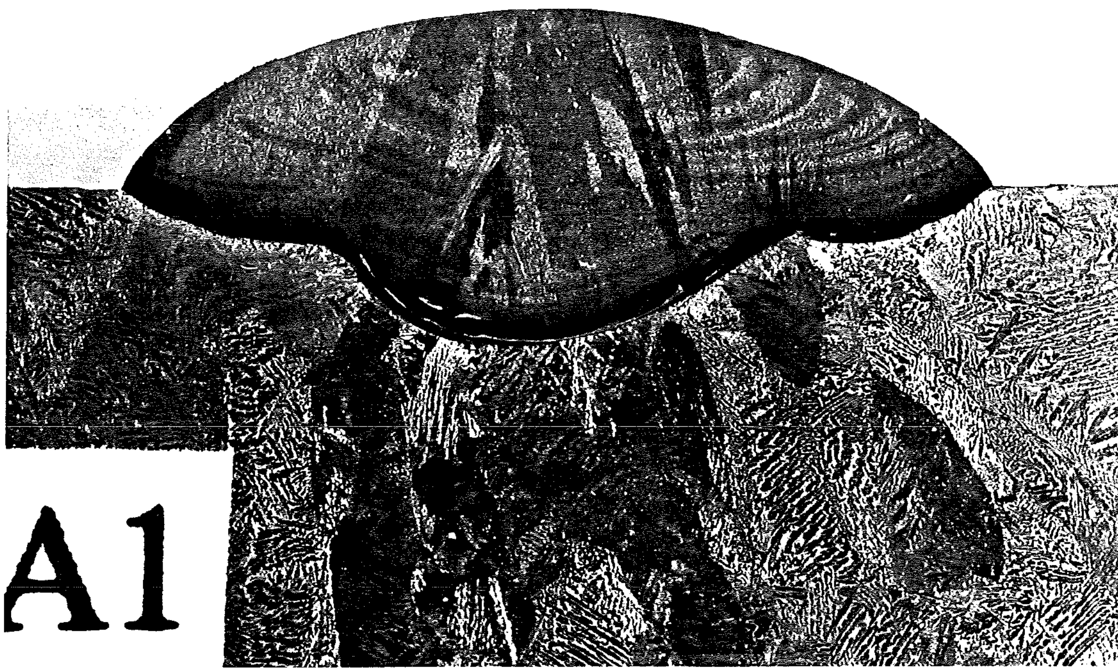


Photograph (7x) of A1 : BOP test I (I = 260 A, v = 400 mm/min, V = 26 V)

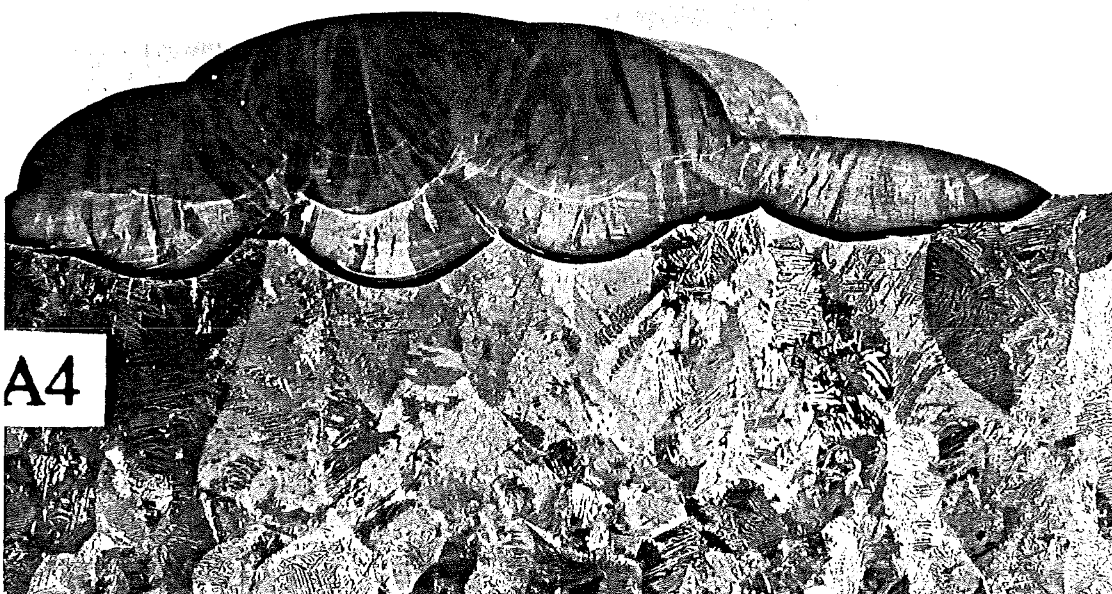


Photograph (3x) of A4 : BOP test I (I = 260 A, v = 400 mm/min, V = 26 V)

Photograph (7x) of B1 : BOP test I (I = 260 A, v = 500 mm/min, V = 26V)

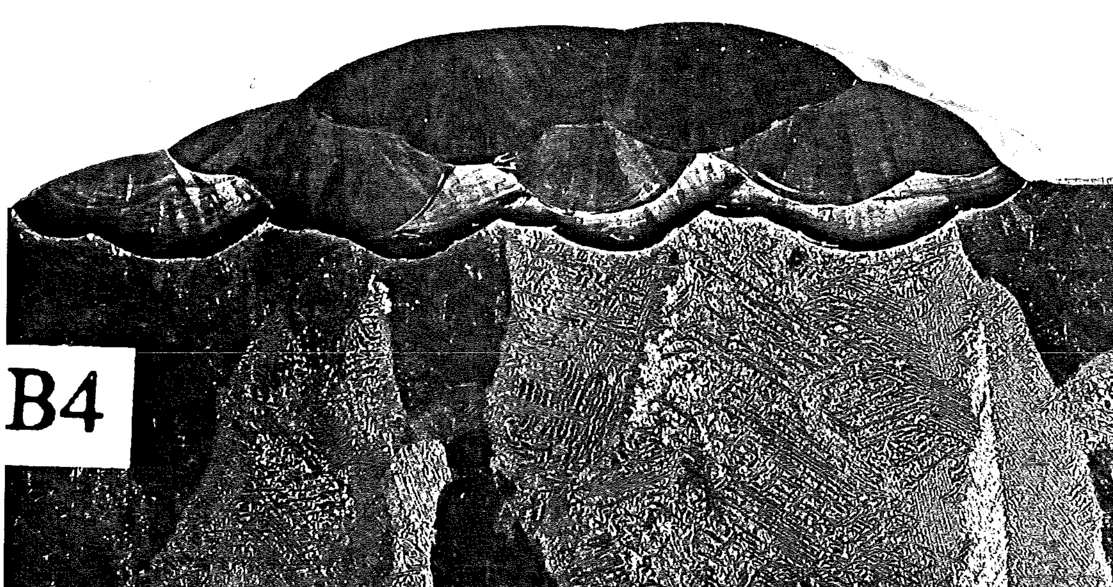


Photograph (3x) of B4 : BOP test I (I = 260 A, v = 500 mm/min, V = 26 V)

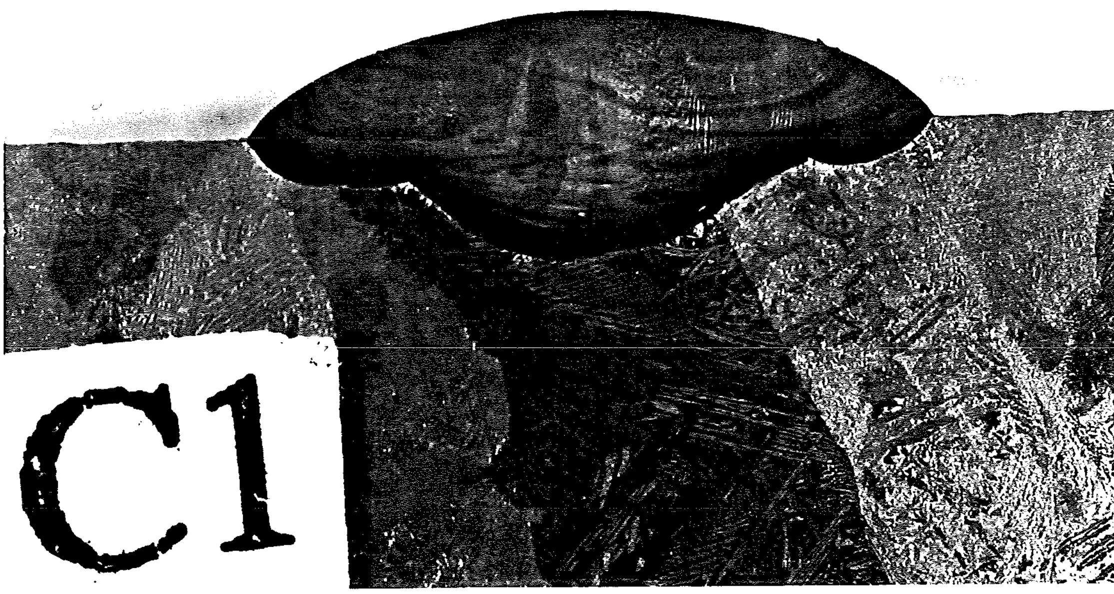


Photograph (7x) of C1 : BOP test I (I = 260 A, v = 500 mm/min, V = 28V)

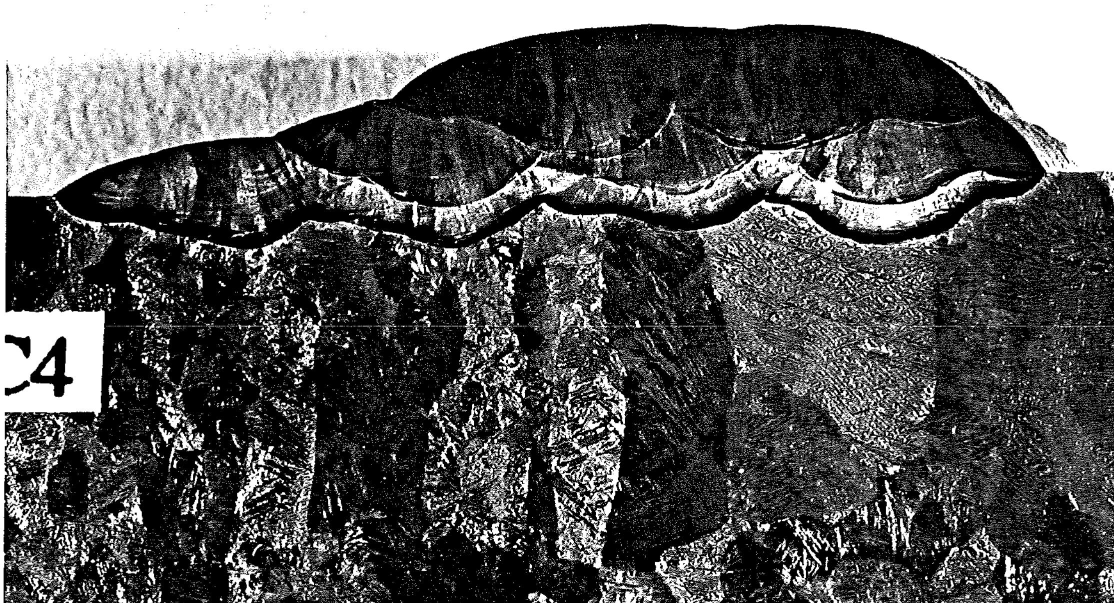

Photograph (3x) of C4 : BOP test I (I = 260 A, v = 500 mm/min, V = 28 V)

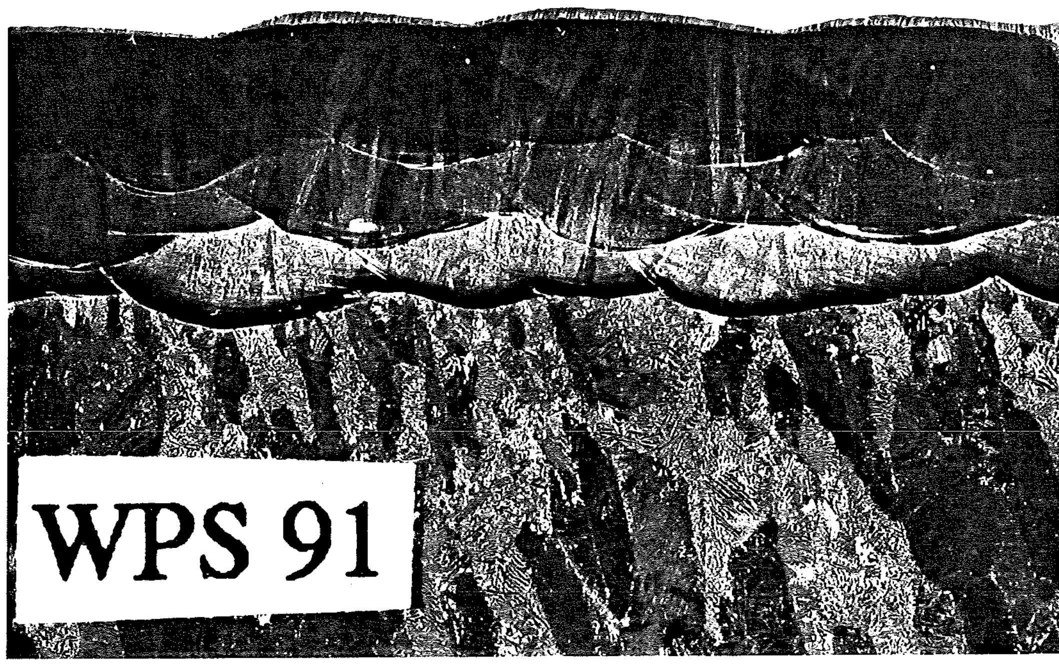


Photograph (3x) of WPS 91 including bufferlayer (I = 260 A, v = 470 mm/min, V = 28V)

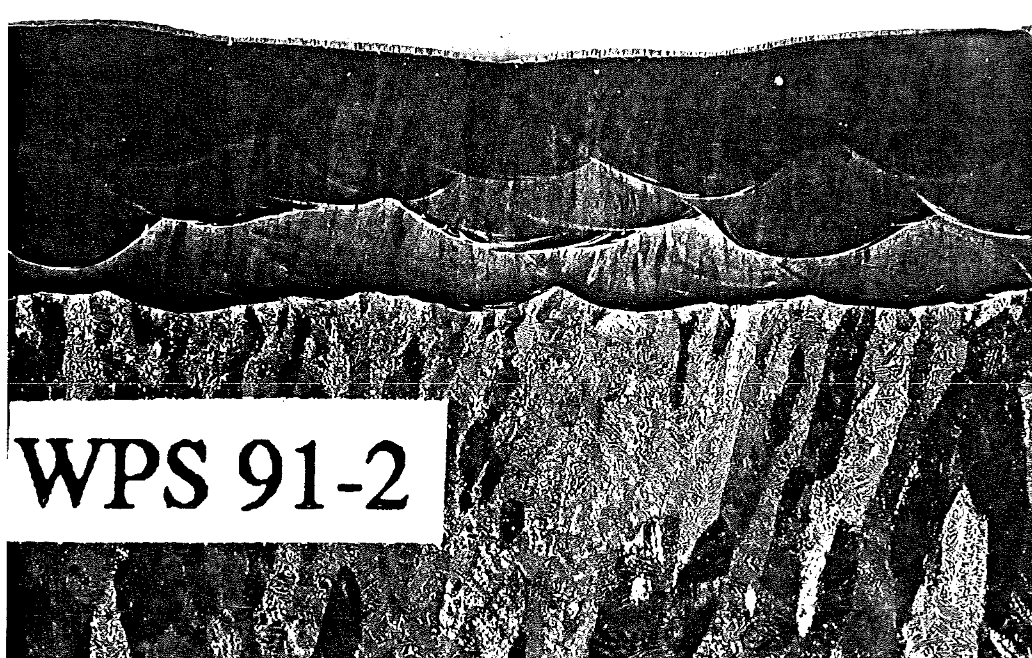


Photograph (3x) of WPS 91-2 without bufferlayer (I = 260 A, v = 470 mm/min, V = 28 V)

# APPENDIX II

**Data and photographs of Bead-on-Plate test II**

| weld no. | T (before) °C | T (after) °C | T (water) °C | I (A) | V (V) | Cooling-time (min) |
|---|---|---|---|---|---|---|
| LAYER A (S59) | | Travelspeed : 470 mm/min | | | | |
| 1 | 23 | 43 | 24 | 174 | 28 | – |
| 2 | 42 | 53 | 28 | 177 | 28 | 6 |
| 3 | 34 | 58 | 29 | 168 | 28 | 12 |
| 4 | 40 | 60 | 29 | 171 | 28 | 7 |
| 5 | 43 | 65 | 30 | 165 | 28 | 8 |
| 6 | 37 | 67 | 32 | 166 | 28 | 10 |
| 7 | 46 | 63 | 33 | 170 | 28 | 8 |
| 8 | 41 | 56 | 35 | 170 | 28 | 15 |
| Average | 38 | 58 | 30 | 172 | 28 | 9, |
| LAYER B (Inconel 625) | | Travelspeed : 500 mm/min | | | | |
| 9 | 32 | 68 | 30 | 275 | 28 | 49 |
| 10 | 43 | 70 | 32 | 274 | 28 | 7 |
| 11 | 46 | 64 | 36 | 269 | 28 | 20 |
| 12 | 46 | 79 | 38 | 266 | 28 | 10 |
| 13 | 51 | 69 | 40 | 267 | 28 | 9 |
| Average | 43 | 70 | 35 | 270 | 28 | 19 |
| LAYER C (Inconel 625) | | Travelspeed : 500 mm/min | | | | |
| 14 | 31 | 74 | 29 | 286 | 28 | 87 |
| 15 | 45 | 90 | 33 | 293 | 28 | 8 |
| | | | FRESH COOLING WATER | | | |
| 16 | 42 | 71 | 23 | 288 | 28 | 13 |
| 17 | 40 | 70 | 27 | 284 | 28 | 9 |
| Average | 39 | 76 | 28 | 287 | 28 | 29 |
| LAYER D (Inconel 625) | | Travelspeed : 500 mm/min | | | | |
| 18 | 38 | 83 | 33 | 276 | 28 | 17 |
| 19 | 37 | 80 | 34 | 280 | 28 | 37 |
| 20 | 37 | 93 | 35 | 281 | 28 | 13 |
| Average | 37 | 85 | 34 | 279 | 28 | 22 |

Table 2.2 : Welding parameters including temperature measurements

Remarks :
1. Bead shape on Zeron 100 is wider than on Zeron 25.
2. Base metal is cooled by a waterbath, this water is cooled after every weld with liquid Nitrogen.
3. T(before) and T(after) are measured right next to the weldbead on the base metal or the previous layer.
4. The temperatures are taken just before and just after the bead is deposited.
5. S59 is welded with 1.2 mm wire; Inconel 625 is welded with 1.6 mm wire.

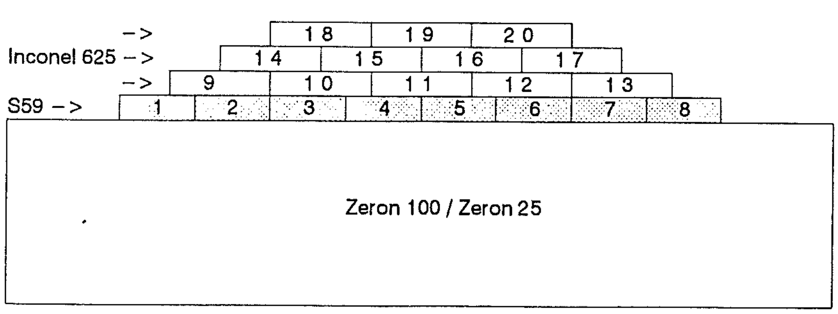


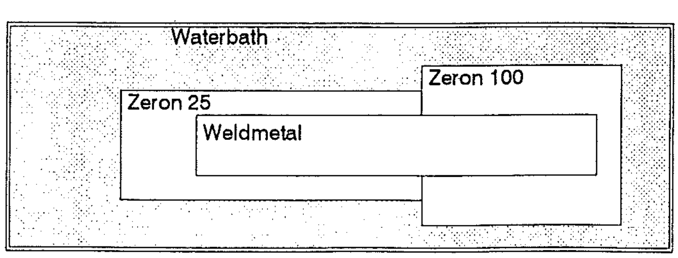


# Welding dat Bead-on-Plate II

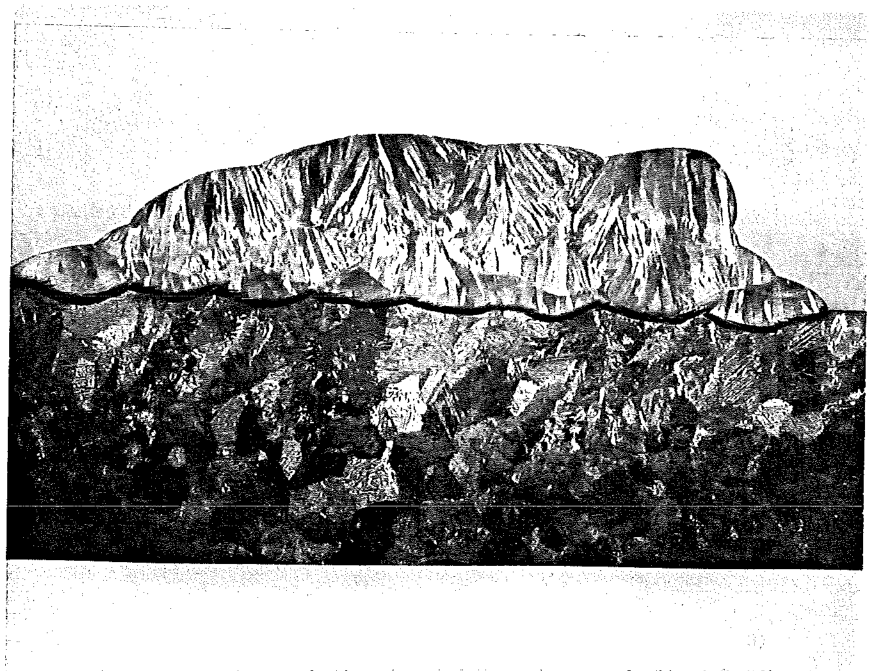

**Cross-section of BOP II welded on Zeron 25**

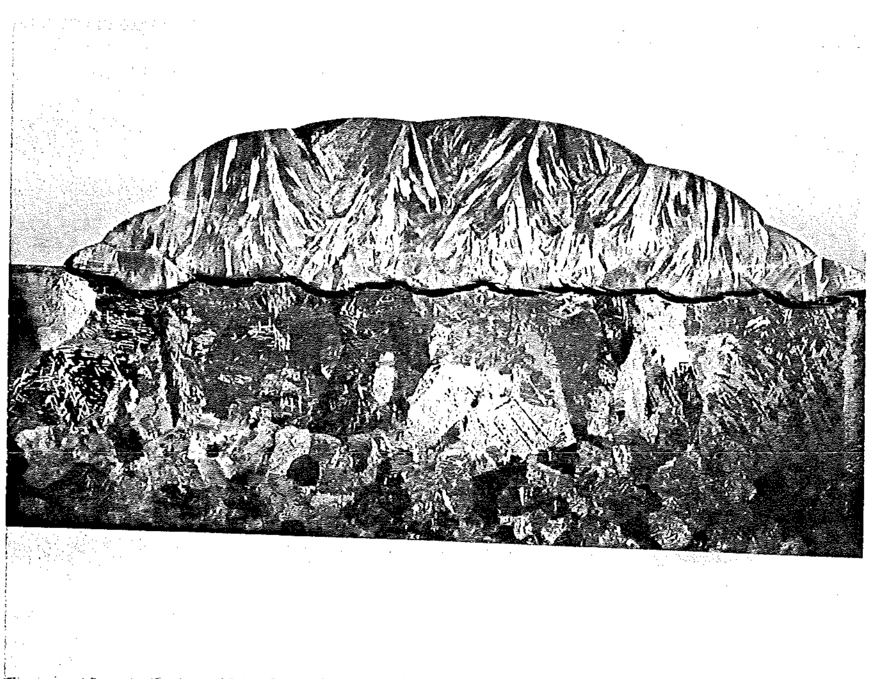

**Cross-section of BOP II welded on Zeron 100**

# APPENDIX III

**Data and photographs of Bead-on-Plate test III**

| RESULT | A | B | C | D | E | F | G | H |
|---|---|---|---|---|---|---|---|---|
| I (Ampere) | 279 | 283 | 286 | 291 | 266 | 298 | 296 | 290 |
| V (Volts) | 25,2 | 28,4 | 32,8 | 33,1 | 25 | 36,8 | 36,8 | 36,8 |
| v (mm/min) | 500 | 500 | 500 | 560 | 500 | 440 | 500 | 560 |
| HI (kJ/mm) | 0,84 | 0,96 | 1,13 | 1,03 | 0,80 | 1,50 | 1,31 | 1,14 |
| HI (J/mm ^ 2) | 70,3 | 68,4 | 77,1 | 71,7 | 69,4 | 88,5 | 82,7 | 81,1 |
| W (mm) | 12 | 14,1 | 14,6 | 14,4 | 11,5 | 16,9 | 15,8 | 14,1 |
| D (mm) | 6,1 | 5,2 | 4,9 | 5,3 | 5,9 | 5,8 | 5,9 | 5,1 |
| D/W | 0,51 | 0,37 | 0,34 | 0,37 | 0,51 | 0,34 | 0,37 | 0,36 |
| R (mm) | 2,8 | 2,5 | 2,1 | 2,3 | 2,6 | 2,4 | 2,3 | 2,1 |
| P (mm) | 3,3 | 2,7 | 2,8 | 3 | 3,3 | 3,4 | 3,6 | 3 |

HI = Heat Input
W = Bead width
D = Bead Depth
R = Reinforcement
P = Penetration

Welding data and bead dimensions of BOP III

A

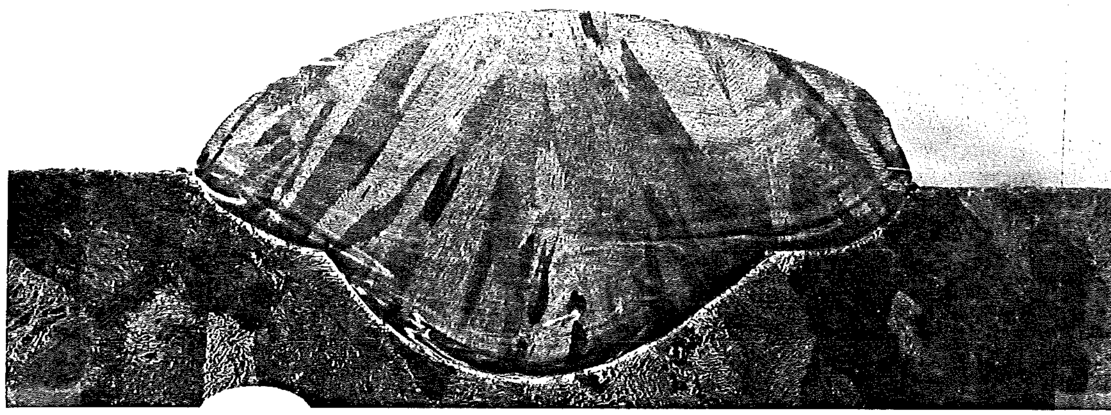

B

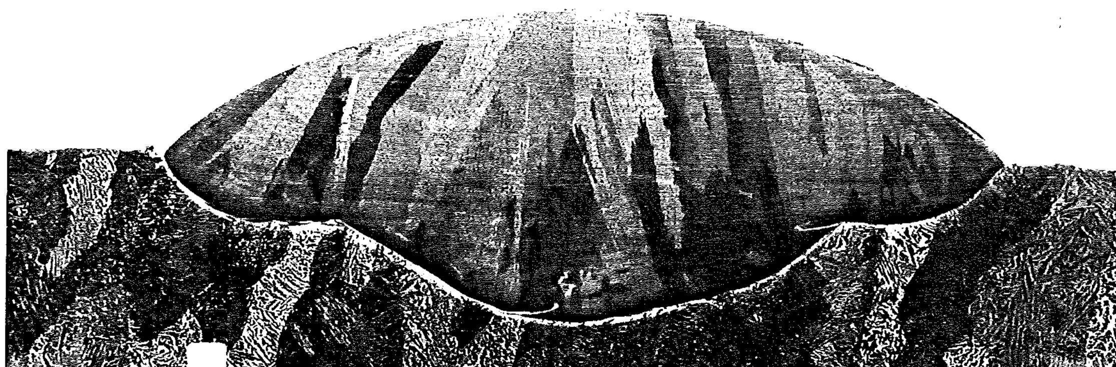

C

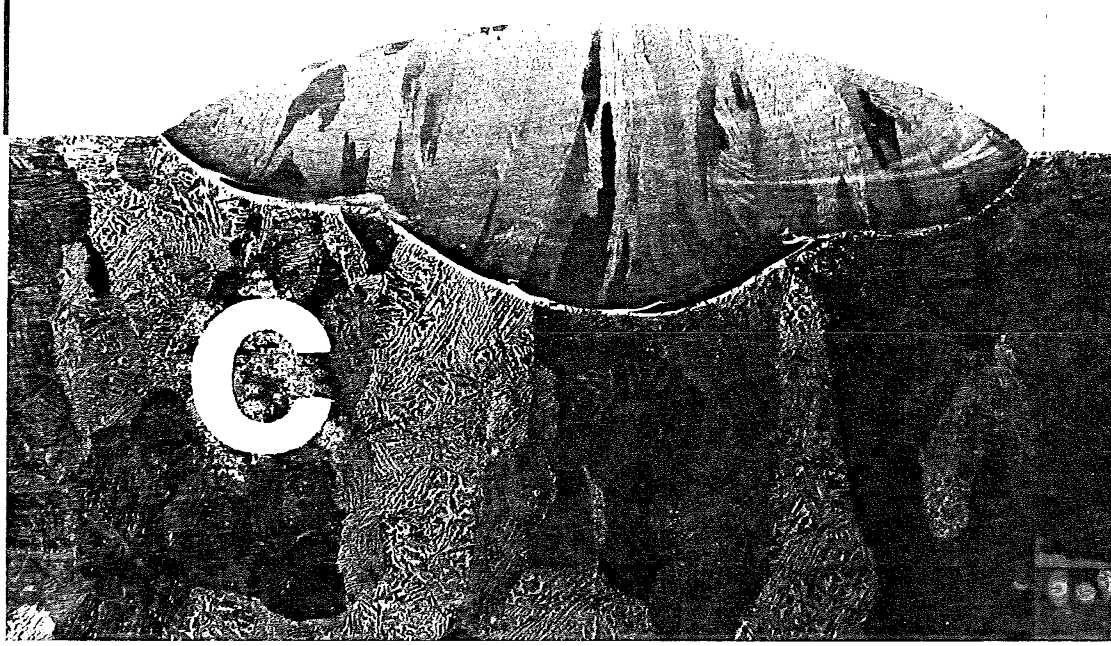


Bead-on-Plate III: welding with increasing voltage (7.5x)

F

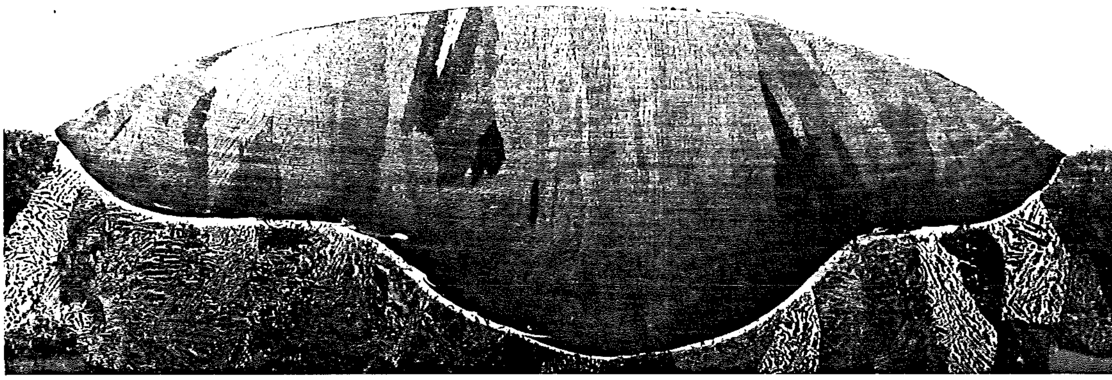

G

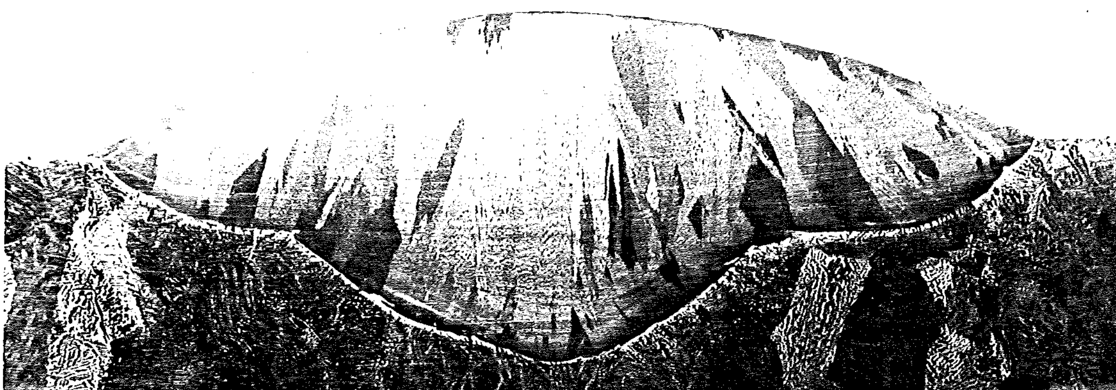

H


Bead-on-Plate III: welding with high voltage and increasing travel speed (7.5x)

**D**

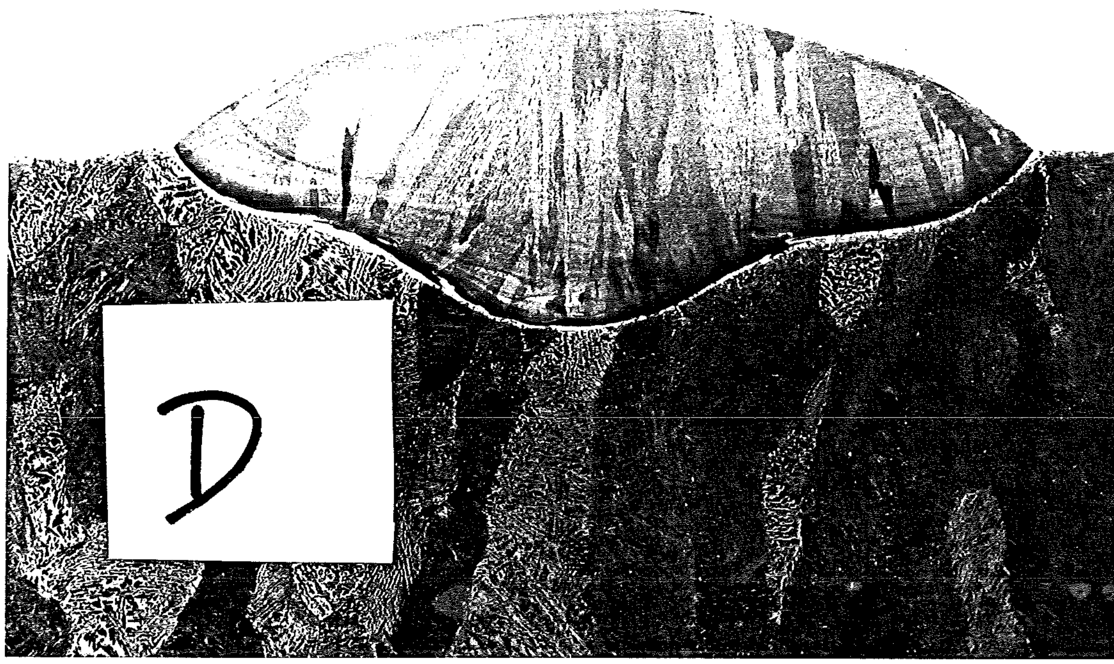


Bead-on-Plate III: Welding with high voltage and travel speed (7.5x)

**E**

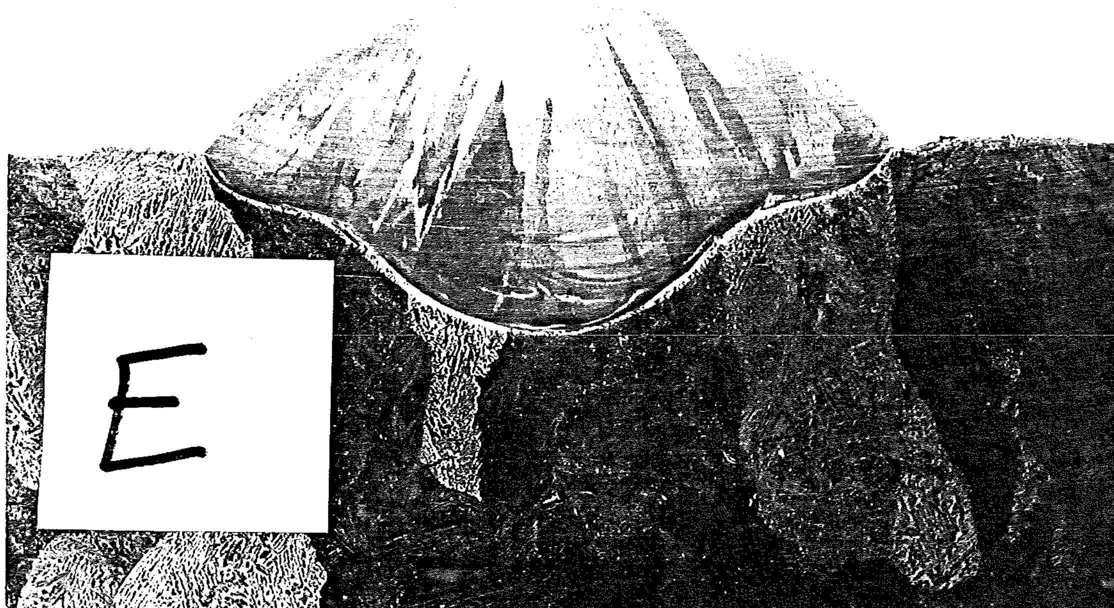


Bead-on-Plate III : Welding with low current and voltage (7.5x)

1 :

B = 12.0 mm
D = 5.0 mm
D/B = 0.42
OD = 2.2 mm
ID = 2.8 mm

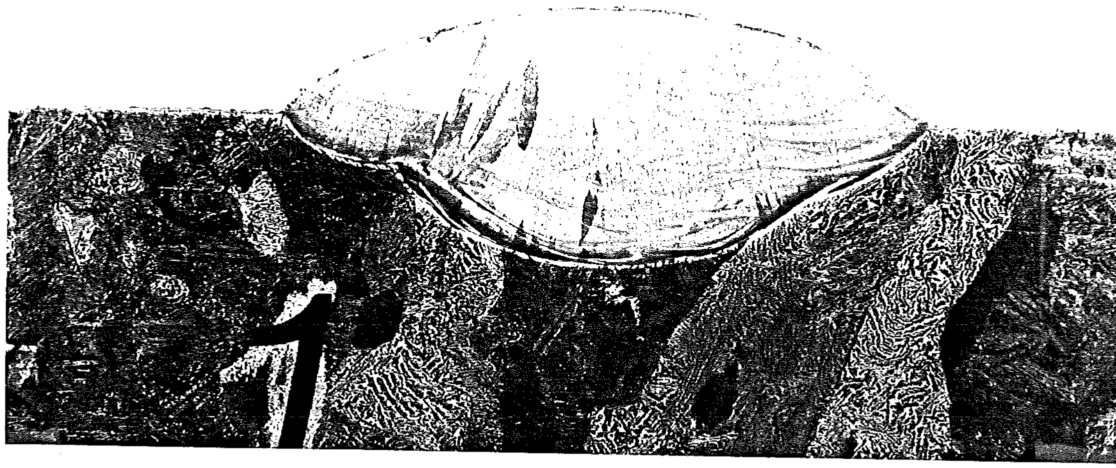

2 :

B = 11.9 mm
D = 4.7 mm
D/B = 0.39
OD = 2.2 mm
ID = 2.5 mm

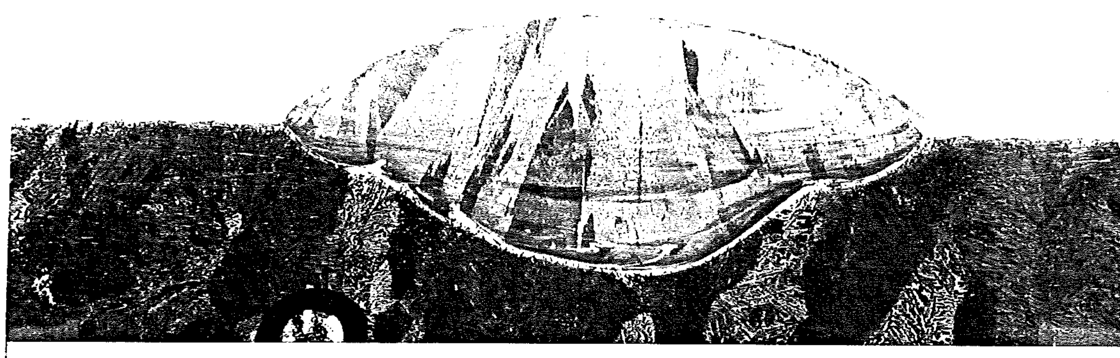

3 :

B = 11.8 mm
D = 4.6 mm
D/B = 0.39
OD = 2.3 mm
ID = 2.3 mm

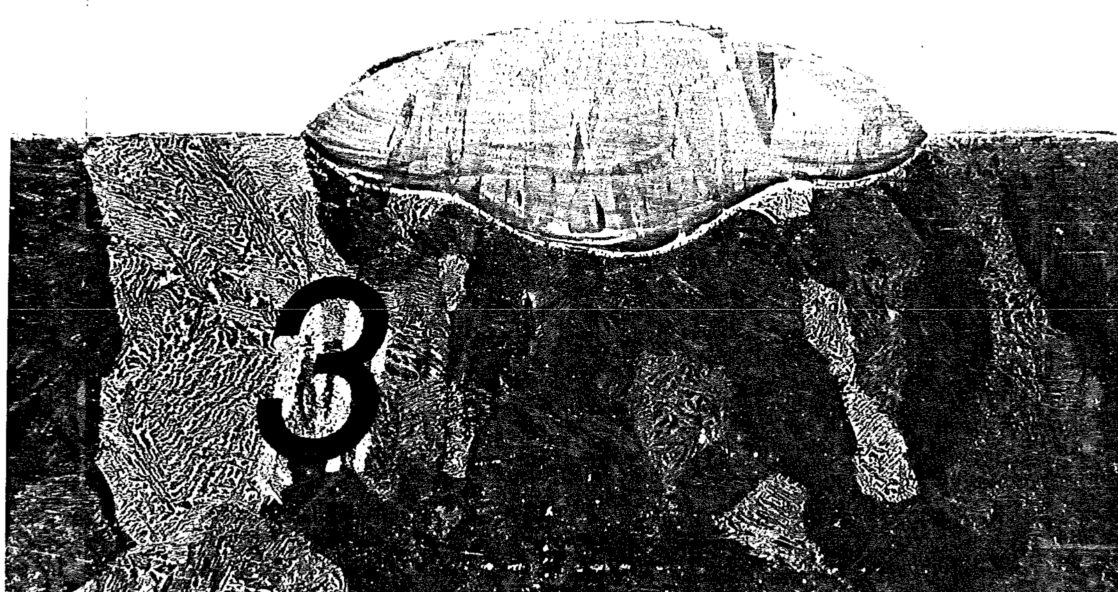

Macrographs (7x) of current welding method (250 A, 28 V, 500 mm/min)

# APPENDIX IV

**Data and photographs of Bead-on-Plate test IV**

# DATASHEET LASPROEF A (S59/INC. 625) A

| Las nr. | Lasspan- ning (V) | Lasstroom (A) | Voortloop- snelheid (mm/min) | Heatinput (kJ/mm) |
|---|---|---|---|---|
| **LAAG 1 :** | S59 Ø 2.0 mm gevulde draad | | | |
| | **28 V** | **280 A** | **420 mm/min** | **1,12 kJ/mm** |
| A1 | 28,1 | 275 | 428 | 1,08 |
| A2 | 28,1 | 274 | 428 | 1,08 |
| A3 | 28,1 | 275 | 428 | 1,08 |
| A4 | 28,2 | 268 | 428 | 1,06 |
| A5 | 28,2 | 269 | 428 | 1,06 |
| A6 | 28,2 | 275 | 428 | 1,09 |
| A7 | – | – | 428 | – |
| **GEM.** | **28,2** | **273** | **428** | **1,08** |
| **LAAG 2 :** | INCONEL 625 Ø 1.6 mm massieve draad (od. param's) | | | |
| | **28 V** | **280 A** | **400 mm/min** | **1,18 kJ/mm** |
| A8 | 28,0 | 284 | 395 | 1,21 |
| A9 | 28,0 | 280 | 395 | 1,19 |
| A10 | 28,0 | 279 | 395 | 1,19 |
| A11 | 27,9 | 279 | 395 | 1,18 |
| A12 | 28,0 | 279 | 395 | 1,19 |
| A13 | 27,9 | 284 | 395 | 1,20 |
| **GEM.** | **28,0** | **281** | **395** | **1,19** |
| **LAAG 3 :** | INCONEL 625 Ø 1.6 mm massieve draad | | | |
| A14 | 27,9 | 280 | 395 | 1,19 |
| A15 | 27,9 | 280 | 395 | 1,19 |
| A16 | 27,9 | 279 | 395 | 1,18 |
| A17 | 27,9 | 279 | 395 | 1,18 |
| A18 | 28,0 | 269 | 395 | 1,14 |
| A19 | 28,0 | 275 | 395 | 1,17 |
| **GEM.** | **27,9** | **277** | **395** | **1,18** |
| **LAAG 4 :** | INCONEL 625 Ø 1.6 mm massieve draad | | | |
| A20 | 27,9 | 279 | 395 | 1,18 |
| A21 | 28,0 | 280 | 395 | 1,19 |
| A22 | 28,0 | 271 | 395 | 1,15 |
| A23 | 28,0 | 278 | 395 | 1,18 |
| A24 | 27,9 | 274 | 395 | 1,16 |
| **GEM.** | **23,3** | **276** | **395** | **1,17** |

## DATASHEET LASPROEF B (S59/INC. 625) **B**

| Las nr. | Lasspan– ning (V) | Lasstroom (A) | Voortloop– snelheid (mm/min) | Heatinput (kJ/mm) |
|---|---|---|---|---|
| **LAAG 1 :** | S59 Ø 2.0 mm gevulde draad | | | |
| | **28 V** | **280 A** | **420 mm/min** | **1,12 kJ/mm** |
| B1 | 28,2 | 272 | 428 | 1,08 |
| B2 | 28,2 | 275 | 428 | 1,09 |
| B3 | 28,2 | 273 | 428 | 1,08 |
| B4 | 28,2 | 272 | 428 | 1,08 |
| B5 | 28,2 | 273 | 428 | 1,08 |
| B6 | 28,2 | 268 | 428 | 1,06 |
| B7 | 28,2 | 269 | 428 | 1,06 |
| **GEM.** | **28,2** | **272** | **428** | **1,07** |
| **LAAG 2 :** | INCONEL 625 Ø 1.6 mm massieve draad (nw. param's) | | | |
| | **28 V** | **250 A** | **500 mm/min** | **0,84 kJ/mm** |
| B8 | – | – | 485 | – |
| B9 | – | – | 485 | – |
| B10 | – | – | 485 | – |
| B11 | 28,3 | 247 | 485 | 0,86 |
| B12 | 28,3 | 246 | 485 | 0,86 |
| B13 | 28,0 | 247 | 485 | 0,86 |
| B14 | 28,0 | 249 | 485 | 0,86 |
| B15 | 28,1 | 247 | 485 | 0,86 |
| **GEM.** | **28,1** | **247** | **485** | **0,86** |
| **LAAG 3 :** | INCONEL 625 Ø 1.6 mm massieve draad | | | |
| B16 | 28,0 | 247 | 485 | 0,86 |
| B17 | 28,1 | 251 | 485 | 0,87 |
| B18 | 28,1 | 247 | 485 | 0,86 |
| B19 | 28,0 | 251 | 485 | 0,87 |
| B20 | 28,1 | 247 | 485 | 0,86 |
| B21 | 28,0 | 249 | 485 | 0,86 |
| **GEM.** | **28,1** | **249** | **485** | **0,86** |
| **LAAG 4 :** | INCONEL 625 Ø 1.6 mm massieve draad | | | |
| B22 | 28,0 | 246 | 485 | 0,85 |
| B23 | 28,0 | 247 | 485 | 0,86 |
| B24 | 28,2 | 247 | 485 | 0,86 |
| B25 | 28 | 239 | 485 | 0,83 |
| B26 | 27,9 | 245 | 485 | 0,85 |
| **GEM.** | **28,0** | **245** | **485** | **0,85** |

## DATASHEET LASPROEF C (Nb–ARM INC. 625)

**C**

| Las nr. | Lasspan–ning (V) | Lasstroom (A) | Voortloop–snelheid (mm/min) | Heatinput (kJ/mm) |
|---|---|---|---|---|
| **LAAG 1 :** | Nb–ARM INCONEL 625 Ø 1.6 mm (gevulde draad) | | | |
| | **28 V** | **250 A** | **500 mm/min** | **0,84 kJ/mm** |
| C1 | 28,1 | 248 | 470 | 0,89 |
| C2 | 28,1 | 249 | 470 | 0,89 |
| C3 | 28,1 | 248 | 470 | 0,89 |
| C4 | 28,0 | 250 | 470 | 0,89 |
| C5 | 28,0 | 252 | 470 | 0,90 |
| C6 | 27,9 | 251 | 470 | 0,89 |
| C7 | 28,1 | 248 | 470 | 0,89 |
| C8 | 28,0 | 252 | 470 | 0,90 |
| **GEM.** | **28,0** | **250** | **470** | **0,89** |
| **LAAG 2 :** | Nb–ARM INCONEL 625 Ø 1.6 mm (gevulde draad) | | | |
| C9 | 28,1 | 250 | 470 | 0,90 |
| C10 | 28,1 | 254 | 470 | 0,91 |
| C11 | 28,2 | 250 | 470 | 0,90 |
| C12 | 28,2 | 239 | 470 | 0,86 |
| C13 | 28,1 | 248 | 470 | 0,89 |
| C14 | 28,0 | 249 | 470 | 0,89 |
| C15 | 28,0 | 252 | 470 | 0,90 |
| **GEM.** | **28,1** | **249** | **470** | **0,89** |
| **LAAG 3 :** | Nb–ARM INCONEL 625 Ø 1.6 mm (gevulde draad) | | | |
| C16 | 28,0 | 253 | 470 | 0,90 |
| C17 | 28,0 | 253 | 470 | 0,90 |
| C18 | 28,1 | 248 | 470 | 0,89 |
| C19 | 28,1 | 246 | 470 | 0,88 |
| C20 | 28,1 | 248 | 470 | 0,89 |
| C21 | 28,0 | 248 | 470 | 0,89 |
| **GEM.** | **28,1** | **249** | **470** | **0,89** |
| **LAAG 4 :** | Nb–ARM INCONEL 625 Ø 1.6 mm (gevulde draad) | | | |
| C22 | 28,1 | 250 | 470 | 0,90 |
| C23 | 28,1 | 253 | 470 | 0,91 |
| C24 | 28,1 | 247 | 470 | 0,89 |
| C25 | 28,1 | 246 | 470 | 0,88 |
| C26 | 28,0 | 246 | 470 | 0,88 |
| **GEM.** | **28,1** | **248** | **470** | **0,89** |

## DATASHEET LASPROEF D (HASTELLOY C−4)

# D

| Las nr. | Lasspan–ning (V) | Lasstroom (A) | Voortloop–snelheid (mm/min) | Heatinput (kJ/mm) |
|---|---|---|---|---|
| **LAAG 1 :** | HASTELLOY C−4 Ø 1.6 mm | | | |
| | **28 V** | **250 A** | **500 mm/min** | **0,84 kJ/mm** |
| D1 | 28,3 | 245 | 475 | 0,88 |
| D2 | 28,0 | 249 | 475 | 0,88 |
| D3 | 28,0 | 251 | 475 | 0,89 |
| D4 | 27,9 | 252 | 475 | 0,89 |
| D5 | 27,9 | 247 | 475 | 0,87 |
| D6 | 27,9 | 251 | 475 | 0,88 |
| D7 | 27,9 | 250 | 475 | 0,88 |
| **GEM.** | **28,0** | **249** | **475** | **0,88** |
| **LAAG 2 :** | HASTELLOY C−4 Ø 1.6 mm | | | |
| D8 | 28,0 | 248 | 475 | 0,88 |
| D9 | 28,0 | 244 | 475 | 0,86 |
| D10 | 28,0 | 248 | 475 | 0,88 |
| D11 | 27,9 | 245 | 475 | 0,86 |
| D12 | 27,8 | 247 | 475 | 0,87 |
| D13 | 28,0 | 250 | 475 | 0,88 |
| **GEM.** | **28,0** | **247** | **475** | **0,87** |
| **LAAG 3 :** | HASTELLOY C−4 Ø 1.6 mm | | | |
| D14 | 28,7 | 245 | 475 | 0,89 |
| D15 | 28,3 | 244 | 475 | 0,87 |
| D16 | 28,0 | 243 | 475 | 0,86 |
| D17 | 28,4 | 239 | 475 | 0,86 |
| D18 | 28,3 | 245 | 475 | 0,88 |
| **GEM.** | **28,3** | **243** | **475** | **0,87** |
| **LAAG 4 :** | HASTELLOY C−4 Ø 1.6 mm | | | |
| D19 | 28,5 | 246 | 475 | 0,89 |
| D20 | 28,5 | 247 | 475 | 0,89 |
| D21 | 28,2 | 247 | 475 | 0,88 |
| D22 | 28,3 | 249 | 475 | 0,89 |
| **GEM.** | **28,4** | **247** | **475** | **0,89** |

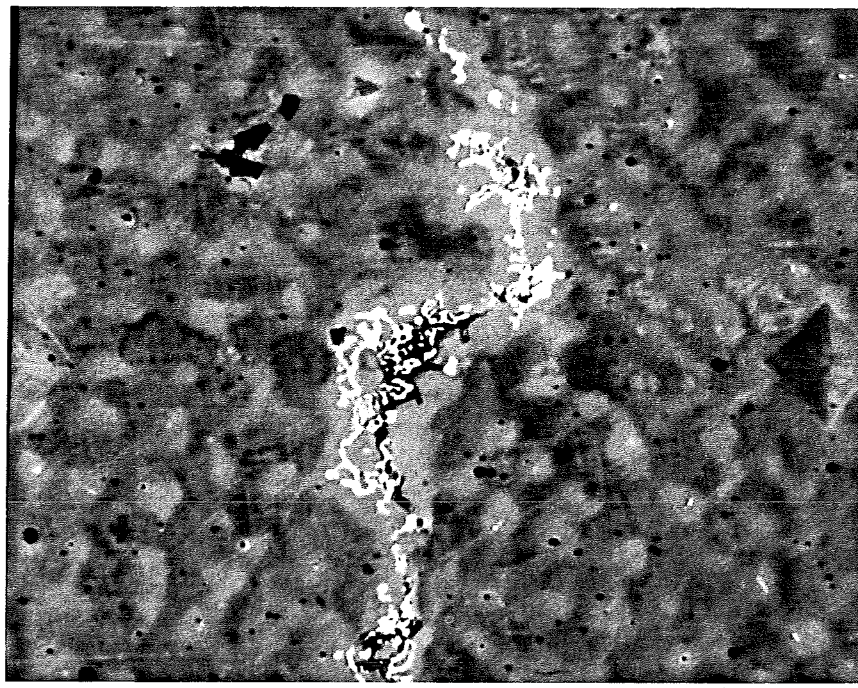

BEI-H photograph (1000x) of scan 1

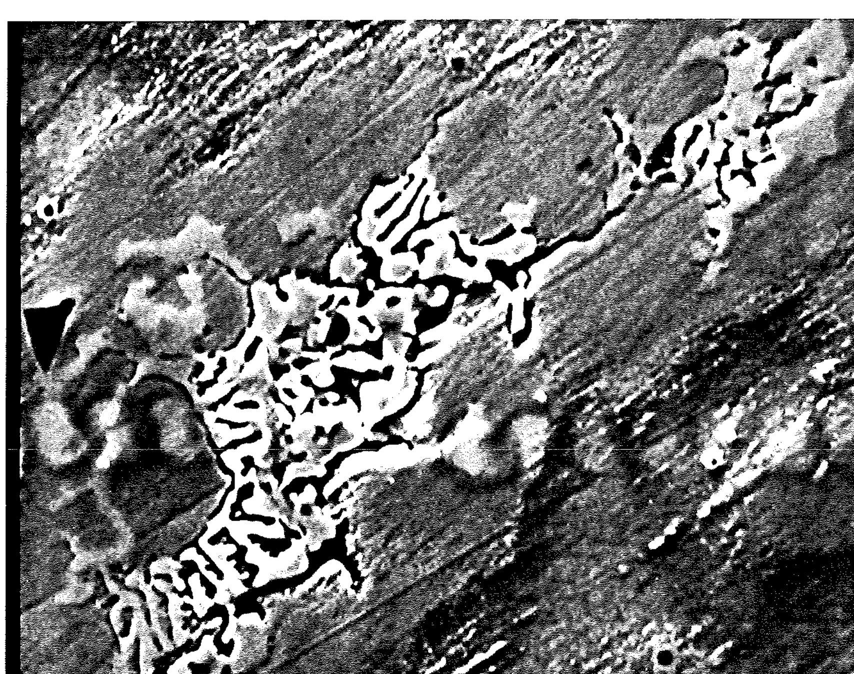

SEM photograph (4000x) of scan 1

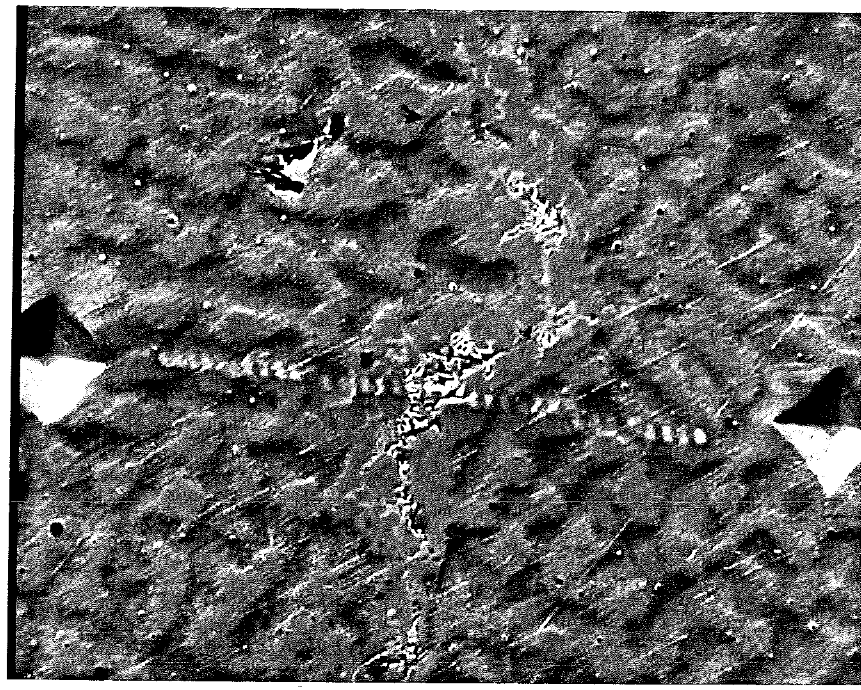

SEM photograph (1000x) of scan 1

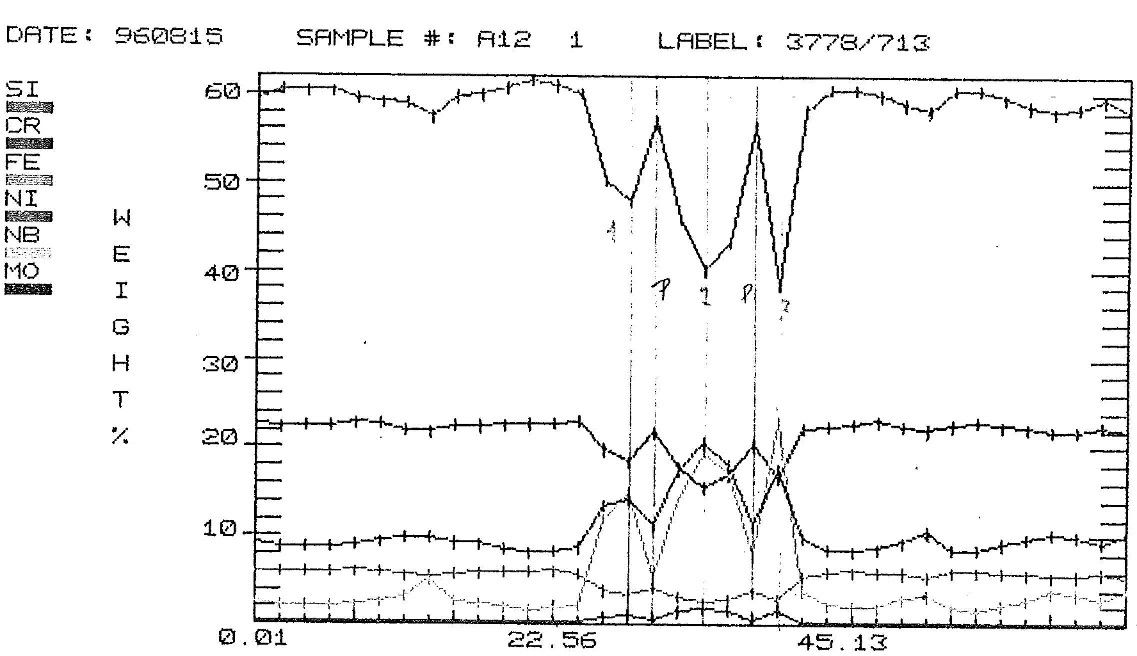


EPMA of scan 1

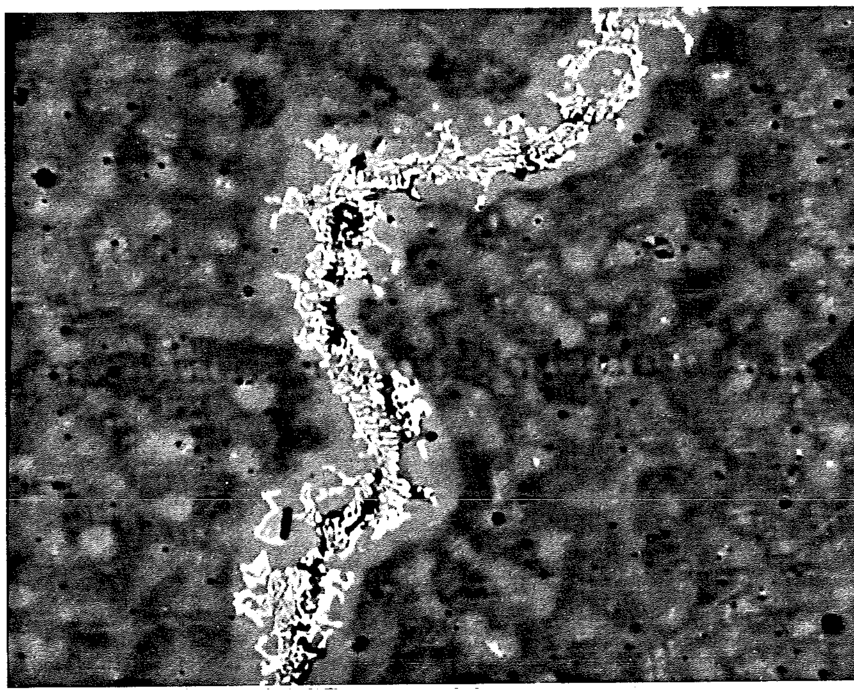

BEI-H photograph (1000x) of scan 2

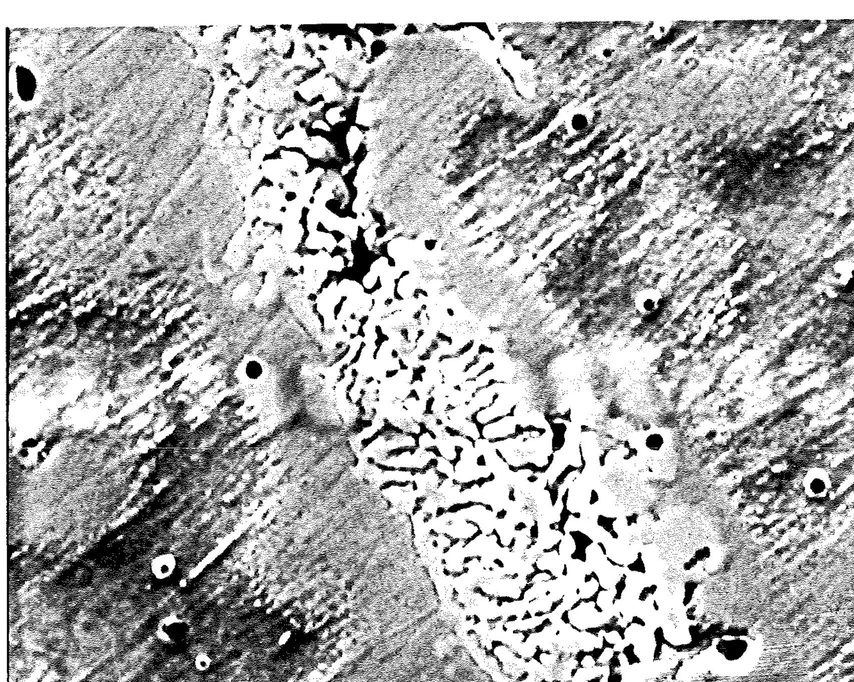

SEM photograph (4000x) of scan 2

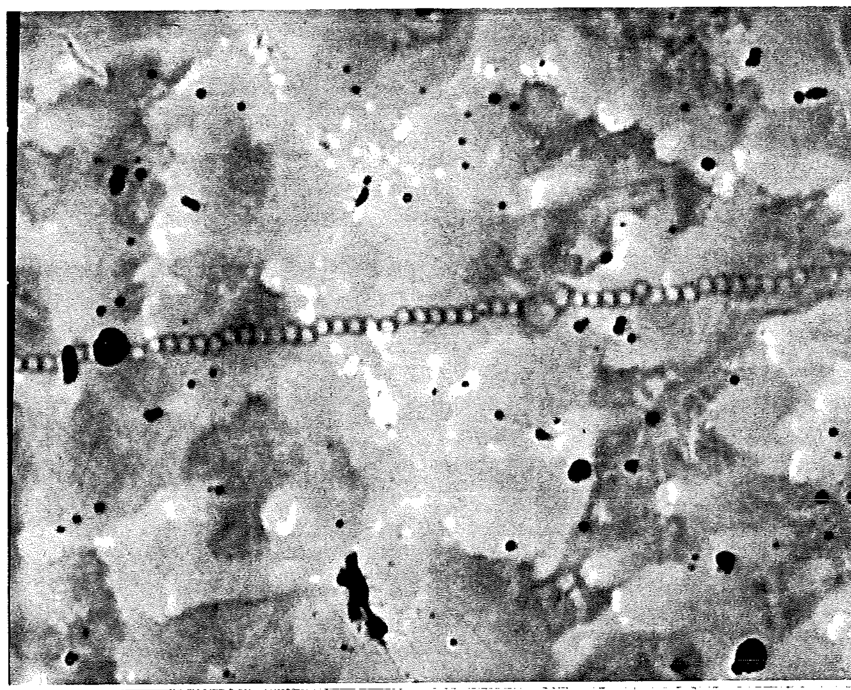

BEI-H photograph (1000x) of scan 3

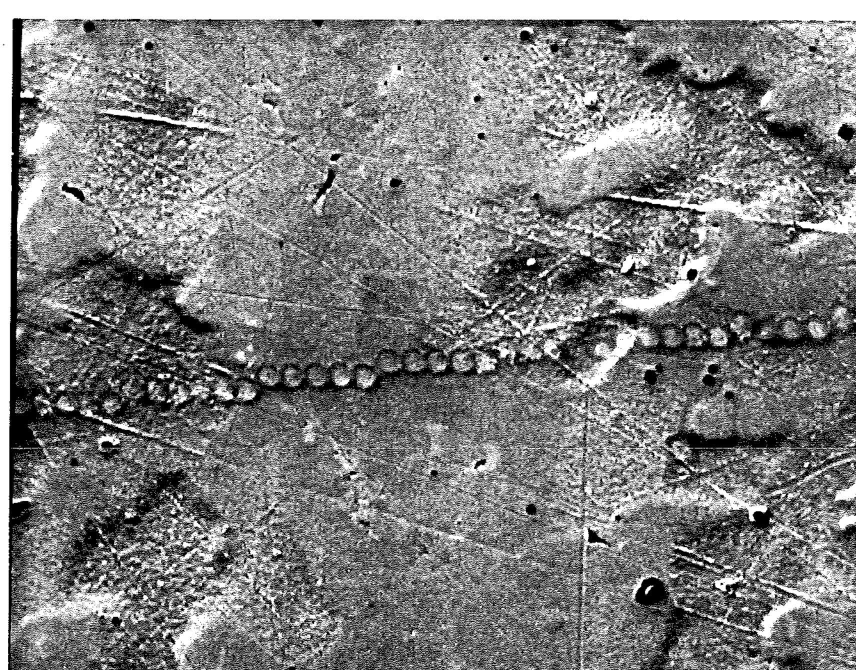

SEM photograph (1500x) of scan 3

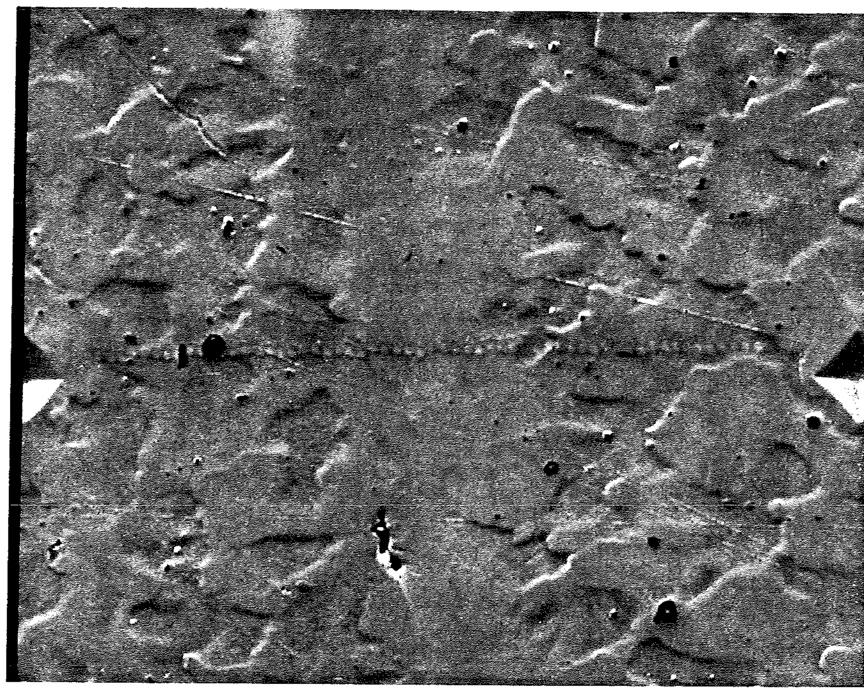

SEM photograph (720x) of scan 3

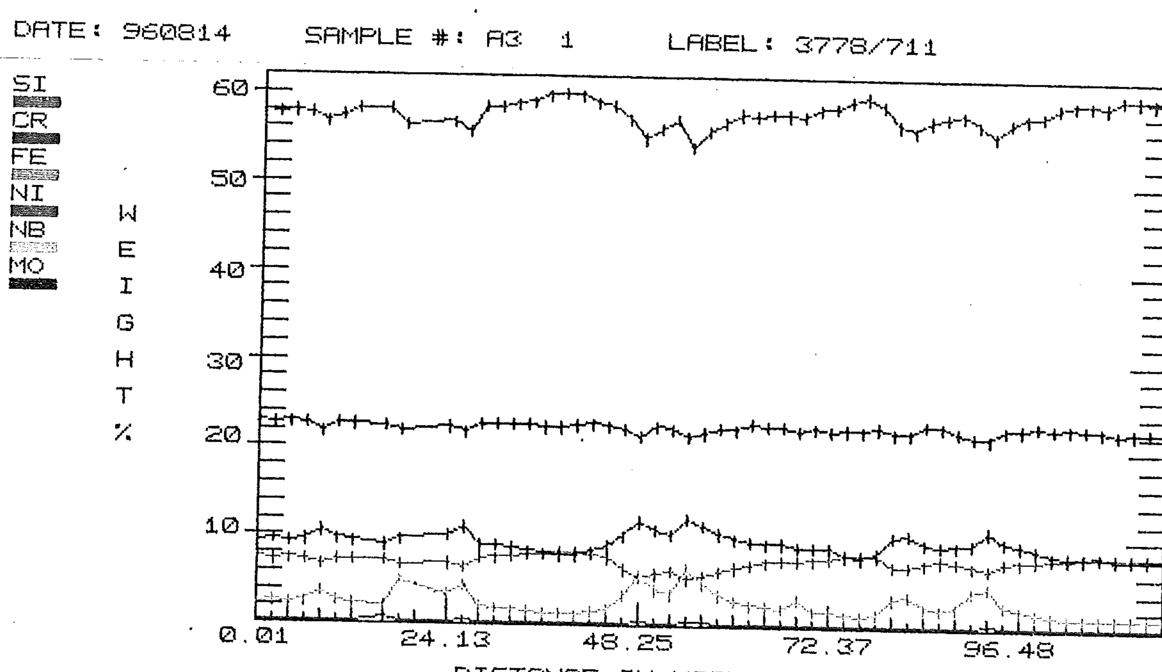


EPMA scan 3

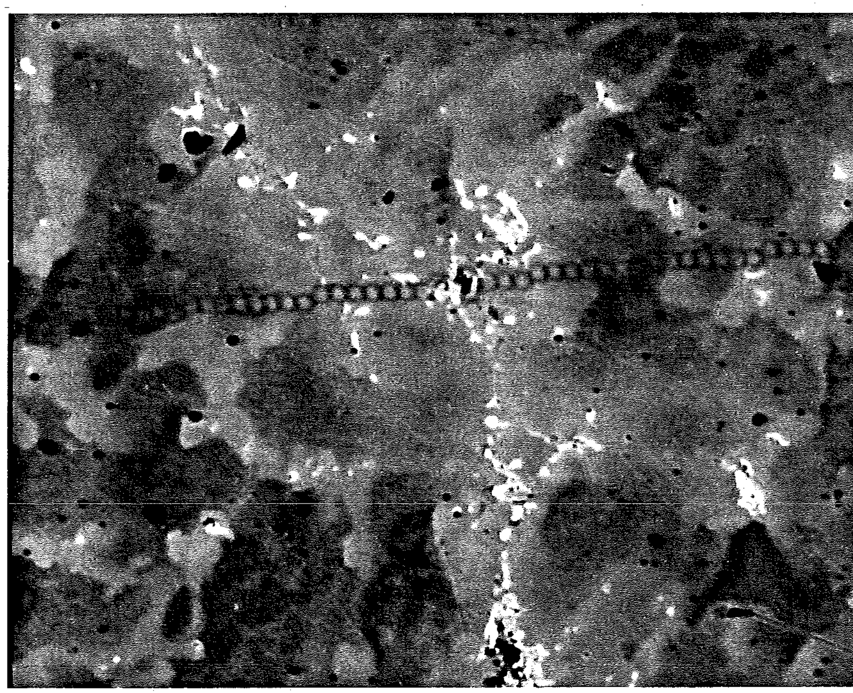

BEI-H photograph (1000x) of scan 4

SEM photograph (1200x) of scan 4

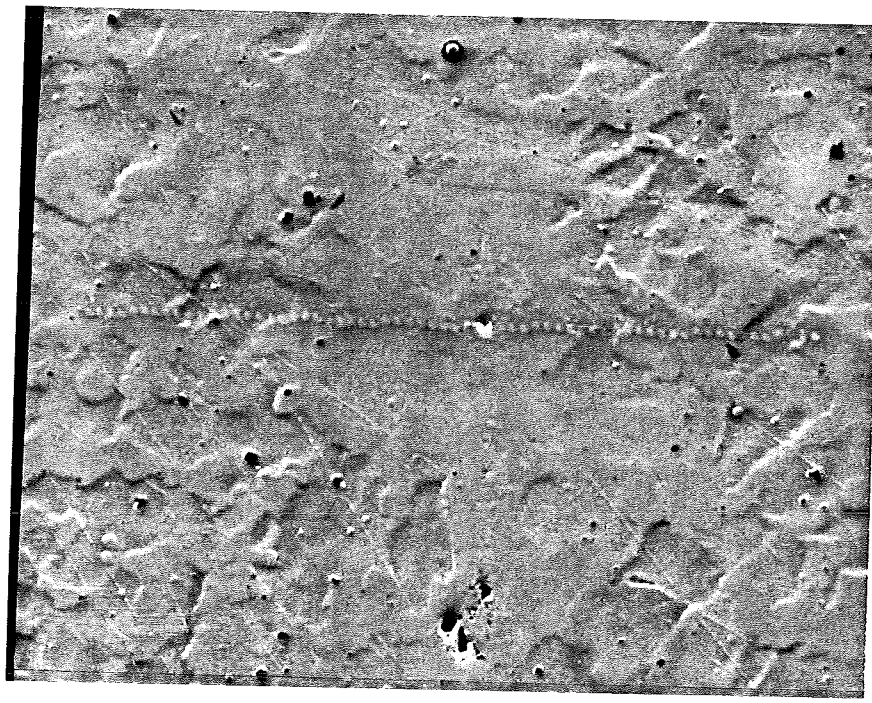

SEM photograph (720x) of scan 4

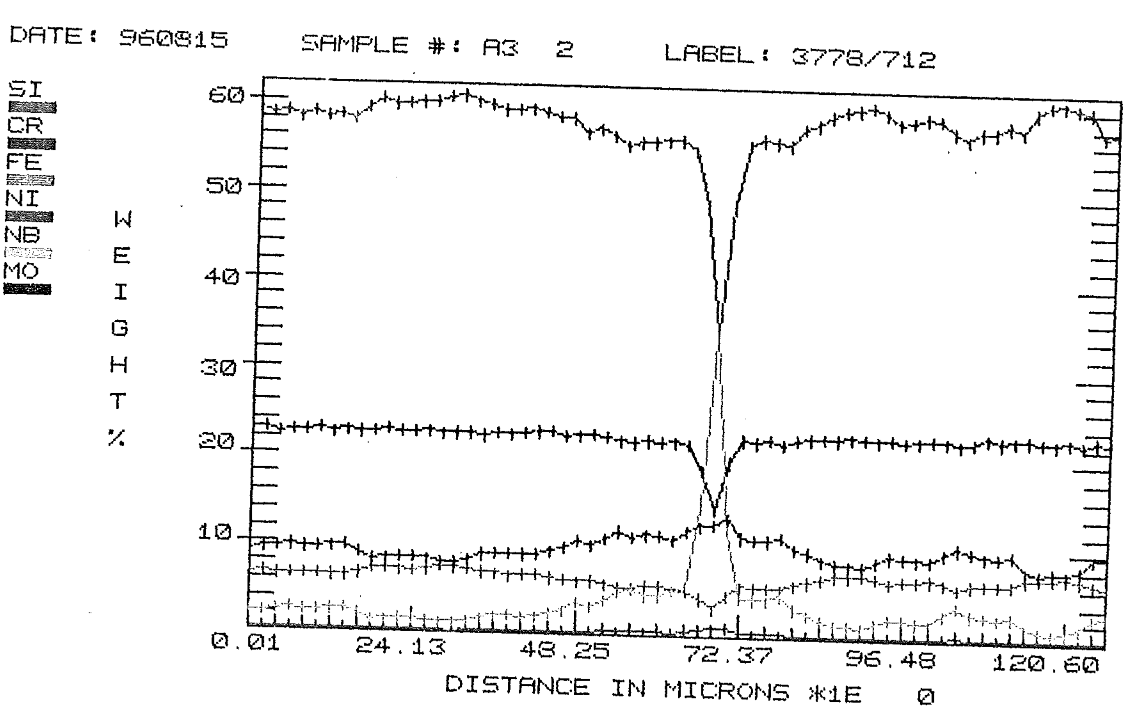


EPMA scan 4

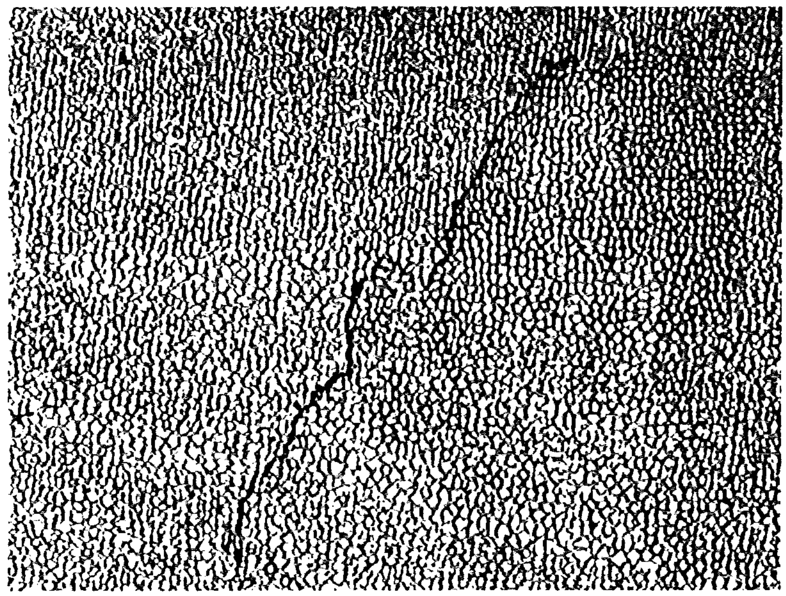

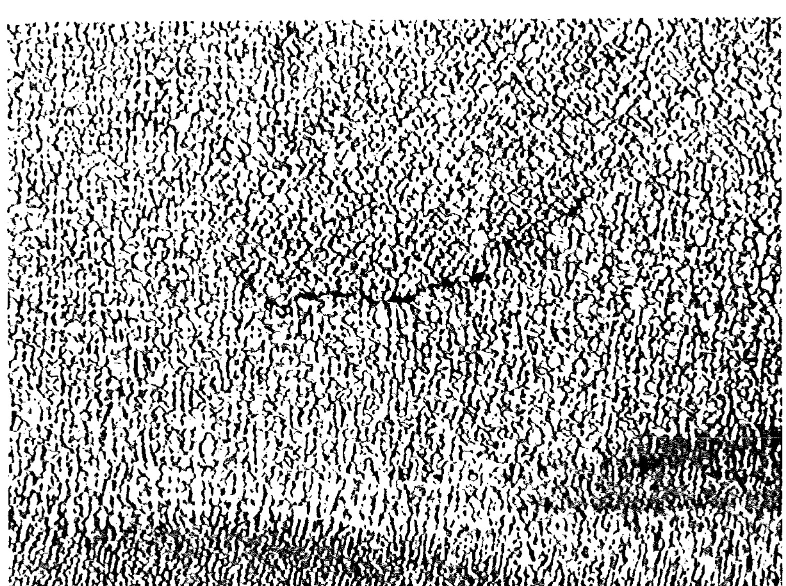

Fissures in Specimen C4 (Low niobium Inconel 625)
Photographs 85x

Fissure in specimen B3 (possible hot-crack)

85x

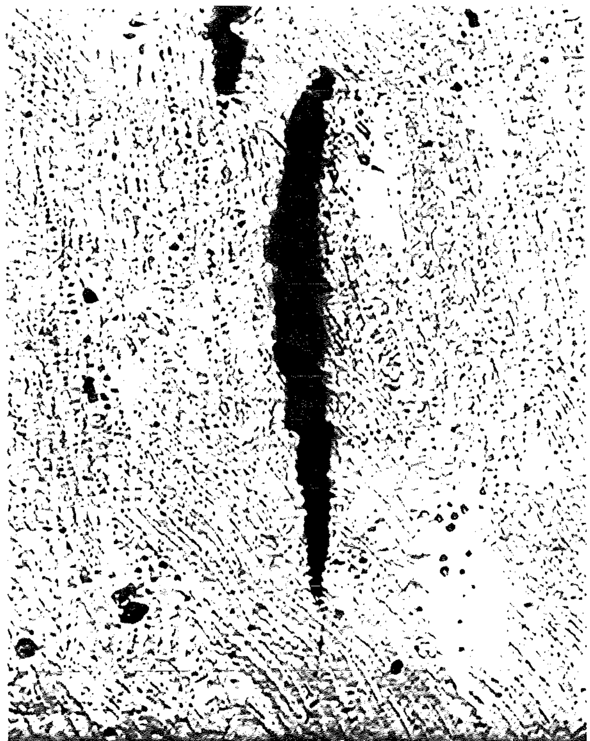

170x

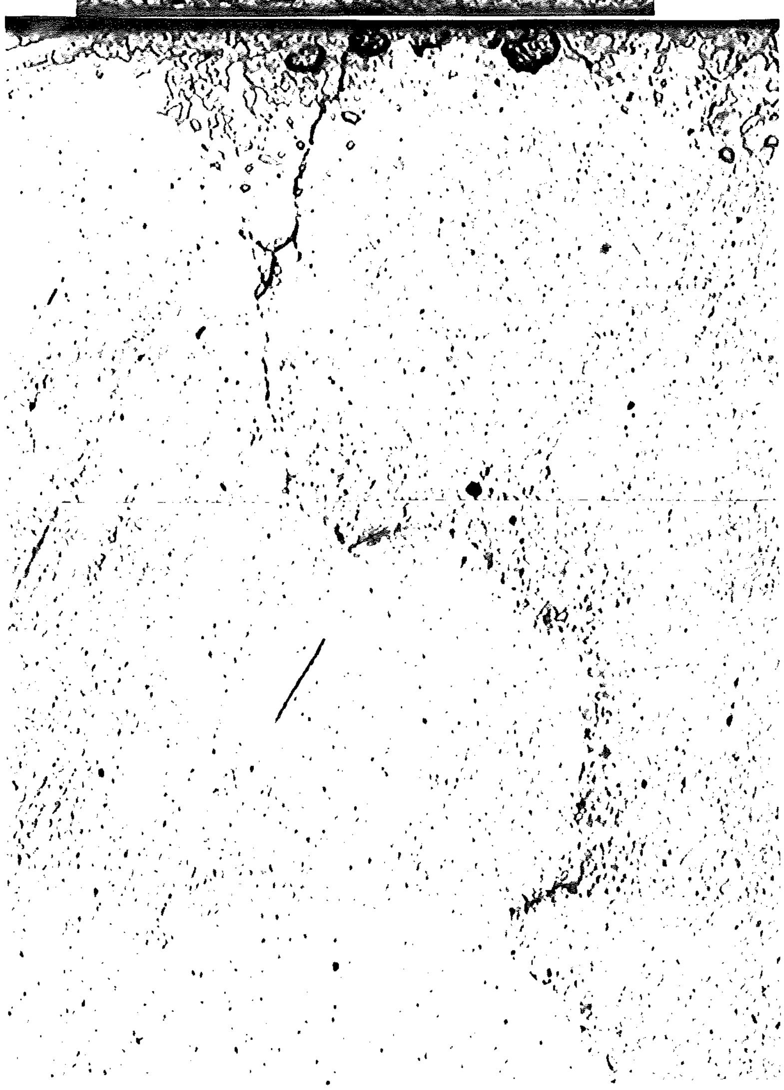

Data of scan 1

| POINT | MICRONS | SI-K | CR-K | FE-K | NI-K | NB-L | MO-L | TOTAL | |
|---|---|---|---|---|---|---|---|---|---|
| 1 | 0.1 | 0.26 | 22.63 | 5.91 | 59.39 | 2.57 | 9.24 | 100.00 | |
| 2 | 1.9 | 0.26 | 22.31 | 6.02 | 60.44 | 2.15 | 8.82 | 100.00 | |
| 3 | 3.8 | 0.26 | 22.43 | 6.01 | 60.35 | 2.12 | 8.85 | 100.01 | |
| 4 | 5.7 | 0.27 | 22.44 | 6.01 | 60.36 | 2.10 | 8.82 | 100.00 | |
| 5 | 7.6 | 0.30 | 22.83 | 6.09 | 59.48 | 2.23 | 9.07 | 100.00 | |
| 6 | 9.5 | 0.30 | 22.69 | 5.98 | 59.07 | 2.51 | 9.45 | 100.00 | |
| 7 | 11.3 | 0.41 | 21.92 | 5.58 | 58.97 | 3.24 | 9.89 | 100.01 | |
| 8 | 13.2 | 0.33 | 21.79 | 5.54 | 57.31 | 5.15 | 9.88 | 100.00 | |
| 9 | 15.1 | 0.28 | 22.42 | 5.73 | 59.61 | 2.69 | 9.28 | 100.00 | |
| 10 | 17.0 | 0.29 | 22.35 | 5.84 | 59.91 | 2.42 | 9.20 | 100.01 | |
| 11 | 18.9 | 0.25 | 22.57 | 6.00 | 60.65 | 2.01 | 8.54 | 100.01 | |
| 12 | 20.7 | 0.20 | 22.60 | 6.05 | 61.49 | 1.51 | 8.15 | 99.99 | |
| 13 | 22.6 | 0.23 | 22.70 | 6.08 | 60.92 | 1.72 | 8.37 | 100.01 | |
| 14 | 24.5 | 0.32 | 22.96 | 5.81 | 59.99 | 2.21 | 8.73 | 100.01 | |
| 15 | 26.4 | 0.87 | 19.81 | 3.87 | 50.21 | 11.84 | 13.42 | 100.00 | |
| 16 | 28.2 | 1.10 | 18.46 | 3.37 | 47.92 | 14.91 | 14.26 | 100.01 | 1 |
| 17 | 30.1 | 0.45 | 21.77 | 4.27 | 56.82 | 5.43 | 11.26 | 100.00 | |
| 18 | 32.0 | 1.52 | 17.87 | 3.19 | 45.93 | 14.09 | 17.40 | 99.99 | |
| 19 | 33.9 | 1.95 | 15.52 | 2.51 | 40.11 | 19.33 | 20.58 | 100.00 | 2 - Laves |
| 20 | 35.8 | 1.58 | 16.89 | 2.88 | 43.33 | 17.33 | 17.99 | 100.00 | |
| 21 | 37.7 | 0.52 | 20.28 | 3.78 | 56.26 | 7.93 | 11.23 | 100.00 | |
| 22 | 39.5 | 1.59 | 16.70 | 2.97 | 38.40 | 22.87 | 17.46 | 99.99 | 3 |
| 23 | 41.4 | 0.41 | 22.25 | 5.51 | 58.23 | 3.80 | 9.81 | 100.00 | |
| 24 | 43.3 | 0.26 | 22.43 | 6.06 | 60.52 | 2.22 | 8.52 | 100.00 | |
| 25 | 45.2 | 0.26 | 22.67 | 6.13 | 60.51 | 2.03 | 8.39 | 99.99 | |
| 26 | 47.1 | 0.31 | 23.08 | 6.03 | 59.88 | 2.01 | 8.70 | 100.01 | |
| 27 | 48.9 | 0.36 | 22.42 | 5.89 | 58.88 | 3.01 | 9.46 | 100.01 | |
| 28 | 50.8 | 0.39 | 22.08 | 5.54 | 58.14 | 3.35 | 10.51 | 100.00 | |
| 29 | 52.7 | 0.23 | 22.64 | 6.10 | 60.50 | 1.97 | 8.57 | 100.00 | |
| 30 | 54.6 | 0.24 | 22.95 | 6.11 | 60.47 | 1.69 | 8.55 | 100.00 | |
| 31 | 56.4 | 0.36 | 22.52 | 5.98 | 59.58 | 2.30 | 9.26 | 100.00 | |
| 32 | 58.3 | 0.36 | 22.32 | 5.87 | 58.62 | 2.92 | 9.90 | 99.99 | |
| 33 | 60.2 | 0.35 | 21.92 | 5.56 | 58.03 | 3.81 | 10.34 | 100.01 | |
| 34 | 62.1 | 0.33 | 21.92 | 5.64 | 58.44 | 3.60 | 10.09 | 100.01 | |
| ~~35~~ | ~~64.0~~ | ~~0.31~~ | ~~22.43~~ | ~~5.88~~ | ~~59.29~~ | ~~2.81~~ | ~~9.29~~ | ~~100.01~~ | |
| 36 | 65.8 | 0.37 | 21.90 | 5.43 | 58.06 | 4.01 | 10.23 | 100.00 | |

Data of scan 2

| POINT | MICRONS | SI-K | CR-K | FE-K | NI-K | NB-L | MO-L | TOTAL |
|---|---|---|---|---|---|---|---|---|
| 1 | 0.1 | 0.23 | 22.51 | 5.91 | 58.03 | 4.28 | 9.05 | 100.00 |
| 2 | 2.1 | 0.32 | 22.70 | 5.87 | 58.16 | 3.10 | 9.85 | 99.99 |
| 3 | 4.1 | 0.30 | 22.87 | 5.94 | 58.85 | 2.78 | 9.27 | 100.00 |
| 4 | 6.1 | 0.26 | 22.65 | 6.21 | 59.96 | 2.12 | 8.81 | 100.00 |
| 5 | 8.0 | 0.33 | 23.01 | 6.40 | 59.20 | 2.08 | 8.98 | 100.00 |
| 6 | 10.0 | 0.22 | 22.73 | 6.24 | 60.50 | 1.79 | 8.53 | 100.00 |
| 7 | 12.0 | 0.26 | 22.61 | 6.00 | 59.66 | 2.19 | 9.30 | 100.01 |
| 8 | 14.0 | 0.33 | 22.27 | 5.70 | 58.32 | 3.85 | 9.52 | 100.00 |
| 9 | 16.0 | 0.34 | 22.03 | 5.67 | 58.52 | 3.29 | 10.15 | 100.00 |
| 10 | 18.0 | 0.43 | 21.79 | 5.28 | 56.38 | 4.94 | 11.18 | 100.00 |
| 11 | 20.0 | 0.37 | 22.02 | 5.58 | 58.15 | 3.56 | 10.32 | 100.00 |
| 12 | 22.0 | 0.32 | 22.46 | 5.70 | 58.63 | 2.97 | 9.93 | 100.02 |
| 13 | 24.0 | 0.29 | 22.93 | 5.80 | 58.85 | 2.58 | 9.56 | 100.01 |
| 14 | 26.0 | 0.28 | 22.97 | 6.00 | 58.84 | 2.62 | 9.29 | 100.00 |
| 15 | 28.0 | 0.29 | 22.53 | 5.91 | 59.45 | 2.42 | 9.40 | 100.00 |
| 16 | 30.0 | 0.27 | 22.89 | 5.91 | 59.09 | 2.38 | 9.46 | 100.00 |
| 17 | 32.1 | 0.30 | 22.57 | 5.78 | 59.11 | 2.67 | 9.57 | 100.00 |
| 18 | 34.1 | 0.39 | 21.57 | 4.88 | 56.21 | 6.23 | 10.73 | 100.01 |
| 19 | 36.1 | 0.89 | 19.50 | 3.35 | 50.65 | 11.31 | 14.30 | 100.00 |
| 20 | 38.1 | 1.28 | 18.05 | 2.94 | 47.71 | 13.27 | 16.75 | 100.00 |
| 21 | 40.1 | 1.17 | 18.19 | 2.98 | 48.43 | 12.90 | 16.34 | 100.01 |
| 22 | 42.1 | 0.94 | 18.95 | 3.12 | 48.63 | 13.62 | 14.76 | 100.01 |
| 23 | 44.1 | 0.49 | 21.07 | 3.92 | 55.66 | 7.02 | 11.84 | 100.00 |
| 24 | 46.1 | 0.43 | 21.47 | 5.07 | 56.98 | 4.70 | 11.35 | 100.00 |
| 25 | 48.1 | 0.30 | 22.71 | 6.17 | 58.71 | 2.66 | 9.46 | 100.01 |
| 26 | 50.1 | 0.33 | 22.40 | 6.07 | 57.98 | 3.12 | 10.09 | 99.99 |
| 27 | 52.1 | 0.28 | 22.54 | 6.08 | 58.98 | 2.73 | 9.40 | 100.01 |
| 28 | 54.1 | 0.20 | 22.84 | 6.50 | 60.03 | 1.83 | 8.62 | 100.00 |
| 29 | 56.1 | 0.25 | 22.97 | 6.29 | 59.56 | 1.96 | 8.98 | 100.00 |
| 30 | 58.1 | 0.33 | 22.68 | 6.05 | 58.80 | 2.80 | 9.34 | 99.99 |
| 31 | 60.1 | 0.34 | 22.06 | 5.75 | 58.24 | 3.44 | 10.17 | 100.00 |
| 32 | 62.1 | 0.31 | 22.19 | 5.94 | 58.50 | 3.12 | 9.95 | 100.00 |
| 33 | 64.1 | 0.19 | 22.23 | 6.47 | 61.02 | 1.65 | 8.45 | 99.99 |
| 34 | 66.1 | 0.21 | 22.60 | 6.24 | 60.57 | 1.69 | 8.70 | 100.00 |
| 35 | 68.1 | 0.28 | 22.48 | 6.02 | 59.77 | 2.10 | 9.35 | 100.01 |
| 36 | 70.1 | 0.39 | 22.18 | 5.47 | 56.95 | 4.60 | 10.42 | 100.00 |
| 37 | 72.1 | 0.37 | 21.67 | 5.45 | 57.32 | 4.50 | 10.70 | 100.00 |
| 38 | 74.1 | 0.32 | 22.02 | 5.66 | 58.63 | 3.32 | 10.04 | 100.00 |
| 39 | 76.1 | 0.27 | 22.49 | 6.12 | 59.93 | 2.29 | 8.91 | 100.01 |
| 40 | 78.1 | 0.30 | 22.67 | 5.92 | 59.18 | 2.60 | 9.34 | 100.00 |
| 41 | 80.1 | 0.37 | 21.80 | 5.54 | 57.96 | 4.09 | 10.26 | 100.01 |
| 42 | 82.1 | 0.33 | 22.20 | 5.69 | 58.26 | 3.47 | 10.04 | 100.00 |
| 43 | 84.1 | 0.28 | 22.51 | 5.91 | 59.07 | 2.74 | 9.48 | 100.00 |
| 44 | 86.1 | 0.29 | 22.65 | 5.86 | 59.10 | 2.62 | 9.48 | 100.00 |
| 45 | 88.1 | 0.36 | 22.12 | 5.63 | 58.23 | 3.42 | 10.24 | 100.00 |

Laves

## Data of scan 3

| POINT | MICRONS | SI-K | CR-K | FE-K | NI-K | NB-L | MO-L | TOTAL |
|---|---|---|---|---|---|---|---|---|
| 1 | 0.1 | 0.27 | 22.88 | 7.43 | 57.87 | 2.35 | 9.23 | 100.01 |
| 2 | 2.1 | 0.30 | 22.64 | 7.22 | 57.67 | 2.54 | 9.63 | 100.00 |
| 3 | 4.1 | 0.27 | 22.79 | 7.41 | 57.83 | 2.30 | 9.39 | 100.00 |
| 4 | 6.1 | 0.31 | 22.74 | 7.29 | 57.65 | 2.49 | 9.52 | 100.00 |
| 5 | 8.1 | 0.41 | 21.78 | 6.79 | 56.75 | 3.73 | 10.55 | 100.01 |
| 6 | 10.1 | 0.28 | 22.66 | 7.30 | 57.42 | 2.66 | 9.68 | 100.00 |
| 7 | 12.1 | 0.27 | 22.60 | 7.28 | 58.14 | 2.30 | 9.42 | 100.02 |
| 9 | 16.1 | 0.71 | 22.49 | 7.35 | 58.22 | 2.21 | 9.02 | 100.00 |
| 10 | 18.1 | 0.32 | 22.00 | 6.74 | 56.35 | 4.92 | 9.67 | 100.00 |
| 13 | 24.2 | 0.35 | 22.37 | 6.97 | 56.70 | 3.47 | 10.14 | 100.00 |
| 14 | 26.2 | 0.43 | 21.80 | 6.54 | 55.66 | 4.50 | 11.07 | 100.00 |
| 15 | 28.2 | 0.26 | 22.69 | 7.52 | 58.45 | 2.07 | 9.01 | 100.00 |
| 16 | 30.2 | 0.24 | 22.71 | 7.66 | 58.37 | 1.90 | 9.12 | 99.99 |
| 17 | 32.2 | 0.23 | 22.77 | 7.75 | 58.78 | 1.76 | 8.73 | 100.00 |
| 18 | 34.2 | 0.22 | 22.77 | 8.06 | 59.02 | 1.53 | 8.42 | 100.01 |
| 19 | 36.2 | 0.20 | 22.38 | 8.09 | 59.80 | 1.37 | 8.17 | 100.00 |
| 20 | 38.2 | 0.20 | 22.38 | 8.21 | 59.95 | 1.29 | 7.98 | 100.01 |
| 21 | 40.3 | 0.18 | 22.60 | 8.23 | 59.81 | 1.21 | 7.99 | 100.00 |
| 22 | 42.3 | 0.22 | 22.78 | 8.01 | 59.03 | 1.58 | 8.41 | 100.01 |
| 23 | 44.3 | 0.26 | 22.56 | 7.72 | 58.64 | 1.85 | 8.99 | 100.01 |
| 24 | 46.3 | 0.35 | 22.26 | 6.45 | 57.25 | 3.47 | 10.21 | 100.00 |
| 25 | 48.3 | 0.52 | 21.37 | 5.49 | 54.99 | 5.79 | 11.84 | 100.00 |
| 26 | 50.3 | 0.41 | 22.56 | 5.90 | 56.15 | 4.10 | 10.89 | 100.01 |
| 27 | 52.3 | 0.36 | 22.30 | 6.25 | 57.10 | 3.57 | 10.43 | 100.01 |
| 28 | 54.3 | 0.55 | 21.42 | 5.34 | 54.05 | 6.52 | 12.13 | 100.01 |
| 29 | 56.3 | 0.47 | 21.84 | 5.65 | 55.81 | 4.88 | 11.35 | 100.00 |
| 30 | 58.3 | 0.37 | 22.46 | 6.21 | 56.84 | 3.60 | 10.52 | 99.99 |
| 31 | 60.3 | 0.32 | 22.32 | 6.70 | 57.80 | 2.94 | 9.93 | 100.01 |
| 32 | 62.4 | 0.29 | 22.97 | 7.06 | 57.61 | 2.49 | 9.59 | 100.00 |
| 33 | 64.4 | 0.27 | 22.72 | 7.38 | 57.91 | 2.29 | 9.43 | 100.00 |
| 34 | 66.4 | 0.26 | 22.77 | 7.52 | 57.83 | 2.10 | 9.53 | 100.00 |
| 35 | 68.4 | 0.25 | 22.20 | 7.60 | 57.65 | 3.19 | 9.13 | 100.01 |
| 36 | 70.4 | 0.25 | 22.54 | 7.64 | 58.55 | 1.91 | 9.13 | 100.01 |
| 37 | 72.4 | 0.26 | 22.21 | 7.76 | 58.73 | 1.92 | 9.13 | 100.00 |
| 38 | 74.4 | 0.22 | 22.34 | 8.23 | 59.52 | 1.47 | 8.23 | 100.00 |
| 39 | 76.4 | 0.18 | 22.29 | 8.35 | 59.85 | 1.35 | 7.99 | 100.00 |
| 40 | 78.4 | 0.21 | 22.62 | 8.13 | 58.90 | 1.67 | 8.48 | 100.00 |
| 41 | 80.5 | 0.39 | 22.06 | 7.05 | 56.79 | 3.35 | 10.38 | 100.01 |
| 42 | 82.5 | 0.39 | 22.06 | 7.05 | 56.23 | 3.67 | 10.62 | 100.00 |
| 43 | 84.5 | 0.29 | 22.91 | 7.41 | 57.33 | 2.51 | 9.55 | 100.00 |
| 44 | 86.5 | 0.27 | 22.82 | 7.68 | 57.72 | 2.15 | 9.37 | 100.01 |
| 45 | 88.5 | 0.28 | 22.22 | 7.54 | 58.02 | 2.51 | 9.45 | 100.01 |
| 46 | 90.5 | 0.39 | 21.68 | 7.11 | 57.01 | 4.19 | 9.63 | 100.00 |
| 47 | 92.5 | 0.43 | 21.50 | 6.75 | 55.55 | 4.76 | 11.03 | 100.01 |
| 48 | 94.5 | 0.29 | 22.53 | 7.50 | 57.21 | 2.62 | 9.87 | 100.00 |
| 49 | 96.5 | 0.28 | 22.59 | 7.65 | 57.74 | 2.26 | 9.49 | 100.00 |
| 50 | 98.5 | 0.26 | 22.96 | 7.81 | 57.97 | 1.95 | 9.05 | 100.00 |
| 51 | 100.6 | 0.23 | 22.68 | 8.10 | 59.00 | 1.56 | 8.45 | 100.00 |
| 52 | 102.6 | 0.20 | 22.80 | 8.12 | 59.30 | 1.40 | 8.20 | 100.00 |
| 53 | 104.6 | 0.20 | 22.76 | 8.15 | 59.30 | 1.35 | 8.24 | 100.00 |
| 54 | 106.6 | 0.22 | 22.58 | 8.27 | 59.12 | 1.42 | 8.40 | 100.00 |
| 55 | 108.6 | 0.19 | 22.26 | 8.31 | 59.93 | 1.30 | 8.02 | 100.00 |
| 56 | 110.6 | 0.18 | 22.38 | 8.24 | 59.88 | 1.27 | 8.06 | 100.00 |
| 57 | 112.6 | 0.20 | 22.46 | 8.26 | 59.65 | 1.31 | 8.14 | 100.00 |
| 58 | 114.6 | 0.19 | 22.51 | 8.29 | 59.45 | 1.37 | 8.20 | 100.00 |

## Data of scan 4

| POINT | MICRONS | SI-K | CR-K | FE-K | NI-K | NB-L | MO-L | TOTAL |
|---|---|---|---|---|---|---|---|---|
| 1 | 0.1 | 0.26 | 22.99 | 6.56 | 58.87 | 2.21 | 9.12 | 100.00 |
| 2 | 2.1 | 0.32 | 22.95 | 6.71 | 58.42 | 2.17 | 9.42 | 100.00 |
| 3 | 4.1 | 0.34 | 22.49 | 6.44 | 58.73 | 2.39 | 9.62 | 100.00 |
| 4 | 6.1 | 0.32 | 22.70 | 6.49 | 57.99 | 2.71 | 9.79 | 100.00 |
| 5 | 8.1 | 0.29 | 22.69 | 6.47 | 58.67 | 2.35 | 9.53 | 100.00 |
| 6 | 10.1 | 0.30 | 22.95 | 6.57 | 58.12 | 2.46 | 9.62 | 100.00 |
| 7 | 12.1 | 0.31 | 22.57 | 6.45 | 58.42 | 2.55 | 9.71 | 100.01 |
| 8 | 14.1 | 0.32 | 22.84 | 6.45 | 57.86 | 2.73 | 9.80 | 100.00 |
| 9 | 16.1 | 0.27 | 22.59 | 6.71 | 59.21 | 2.14 | 9.09 | 100.00 |
| 10 | 18.1 | 0.23 | 22.73 | 7.29 | 60.20 | 1.34 | 8.23 | 100.01 |
| 11 | 20.2 | 0.21 | 23.03 | 7.23 | 59.63 | 1.48 | 8.43 | 100.00 |
| 12 | 22.2 | 0.24 | 22.77 | 7.12 | 59.74 | 1.53 | 8.62 | 100.01 |
| 13 | 24.2 | 0.23 | 22.72 | 7.08 | 59.86 | 1.54 | 8.59 | 100.01 |
| 14 | 26.2 | 0.24 | 22.84 | 7.16 | 60.01 | 1.37 | 8.40 | 100.01 |
| 15 | 28.2 | 0.18 | 22.56 | 7.52 | 60.53 | 1.24 | 7.98 | 100.00 |
| 16 | 30.2 | 0.17 | 22.60 | 7.37 | 60.63 | 1.22 | 8.02 | 100.00 |
| 17 | 32.2 | 0.22 | 22.61 | 7.32 | 60.09 | 1.40 | 8.37 | 99.99 |
| 18 | 34.2 | 0.24 | 22.39 | 6.97 | 59.69 | 1.74 | 8.98 | 100.01 |
| 19 | 36.2 | 0.28 | 22.76 | 6.86 | 59.08 | 1.96 | 9.07 | 100.01 |
| 20 | 38.2 | 0.26 | 22.56 | 6.63 | 59.22 | 2.21 | 9.14 | 100.01 |
| 21 | 40.3 | 0.25 | 22.75 | 6.82 | 59.27 | 1.90 | 9.02 | 100.00 |
| 22 | 42.3 | 0.27 | 22.90 | 6.74 | 58.93 | 2.03 | 9.14 | 100.00 |
| 23 | 44.3 | 0.33 | 23.01 | 6.44 | 58.39 | 2.40 | 9.43 | 100.00 |
| 24 | 46.3 | 0.35 | 22.40 | 6.32 | 58.33 | 2.74 | 9.87 | 100.00 |
| 25 | 48.3 | 0.39 | 22.54 | 6.10 | 56.68 | 3.69 | 10.62 | 100.00 |
| 26 | 50.3 | 0.36 | 22.76 | 6.15 | 57.25 | 3.24 | 10.23 | 100.00 |
| 27 | 52.3 | 0.45 | 22.47 | 5.84 | 56.50 | 3.90 | 10.87 | 100.02 |
| 28 | 54.3 | 0.47 | 22.05 | 5.41 | 55.35 | 4.92 | 11.81 | 100.01 |
| 29 | 56.3 | 0.47 | 21.87 | 5.51 | 55.77 | 5.24 | 11.15 | 100.00 |
| 30 | 58.3 | 0.47 | 22.10 | 5.64 | 55.75 | 4.57 | 11.48 | 100.00 |
| 31 | 60.3 | 0.47 | 21.96 | 5.66 | 55.98 | 4.55 | 11.39 | 100.00 |
| 32 | 62.4 | 0.39 | 22.05 | 5.31 | 56.04 | 5.25 | 10.95 | 99.99 |
| 33 | 64.4 | 0.51 | 21.68 | 5.26 | 54.95 | 5.73 | 11.87 | 100.00 |
| 34 | 66.4 | 0.75 | 18.92 | 4.34 | 48.86 | 14.62 | 12.51 | 99.99 |
| 35 | 68.4 | 0.97 | 14.45 | 3.28 | 34.45 | 34.10 | 12.76 | 99.99 |
| 36 | 70.4 | 1.09 | 19.78 | 4.76 | 48.93 | 11.87 | 13.57 | 100.00 |
| 37 | 72.4 | 0.45 | 22.38 | 5.83 | 55.55 | 4.51 | 11.29 | 100.01 |
| 38 | 74.4 | 0.43 | 22.07 | 5.67 | 56.30 | 4.36 | 11.17 | 100.00 |
| 39 | 76.4 | 0.45 | 22.42 | 5.77 | 56.03 | 4.33 | 11.02 | 100.01 |
| 40 | 78.4 | 0.47 | 21.97 | 5.57 | 55.77 | 4.81 | 11.41 | 100.00 |
| 41 | 80.5 | 0.35 | 22.43 | 6.08 | 57.61 | 3.35 | 10.18 | 100.00 |
| 42 | 82.5 | 0.32 | 22.63 | 6.45 | 58.07 | 2.78 | 9.76 | 100.01 |
| 43 | 84.5 | 0.26 | 22.71 | 6.82 | 59.14 | 2.16 | 8.91 | 100.01 |
| 44 | 86.5 | 0.24 | 22.61 | 7.19 | 59.78 | 1.64 | 8.55 | 100.00 |
| 45 | 88.5 | 0.23 | 22.79 | 7.13 | 59.90 | 1.55 | 8.41 | 100.00 |
| 46 | 90.5 | 0.20 | 22.69 | 7.23 | 60.21 | 1.42 | 8.27 | 100.01 |
| 47 | 92.5 | 0.25 | 22.54 | 7.07 | 59.57 | 1.80 | 8.79 | 100.02 |
| 48 | 94.5 | 0.30 | 22.69 | 6.58 | 58.45 | 2.46 | 9.52 | 100.00 |
| 49 | 96.5 | 0.28 | 22.48 | 6.79 | 58.66 | 2.44 | 9.37 | 100.01 |
| 50 | 98.5 | 0.29 | 22.54 | 6.79 | 59.14 | 2.07 | 9.18 | 100.01 |
| 51 | 100.6 | 0.26 | 22.73 | 6.97 | 58.98 | 2.03 | 9.04 | 99.99 |
| 52 | 102.6 | 0.39 | 22.58 | 6.64 | 57.56 | 3.01 | 9.85 | 100.01 |
| 53 | 104.6 | 0.43 | 22.30 | 6.06 | 56.73 | 3.97 | 10.53 | 100.01 |
| 54 | 106.6 | 0.33 | 22.51 | 6.43 | 57.57 | 3.06 | 10.10 | 100.01 |
| 55 | 108.6 | 0.32 | 23.04 | 6.50 | 57.55 | 2.94 | 9.67 | 100.01 |
| 56 | 110.6 | 0.31 | 22.62 | 6.49 | 58.31 | 2.69 | 9.60 | 100.01 |
| 57 | 112.6 | 0.32 | 22.78 | 6.49 | 57.74 | 2.85 | 9.84 | 100.00 |
| 58 | 114.6 | 0.24 | 22.87 | 7.11 | 59.86 | 1.75 | 8.18 | 100.00 |

Laves

# APPENDIX V

**Data of test rings 1 an 2**

BEWERKINGSBLAD TESTRING 01 (gelast bij IHC) ORDNR. 60.469–6666–101

| Draaiproef | Vlak | Toeren [omw/min] | | Snelheid [m/min] | Snedediepte [mm] | | Spoed [mm/ omw] | PT: Aantal indic. | Dimensies [mm] | | Cladding dikte [mm] | opmerkingen |
|---|---|---|---|---|---|---|---|---|---|---|---|---|
| | | doel | result. | >50 m/min | doel | resultaat | | | | | | |
| **1** | **1** | 15 | 12,5 | 49,3 | 0.5 – 1 | 0,2 | 0,3 | **1** | D1 | 172,6 | 5,6 | Geschatte claddingdikte voor |
| "schoon– | **2** | 15 | 12,5 | 48,6 | 0.5 – 1 | 0,2 | 0,3 | **0** | H2 | 65,8 | 8,8 | machinale bewerking [mm] |
| draaien" | **3** | 15 | 12,5 | 48,0 | 0.5 – 1 | 0,2 | 0,3 | **1** | D2 | 188,7 | 5,2 | D1 = 7 ± 0,5; D2 = 7 ± 0,5; |
| | **4** | 15 | 12,5 | 47,6 | 0.5 – 1 | 0,2 | 0,3 | **0** | H3 | 30,8 | 5,8 | H2 = 11 ± 1; H3 = 8 ± 1. |
| **2.1** | **1** | 15 | 12,5 | 49,3 | **0.1** | 0,1 | 0,3 | **1** | D1 | 172,5 | 5,5 | |
| variatie in | **2** | 15 | 12,5 | 48,7 | **0.3** | 0,3 | 0,3 | **0** | H2 | 65,5 | 8,5 | |
| snedediep- | **3** | 15 | 12,5 | 48,0 | **0.2** | 0,2 | 0,3 | **1** | D2 | 188,5 | 5,0 | |
| te | **4** | 15 | 12,5 | 47,6 | **0.4** | 0,4 | 0,3 | **0** | H3 | 30,4 | 5,4 | |
| **2.2** | **1** | 15 | 12,5 | 49,3 | **0.35** | 0,35 | 0,3 | **3** | D1 | 172,15 | 5,15 | |
| variatie in | **2** | 15 | 12,5 | 48,7 | **0.15** | 0,15 | 0,3 | **0** | H2 | 65,35 | 8,35 | |
| snedediep- | **3** | 15 | 12,5 | 48,0 | **0.25** | 0,25 | 0,3 | **5** | D2 | 188,25 | 4,75 | |
| te | **4** | 15 | 12,5 | 47,6 | **0.05** | 0,05 | 0,3 | **0** | H3 | 30,35 | 5,4 | |
| **3.1** verder | **1** | 15 | 12,5 | 49,5 | Totaal 2,0 mm | 1: 1,75 | 0,3 | **11** | D1 | 170,15 | 3,15 | Totaal afgedraaide dikte van Inc. |
| afdraaien | **3** | 15 | 12,5 | 48,2 | | 2: 0,25 | 0,3 | **12** | D2 | 186,25 | 2,75 | 625 cladding na bewerking 3.2 |
| **3.2** | **1** | 15 | 12,5 | 49,5 | 0,5 | 0,5 | 0,3 | **58** | D1 | 169,65 | 2,65 | D1 4,35 ± 0,5 mm |
| | **3** | 15 | 12,5 | 48,2 | 0,5 | 0,5 | 0,3 | **15** | D2 | 185,75 | 2,25 | D2 4.75 ± 0,5 mm |

BEWERKINGSBLAD TESTRING 02 (gelast bij FT' ORDNR. 60.469–6666–102

| Draaiproef | Vlak | Toeren [omw/min] | | Snelheid [m/min] | Snedediepte [mm] | | Spoed [mm/ omw] | PT: Aantal indic. | Dimensies [mm] | | Cladding dikte [mm] | opmerkingen |
|---|---|---|---|---|---|---|---|---|---|---|---|---|
| | | doel | result. | >50 m/min | doel | resultaat | | | | | | |
| **1.0** | 1 | | | | | | | | D1 | 176,2 | 9,2 | Claddingdikte voor |
| **Voor** | 2 | | | | | | | | H2 | 56,0 | 6,0 | machinale bewerking [mm] |
| het draaien | 3 | | | | | | | | D3 | 190,0 | 6,5 | D1 = D2 = |
| | 4 | | | | | | | | H4 | 22,0 | 7,0 | H2 = H3 = |
| **1.1** | 1 | 15 | 8 | 23,9 | 0.5 – 1 | 0,75 | 0,32 | **0** | D1 | 175,0 | 8,0 | ZIE OOK BIJGEVOEGDE SCHETS |
| schoon– | 2 | 15 | 10 | 26,4 | 0.5 – 1 | 1,00 | 0,32 | **0** | H2 | 53,5 | 3,5 | |
| draaien | 3 | 15 | 10 | 29,0 | 0.5 – 1 | 1,00 | 0,32 | **0** | D3 | 188,5 | 5,0 | |
| | 4 | 15 | 10 | 28,6 | 0.5 – 1 | 1,00 | 0,32 | **0** | H4 | 21,0 | 6,0 | |
| **2.1** | 1 | 15 | 16 | 47,8 | **0.1** | 0,10 | 0,32 | **0** | D1 | 174,8 | 7,8 | |
| variatie in | 2 | 15 | 16 | 47,1 | **0.3** | 0,30 | 0,32 | **0** | H2 | 53,2 | 3,2 | |
| snedediep- | 3 | 15 | 16 | 46,4 | **0.2** | 0,20 | 0,32 | **0** | D3 | 188,3 | 4,8 | |
| te | 4 | 15 | 16 | 45,8 | **0.4** | 0,40 | 0,32 | **0** | H4 | 20,6 | 5,6 | |
| **2.2** | 1 | 15 | 16 | 47,8 | **0.35** | 0,35 | 0,32 | **0** | D1 | 174,40 | 7,40 | |
| variatie in | 2 | 15 | 16 | 47,1 | **0.15** | 0,15 | 0,32 | **0** | H2 | 53,05 | 3,05 | |
| snedediep- | 3 | 15 | 16 | 46,4 | **0.25** | 0,25 | 0,32 | **0** | D3 | 188,00 | 4,50 | |
| te | 4 | 15 | 16 | 45,8 | **0.05** | 0,05 | 0,32 | **0** | H4 | 20,50 | 5,50 | |
| **3.1** | 1 | 15 | 12 | 35,9 | Totaal | 2,0 mm | 0,32 | **0** | D1 | 173,40 | 6,40 | |
| afdraaien | 3 | 15 | 12 | 34,9 | | | 0,32 | **0** | D3 | 187,00 | 3,50 | |

| Draaiproef | Vlak | Toeren [omw/min] doel | Toeren [omw/min] result. | Snelheid [m/min] >50 m/min | Snedediepte [mm] doel | Snedediepte [mm] resultaat | Spoed [mm/omw] | PT: Aantal indic. | Dimensies [mm] | | Cladding dikte [mm] | opmerkingen |
|---|---|---|---|---|---|---|---|---|---|---|---|---|
| 3.2.1 | 1 | 15 | 12 | 36,0 | 0,5 | 0,50 | 0,32 | 0 | D1 | 172,90 | 5,90 | |
| | 3 | 15 | 12 | 34,9 | 0,5 | 0,50 | 0,32 | 0 | D3 | 186,50 | 3,00 | |
| 3.2.2 | 1 | 15 | 12 | 36,0 | 0,5 | 0,50 | 0,32 | 0 | D1 | 172,40 | 5,40 | |
| | 3 | 15 | 12 | 35,0 | 0,5 | 0,50 | 0,32 | 0 | D3 | 186,00 | 2,50 | |
| 3.2.3 | 1 | 15 | 12 | 36,0 | 0,5 | 0,50 | 0,32 | 0 | D1 | 171,90 | 4,90 | |
| | 3 | 15 | 12 | 35,0 | 0,5 | 0,50 | 0,32 | 0 | D3 | 185,50 | 2,00 | |
| 3.2.4 | 1 | 15 | 12 | 36,1 | 0,5 | 0,50 | 0,32 | 0 | D1 | 171,40 | 4,40 | |
| | 3 | 15 | 12 | 35,1 | 0,5 | 0,50 | 0,32 | 0 | D3 | 185,00 | 1,50 | |
| 3.2.5 | 1 | 15 | 12 | 36,1 | 0,5 | 0,50 | 0,32 | 1 | D1 | 170,90 | 3,90 | |
| | 3 | 15 | 12 | 35,1 | 0,5 | 0,50 | 0,32 | 0 | D3 | 184,50 | 1,00 | |
| 3.2.6 | 1 | 15 | 12 | 36,2 | 0,5 | 0,50 | 0,32 | 0 | D1 | 170,10 | 3,10 | |
| | 3 | 15 | 12 | 35,2 | 0,5 | 0,50 | 0,32 | 0 | D3 | 183,60 | 0,10 | |
| 3.2.7 | 1 | 15 | 12 | 36,2 | 0,5 | 0,50 | 0,32 | 0 | D1 | 169,60 | 2,60 | |
| | 3 | 15 | 12 | 35,2 | 0,5 | 0,50 | 0,32 | 0 | D3 | 183,10 | −0,40 | |
| 3.2.8 | 1 | 15 | 12 | 36,3 | 0,5 | 0,50 | 0,32 | 0 | D1 | 169,10 | 2,10 | |
| | 3 | 15 | 12 | 35,2 | 0,5 | 0,50 | 0,32 | 0 | D3 | 182,60 | −0,90 | |

# APPENDIX VI

**Product Status Report and Jobsheet**

**IHC** # JOBSHEET

Datum afgifte:

| | |
|---|---|
| Order : | nr.: |
| Onderdeel : | nr.: |
| Ref. WPS: | Basismateriaal: |
| Proces: | Machine nr.: |
| Lastoevoegmateriaal: | plaats : |

testring 03
Lasproef met Incoflux "7"

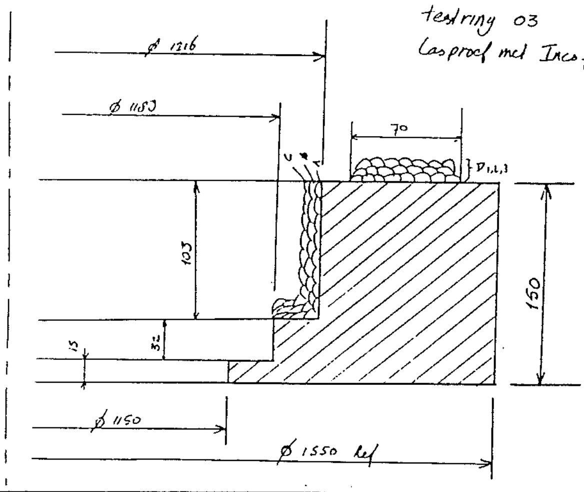


| | |
|---|---|
| Datum start: | |
| Datum einde: | |
| Lasnummer: | |
| Aantal lagen: | |
| Totaal dikte: | |
| Bufferlaag: | Y / N |
| PWHT: | Y / N |

Opmerkingen:

| Datum | Tijd | Lasser | T(interp.) | Draadrol nr | Opmerkingen |
|---|---|---|---|---|---|
| | | | | | |
| | | | | | |
| | | | | | |
| | | | | | |
| | | | | | |
| | | | | | |
| | | | | | |
| | | | | | |
| | | | | | |
| | | | | | |
| | | | | | |
| | | | | | |
| | | | | | |
| | | | | | |
| | | | | | |
| | | | | | |
| | | | | | |
| | | | | | |
| | | | | | |
| | | | | | |
| | | | | | |
| | | | | | |
| | | | | | |

Datum bewerking:

Datum PT: Resultaat:

Datum reparatie

Soort reparatie:

# PRODUCT STATUS REPORT

| | | | |
|---|---|---|---|
| PRODUCT STATUS REPORT | | WEEK 41 | PAGE 1 |
| Project : Mallard | Ordernr. : 60.270 | Part : Inner Part | Partnr. : 6510–101 |

| | | | |
|---|---|---|---|
| Drawingnr. : IHC 6027004 A | WELDING of Overlay | WPS nr. : 194 A | Date : |
| Scetch of overlay UPPER LOWER<br>Material : Zeron 25 | Variation in weldparameters | N.A. | |
| | Heat treatment<br>Target | N.A. | |
| | MACHINING | Comment | |
| | Pre–machining<br>Date : | | |
| | Final machining<br>Date : week 39 | Diameter of lower sealsurfaces 1655.3 (+0.1) and 1690.3 (+0.1) that means 0.15 above final dimension to fit bottom sealring which is machined to wide. | |
| | Superfinish<br>Date : | | |

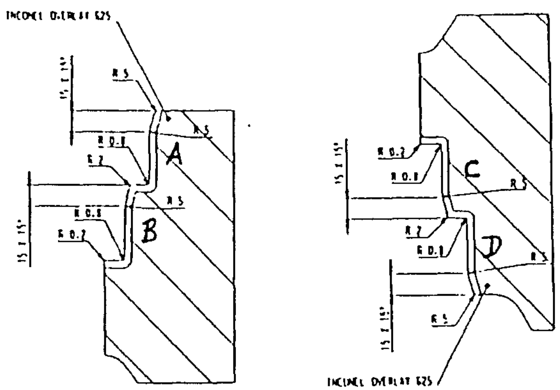


| NON DESTRUCTIVE TESTING :Dye Penetrant Testing | REPAIR |
|---|---|
| I Date : 29/09/95 after machining 0.15 mm in diameter too wide<br>Result : 9 relevant indications in lower sealsurfaces | I Marked indications are repaired with GTAW before fine–turning |
| II Date : 3/10/95 after machining 0.16 mm in diameter too wide<br>Result : 15 relevant indication in upper sealsurface with a linear character on a specific height (see drawing) | II Marked indications are repaired with GTAW before fine–turning |
| III Date :4/10/95 After final machining 9 indications in upper seal surface, these<br>Result : are being repaired | III Marked indications are repaired with GTAW followed by hand–grinding |
| IV Date :9/10/1995 Sealrings Penetrant Tested after pressurizing assembled swivel if new or old indications occure.<br>Result : NO NEW OR OTHER RELEVANT INDICATIONS FOUND | IV N.A. |

| Place in shop | Hal 5A | Hal 8A | | | | | | | | |
|---|---|---|---|---|---|---|---|---|---|---|
| Date : | 4/10/95 | 09/10/95 | | | | | | | | |

Comparable / same parts : Inner Parts 6520 and 6530

| PRODUCT FINISHED |
|---|
| Planned date : |
| Actual date : 5–10–1995 |